

**LANDSLIDE HAZARD ZONATION AND SLOPE STABILITY
ASSESSMENT TECHNIQUES : APPLICATIONS TO
SRINAGAR-RUDRAPRAYAG, GARHWAL HIMALAYA**

A THESIS

*submitted in fulfilment of the
requirements for the award of the degree
of*
DOCTOR OF PHILOSOPHY
in
EARTH SCIENCES

By

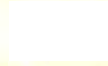
SHANTANU SARKAR



**DEPARTMENT OF EARTH SCIENCES
UNIVERSITY OF ROORKEE
ROORKEE-247 667 (INDIA)**

SEPTEMBER, 1996

Gratis



CANDIDATE'S DECLARATION

I hereby certify that the work which is being presented in the thesis entitled " **LANDSLIDE HAZARD ZONATION AND SLOPE STABILITY ASSESSMENT TECHNIQUES : APPLICATIONS TO SRINAGAR-RUDRAPRAYAG, GARHWAL HIMALAYA**" in fulfilment of the requirement for the award of the Degree of **Doctor of Philosophy**, submitted in the **Department of Earth Sciences, University of Roorkee**, is an authentic record of my own work carried out during the period from April, 1990 to September, 1996 under the supervision of Dr. R. Anbalagan, Dr. G.S. Mehrotra and Dr. P.K. Gupta.

The matter embodied in this thesis has not been submitted by me for the award of any other degree.

Shantanu Sarkar

(SHANTANU SARKAR)

This is to certify that the above statement made by the candidate is correct to the best of our knowledge.

R. Anbalagan
2/9/96

(R. Anbalagan)
Asst. Professor
Dept. of Earth Sciences
University of Roorkee
Roorkee, India

G.S. Mehrotra
2.9.96

(G.S. Mehrotra)
Dy. Director & Head
G.E. Division
C.B.R.I.
Roorkee, India

P.K. Gupta

(P.K. Gupta)
Asst. Professor
Dept. of Earth Sciences
University of Roorkee
Roorkee, India

Date : 2. 9. 96.

The Ph.D. Viva-Voce of **Mr. S. Sarkar**, Research Scholar has been held on

24/5/97

R. Anbalagan
24/5/97
Signature of Supervisor(s)

V.N. Singh
24/5/97
Signature of H.O.D.

Doobani
Signature of External Examiner

G.S. Mehrotra

ACKNOWLEDGEMENTS

I take this opportunity to express profound gratitude to my supervisors, Dr G.S. Mehrotra, Dr P.K. Gupta and Dr R. Anbalagan, for their valuable guidance and constructive criticism during the course of my Ph.D. work.

I am grateful to Prof. R.N. Iyengar, Director, Central Building Research Institute, for providing the necessary facilities to complete this work.

I express my unfathomable gratitude to Dr R.K. Bhandari who introduced to me the field of landslides and inspired me to take up this work. My most sincere thanks to Dr P.K. Gupta without whose constant guidance and valuable suggestions the thesis would not have been completed.

I am grateful to Dr Bhawani Singh for his critical suggestions during the course of the work.

I am thankful to Mr D.P. Kanungo who has helped me at various stages of the work, particularly assisting me in carrying out field investigations. My sincere thanks are also to Mr Anil Swarup and Dr Sudhir Kumar who helped me in different stages during the compilation of the thesis. Valuable suggestions rendered by Mr A. Ghosh, Mr J.N. Vaish, Dr D.K. Mukhopadhyay and Dr A.K. Sen are greatly acknowledged.

I would like to acknowledge the cooperation rendered by Haragopal, Radha, Sandeep, Anupma, Dr Vineet, Dr Kalpana, Yashpal, Dr Sandeep, Dr R.K. Goel and Mr A.K. Jethi. I also thank to Mr Bhagat Bist for drafting the figures. The moral encouragement received through Mrs Mamta Gupta is greatly acknowledged.

I acknowledge my parents and sister for their constant encouragement and inspiration. My wife Archana and daughter Ishita sacrificed a lot during this period.

I dedicate this thesis to my mother who had a desire to see my Ph.D complete but unfortunately she passed away a few months ago.

I am thankful to all, who in any manner, directly or indirectly helped me during the course of this work.



(SHANTANU SARKAR)

ABSTRACT

Landslide is one of the most destructive geological processes which not only causes extensive damage to roads, bridges and houses but may also lead to loss of lives. Recent anthropogenic activities, particularly the road construction on vulnerable slopes, have greatly deteriorated slope stability and triggered landslides. This implies that the existing slope stability conditions must be systematically studied before implementing any developmental project. Such a study calls for slope stability assessment through spatial prediction of landslide potential zones. The present study, carried out in Srinagar-Rudraprayag area of Garhwal Himalaya, is an attempt towards development and evaluation of techniques for landslide hazard zonation and slope stability assessment.

The work has been initiated with the selection of important terrain factors which govern the slope stability. The terrain factors considered are lithology, distance from major thrust, slope, relative relief, drainage density and landuse. To determine the spatial distribution of various categories of these factors and of the existing landslides in the area, various terrain factor maps and a landslide map of the area have been prepared. Then the binary relationships between these factors and landslides have been identified on the basis of landslide density for each category of the factors. This study has revealed the degree of susceptibility of the factor categories to the landslide occurrence. The study has also highlighted the complex dependence of landslide occurrence on various factors.

The two techniques developed for the regional landslide hazard zonation study are the Subjective Regional Zonation (SRZ) and the Objective Regional Zonation (ORZ). Although the SRZ technique employs the inferred relationships between the landslide occurrence and the terrain factors to assign ratings to the factor categories, yet the rating assignment is subjective. The ORZ technique reduces the impact of subjectivity in rating assignment, by deriving these from the frequency distribution of landslides. In this technique, an attempt has been also made for a judicious classification of different hazard classes. Following these two techniques, the SRZ and ORZ maps of the study area have been prepared. Next, to obtain finer details of the hazard zones in a small sub-area, a third zonation technique, the Detailed Regional Zonation

(DRZ), has been employed. DRZ technique requires detailed field investigations to acquire additional field data pertaining to the weathering condition of rocks, the relation of discontinuities with reference to slope and the surface water conditions. Using this technique, the DRZ map of the sub-area has been prepared. The quality of hazard assessment for all the three zonation maps has been determined and it is found that these maps broadly show hazard zones in accordance with the existing landslide distribution. A comparative study of the results of the three zonation maps shows that considerable amount of information, available from the DRZ map, is present in the SRZ and ORZ maps. Further, the general trends of zonation in the three maps are found to be in broad agreement, particularly for the very high and high hazard zones. This study has demarcated the applicability of all the three techniques depending on the nature of available data and the purpose of study. When sufficient apriori information about the terrain is available so as to enable judicious choice of ratings, the SRZ technique should be used. Otherwise, the ORZ technique should be used, particularly when large data set are available. In case of a need for detailed regional zonation, the DRZ technique should be used provided the necessary detailed field investigation is possible.

The assessment of stability of an individual slope is always not possible from the regional zonation maps. For this purpose the Slope Mass Rating (SMR) technique has been used. This technique is based on the Rock Mass Rating (RMR), coupled with adjustment factor ratings for joint orientation and method of excavation of slopes. The technique has been used for thirty slopes along the Srinagar-Rudraprayag road. With the help of SMR technique, the slopes have been classified into different classes of stability conditions. The results arrived at are consistent with the existing field conditions and therefore point at the potentiality of the technique. The study has also revealed the importance of the relation between joint and slope orientations for a better understanding of various modes of slope failure. A conservative stability estimate has been obtained by anticipating the worst stability condition under water saturation.

The present work provides a systematic approach to the comprehensive slope stability assessment of a large region.

LIST OF FIGURES

	Page No.
1.1 Location map of the study area	9
1.2 Physiographic map of the study area	11
2.1 Longitudinal sub-divisions of the Himalaya	14
2.2 Tectonic map of Srinagar-Nandprayag area	17
2.3 Geological map of Srinagar-Rudraprayag area	18
3.1 Landslide map of the study area	32
3.2 Slope map of the study area	36
3.3 Relative relief map of the study area	37
3.4 Drainage map showing sub-basins of the study area	39
3.5 Landuse map of the study area	44
3.6 Density of landslide vs lithology	47
3.7 Density of landslide vs distance from NAT	47
3.8 Density of landslide vs slope	47
3.9 Density of landslide vs relative relief	51
3.10 Density of landslide vs drainage density	51
3.11 Density of landslide vs landuse	51
4.1 Cell map of the study area	60
4.2 SRZ map of the study area showing landslide hazard zones	63
4.3 Contours of landslide potential scores of ORZ technique	71
4.4 Frequency plots of landslide potential score	73
4.5 Composite graph obtained after superposing the curves (a), (b), (c) & (d) of figure 4.4.	74
4.6 ORZ map of the study area showing landslide hazard zones	76
4.7 Facet map of the sub-area	84
4.8 Structural map of the sub-area showing attitude of discontinuities	85
4.9 DRZ map of the sub-area showing landslide hazard zones	87
4.10 SRZ1 map of the sub-area showing landslide hazard zones	90

4.11 ORZ1 map of the sub-area showing landslide hazard zones	91
4.12 DRZ1 map of the sub-area showing landslide hazard zones	92
4.13 SRZ2 map of the sub-area showing landslide hazard zones when class boundaries of ORZ map are used	95
4.14 DRZ2 map of the sub-area showing landslide hazard zones when class boundaries of ORZ map are used	96
5.1 Slope locations along Srinagar-Rudraprayag road	100
5.2 Modes of failure in rock slopes	121
5.3 Stereoplots of slope 1 to 6 showing orientations of slope and joints	122
5.4 Stereoplots of slope 7 to 12 showing orientations of slope and joints	123
5.5 Stereoplots of slope 13 to 18 showing orientations of slope and joints	124
5.6 Stereoplots of slope 19 to 24 showing orientations of slope and joints	125
5.7 Stereoplots of slope 25 to 30 showing orientations of slope and joints	126

LIST OF TABLES

	Page No.
2.1 Lithological succession in Srinagar-Rudraprayag area	19
3.1 Main factors controlling instability and degree of uncertainty	34
3.2 Drainage density of sub-basins	40
3.3 Photo recognition elements for landuse classification	43
3.4 Frequency distribution of landslide in relation to lithology	46
3.5 Frequency distribution of landslide in relation to distance from NAT	46
3.6 Frequency distribution of landslide in relation to slope	46
3.7 Frequency distribution of landslide in relation to relative relief	50
3.8 Frequency distribution of landslide in relation to drainage density	50
3.9 Frequency distribution of landslide in relation to landuse	50
4.1 LSI of lithology categories	57
4.2 LSI of distances from NAT	57
4.3 LSI of slope categories	57
4.4 LSI of relative relief categories	58
4.5 LSI of drainage density categories	58
4.6 LSI of landuse categories	58
4.7 Hazard index for SRZ map	62
4.8 LSG of lithology categories	67
4.9 LSG of distances from NAT	67
4.10 LSG of slope categories	67
4.11 LSG of relative relief categories	68
4.12 LSG of drainage density categories	68
4.13 LSG of landuse categories	68
4.14 Hazard index for ORZ map	75
4.15 Landslide Hazard Evaluation Factor (LHEF) rating scheme	78
4.16 Hazard index for DRZ map	86
4.17 Comparison of cells for SRZ and ORZ maps	89
4.18 Comparison of cells for sub-area maps	93

4.19 Comparison of cells for sub-area maps with similar classification	97
5.1 Rock Mass Rating of Bieniawski, 1979	103
5.2 Adjustment ratings for joint orientations	104
5.3 Adjustment rating for methods of excavation of slopes	105
5.4 Joint parameters for RMR of the studied slopes	107
5.5 Strength parameter and orientation of slopes and joints	113
5.6 Ratings of joint parameters for RMR	119
5.7 Adjustment ratings for joint orientation and method of excavation	127
5.8 Description of SMR classes	135
5.9 Stability classes based on SMR	136
5.10 Comparison of SMR under observed and wet conditions	139

LIST OF PLATES

	Page No.
3.1 Planar failure in quartzite	27
3.2 Planar failure in phyllite	27
3.3 Wedge failure in metavolcanic	28
3.4 Debris slide along a drain	28
3.5 Debris slide in metavolcanic	29
3.6 Debris flow due to recent road construction	29
3.7 Rock fall in quartzites	30
3.8 Panoramic view of Kaliasaur slide	30
5.1 Highly jointed quartzite showing low RQD	109
5.2 Joints showing large spacing	109
5.3 Joint opening without filling material	110
5.4 Use of Schmidt hammer on joint planes	110

CONTENTS

	Page No.
Acknowledgements	(i)
Abstract	(ii)
List of Figures	(iv)
List of Tables	(vi)
List of Plates	(viii)
CHAPTER 1 INTRODUCTION	1
1.1 Landslides in Himalaya	1
1.2 Need for landslide hazard zonation	2
1.3 Review of literature on landslide hazard zonation	3
1.3.1 Global scenario	3
1.3.2 Indian scenario	6
1.4 Objectives and scope of study	7
1.5 Area of study	8
1.5.1 General physiography of the study area	8
1.6 Thesis outlay	10
CHAPTER 2 GEOLICAL SETTING	13
2.1 Regional geology of Alaknanda valley	15
2.2 Geology of Srinagar-Rudraprayag area	16
2.2.1 Dudatoli Group	19
2.2.2 Garhwal Group	20
2.3 Structures and tectonics	21
2.4 Summary	22
CHAPTER 3 LANDSLIDES AND TERRAIN FACTORS	23
3.1 Landslide study	24
3.1.1 Types of landslides in the study area	24

3.1.2	Landslide identification and mapping	26
3.2	Terrain factors	33
3.2.1	Slope	34
3.2.2	Relative relief	35
3.2.3	Drainage density	38
3.2.4	Landuse	42
3.3	Relationships of landslides with terrain factors	45
3.3.1	Landslides in relation to lithology	45
3.3.2	Landslides in relation to distance from North Almora Thrust	45
3.3.3	Landslides in relation to slope	48
3.3.4	Landslides in relation to relative relief	48
3.3.5	Landslides in relation to drainage density	49
3.3.6	Landslides in relation to landuse	49
3.4	Summary	52
 CHAPTER 4 LANDSLIDE HAZARD ZONATION TECHNIQUES		 53
4.1	Basic steps for landslide hazard zonation	54
4.2	Subjective Regional Zonation (SRZ) technique	55
4.2.1	Methodology	55
4.2.2	Data procurement and processing	56
4.2.3	Hazard classes and zonation map	59
4.2.4	Validation of map	61
4.3	Objective Regional Zonation (ORZ) technique	62
4.3.1	Fuzzy set	64
4.3.2	Methodology	64
4.3.3	Data procurement and processing	65
4.3.4	Hazard classes and zonation map	70
4.3.5	Validation of map	75
4.4	Detailed Regional Zonation (DRZ) technique	77
4.4.1	Methodology	77
4.4.2	Data procurement and processing	83

4.4.3 Hazard classes and zonation map	83
4.4.4 Validation of map	86
4.5 Comparative study of zonation maps	88
4.5.1 Parameter for comparison	88
4.5.2 Comparison between SRZ and ORZ maps	88
4.5.3 Comparison of sub-area maps from three techniques	89
4.5.4 Comparison of maps with identical class boundaries	94
4.6 Summary	98

CHAPTER 5 SLOPE STABILITY ASSESSMENT USING SMR

TECHNIQUE	99
5.1 Slope Mass Rating technique	101
5.1.1 Rock Mass Rating system	101
5.1.2 Adjustment rating for joint orientations	102
5.1.3 Adjustment rating for method of excavation	105
5.2 Field data collection	105
5.2.1 Rock Quality Designation (RQD)	106
5.2.2 Spacing of discontinuities	108
5.2.3 Condition of discontinuities	108
5.2.4 Ground water conditions	111
5.2.5 Uniaxial compressive strength	112
5.2.6 Orientation of discontinuities in relation to slope	116
5.3 An overview of the SMR parameters on studied slopes	116
5.4 Data analysis for Rock Mass Rating	118
5.5 Analysis of joint orientation	120
5.6 Method of excavation	133
5.7 Computation of Slope Mass Rating	134
5.8 Slope stability assessment	134
5.8.1 Stability assessment under wet conditions	138
5.9 Summary	141

CHAPTER 6 RESULTS AND DISCUSSIONS	143
6.1 Terrain factors and landslides	143
6.2 Landslide hazard zonation	144
6.3 Comparative study of the results of three techniques	146
6.4 Applicability of SRZ, ORZ and DRZ techniques	146
6.5 Site specific slope stability assessment	147
6.6 Concluding remarks	148
REFERENCES	149

INTRODUCTION

Landslides comprise a wide variety of complex processes that result in downward and outward movements, under gravity, of materials on unstable slopes. Like all the natural hazards, landslides and mass wasting are also of major concern to mankind. These can be considered as one of the most destructive geological processes causing not only the enormous damage to roads, bridges, houses but sometimes even loss of life. Although an individual slope failure is, in general, not so spectacular or devastating as an earthquake, a volcanic eruption, a flood or a hurricane, yet, being much more frequent and wide spread over the years, the slope failures have caused more extensive loss of property and life than any other geologic hazard. For example, vast areas of Darjeeling and Sikkim Himalaya were destroyed by some 20000 landslides in 1968 (Bhandari, 1987).

The imperative need of landslide hazard mitigation has led to persistent researches in this field, particularly on landslide hazard zonation. Such studies may become relevant in this ongoing International Decade for Natural Disaster Reduction (IDNDR).

1.1 LANDSLIDES IN HIMALAYA

The occurrence of landslides is a common phenomenon in the Himalaya which is a conspicuous landscape in the northern part of the Indian subcontinent. The Himalaya presents rock types, tectonic zones, topographic reliefs and slopes of diverse nature. Further, there exists numerous rivers and their tributaries which are intermittently eroding the terrain. In Himalaya, the geological formations have experienced severe folding, faulting and shearing during the successive phases of orogeny. These structurally deformed rocks have been subjected to severe

erosion by toe cutting action of deeply dissecting rivers and streams. All these adverse characteristics contribute in making the terrain susceptible to landslide occurrence. The heavy rainfall in these areas cause high water saturation which, in turn, triggers landslides. In recent years implementation of number of hydro-electric schemes, large scale construction of dams, roads, tunnels, buildings, towers, rope ways and other public utility works as well as indiscriminate mining and quarrying have further aggravated the problem manifold. Himalayan environmental degradation relates deforestation on steep slopes and construction of agricultural terraces to a rapid acceleration in gullying and landslide incidence and increased soil erosion (Ives and Messerli, 1989).

Landslides in the Himalayan region lead to river blockades, increase in siltation, communication disruptions, deforestation and to loss of human life and property. The severity of landslide problems in Himalaya has been highlighted by several workers. The 18th September, 1880 event of less than half a minute duration that took a toll of 143 lives in the upper part of township of Nainital was largely a debris avalanche which swept away Victoria Hotel, some buildings and the Naina Devi temple before plunging into the lake (Valdiya, 1987). Flash floods were caused by the breaching of landslide dams in Alaknanda river in the year 1894 and 1970 (Chansarkar, 1975), in Bhagirathi river in the year 1978 and in Mandakini river in the year 1979 (Prasad and Verma, 1982). The Kaliasaur landslide on the Rishikesh-Badrinath highway and the Ashar, Nerra and Nashri landslides in Chenab valley on the Jammu-Srinagar national highway are a constant threat to human life and property (Negi, 1982).

1.2 NEED FOR LANDSLIDE HAZARD ZONATION

The landslide hazards, in general can not be completely prevented, however, the intensity and severity of their impacts can be minimized by taking effective measures and by planning for disaster preparedness. According to Brabb (1993) at least 90 percent of landslide losses can be avoidable if the problem is recognized before the development or deforestation begins. Hence, there is a dire need for identification of unstable slopes which can be fulfilled by following a systematic approach for spatial prediction of landslide prone slopes. This calls for an assessment of slope instability and for preparation of landslide hazard zonation maps. The landslide hazard zonation can be defined as the division of land surface into uniform zones

and then ranking these according to the degree of actual or potential hazards from landslides on slopes. The zonation maps delineate areas with varying potential for future landslide occurrence. These maps serve as primary tools for planning hill development projects.

1.3 REVIEW OF LITERATURE ON LANDSLIDE HAZARD ZONATION

Most of the landslide hazard zonation schemes are based on the integration of information about spatial distribution of the factors identified to be important in assessing slope instability. The integration is, in general, carried out by superposing the maps of individual factors. The maps, commonly employed, illustrate landslide distribution, slope variation, relief, lithological types, structure, hydrologic conditions, rainfall and seismicity. Till mid seventies the landslide hazard zonation works primarily employed the qualitative integration of spatial data pertaining to some of these factors. Subsequently, the emphasis was laid on quantitative analysis of factors using different rating criteria assigned subjectively or derived numerically. Only a concise review of the literature on landslide hazard zonation is presented here and therefore the list of references is by no means exhaustive.

1.3.1 GLOBAL SCENARIO

Varnes (1984) presented a comprehensive review of the pioneer works on landslide hazard zonation carried out till early eighties. The early zonation maps were prepared in California by Blanc and Cleveland (1968), Brabb et al. (1972) and Radbruch-Hall and Crowther (1973). These maps were prepared by estimating the landslide occurrences in different geological formations and then amalgamating this data with the slope data. A similar grouping based on lithology and prevalence of slope movements was used by Rodriguez and others (1978) in Southern Spain. Nilsen et al. (1979) evaluated slope stability in the San Francisco Bay region by considering geological formations, slope ranges and landslides. The other investigators who used combinations of slope, lithology and landslides are Bowman (1972) in Australia, Dobrovolny and Schmoll (1974) at Anchorage, Alaska and Obermeier (1979) in Virginia.

The method of zonation becomes more and more complex as number of factors incorporated increases. The methodology adopted in France, during 1974-79, considered varied factors to generate maps known as ZERMOS (Zones Exposed to Risks of Soil Movement)

maps. The ZERMOS map of the Moyenne Vesubie region, France, prepared by Meneroud and Calvino (1976) shows four zones of instability defined on the basis of five factors: lithology, structures, slope, morphology and hydrology. Another ZERMOS map prepared by Landry (1979) identified seven classes of hazard on the basis of the factors like geological nature of the soil and sub soil, slope angle, drainage and local history of landslide.

The numerical rating assignment to the contributing factors was employed by Stevenson (1977) to undertake landslide hazard zonation in Tasmania. He estimated the risk by taking the product of the factor ratings. In contrast, Meneroud (1978) in France, rated the factors like topography, discontinuities, vegetation, hydrology and previous failures and obtained the level of risk by adding factor ratings. In a similar way, Huma and Radulescu (1978) prepared a geotechnical zoning map of landslide stability using ranked values of factors related to lithologic composition, structural and hydrologic condition, vegetation, slope angle together with map of landslides.

In Japan, Takei (1982) prepared a debris flow hazard map considering the factors like type of rock, fracturing, weathering characteristics, springs, vegetation cover, valley slopes and the historical records of large landslides. In New Zealand, Eyles (1983), using the factors like lithology, slope and topography, identified thirteen types of erosion and illustrated the severity and location of each erosion type through the computer generated maps. For hazard zonation in Nepal, Wagner et al. (1988) assigned weightages in proportion to the risk associated with structure, lithology, hydrology and tectonics and the total risk values were then divided into three landslide hazard classes. Brand (1988) has carried out landslide risk assessment in Hong Kong using a terrain evaluation approach. The factors considered for terrain evaluation were slope gradient, terrain morphology, erosion and instability, slope condition, hydrology and vegetation. On the basis of selected combinations of attributes from the terrain classification, he prepared the Geotechnical Land Use Map (GLUM), which classifies land into four classes of geotechnical limitations. These GLUM classes indicate the degree of suitability for land development. Kingsbury (1992) has developed a methodology where the terrain characteristics are related to landslide density for grouping the categories in different hazard classes. Bhandari et al. (1994) have developed a landslide hazard zonation approach which is being followed in Srilanka. The factors considered by them are geology, existing landslides and surface deposits, slope range, land form, land use and hydrology.

In addition to the qualitative or the quantitative approaches, considerable amount of work on zonation has also been carried out by different workers using the mathematico-statistical approach. It has been quantitatively shown that the landslide incidence is dependent on the interplay of a large number of interrelated factors which should be treated within the framework of a system approach (Carrara, 1983). Some investigators have isolated the apparently most significant factors by the method of discriminant functions (Neuland, 1976; Reger, 1979). A major contribution from Carrara (1983) presents multivariate models for assessing landslide hazard in Southern Italy. He used discriminant analysis and multiple regression analysis to predict actual and potential landslide hazards. In their study they used a group of geological - geomorphological attributes, directly or indirectly related to the slope instability, to define the discriminant functions or the regression equation.

The quantification theory, a mathematico-statistical method to convert qualitative data into quantitative relations, was employed for landslide risk mapping in Japan by Kawakami and Saito (1984), Haruyama and Kitamura (1984) and Kasa et al. (1992).

Yin and Yan (1988) used the information value method and the regression analysis to establish two statistical prediction models for landslide zonation. The two landslide hazard maps of a same region, prepared using these models, showed close similarity. Mark (1992) produced a debris flow map of San Mateo County, California using the technique of logistic regression and the digitized maps of topography, precipitation, geology and vegetation. Mapping of slope failure potential in Mt. So-San area of Taiwan has been carried out by Juang et al. (1992) using fuzzy sets. They used the fuzzy sets to process the linguistic data of the factors.

In addition to the zonation methods, there exists several conventional engineering methods for slope stability assessment. In these methods the factor of safety is calculated using material properties, slope geometry, hydrological condition and nature of discontinuities. Such analyses are carried out for specific sites only and not for a regional scale mapping. Apart from the stability analysis, the Slope Mass Rating technique, developed by Romana (1985), is being used by several workers for individual slope stability assessment. Tsiambaos & Telli (1992) used this technique to determine the slope stability of road cuts in Greece.

1.3.2 INDIAN SCENARIO

The landslide hazard zonation studies in India started only in the early eighties. However, lately several workers have carried out zonation studies in various parts of the Himalaya. The methodologies developed by different workers vary in selection of factors and in assignment of due weightages to them.

Among the earlier workers, Majumdar (1980) attempted a landslide zonation map of North Eastern Himalaya. He considered the factors such as geology, relief and rainfall intensity and developed a six level landslide zoning system. A landslide hazard zonation map of the Nilgiri hills in South India was prepared by Sheshagiri and Badrinarayanan (1982). They considered slope, soil cover, drainage and landuse as the major factors and assigned numerical weightages.

Gupta and Joshi (1990) considered lithology, landuse, slope aspect and distance from major shear zones as the factors for landslide zonation. The relationship between landslide occurrence and these factors were converted into a risk factor which led to three classes of instability in the study area. The land hazard mapping, carried out by Choubey and Litoria (1990), in Kalsi - Chakrata area of Garhwal Himalaya, was based on the studies on factors like steepness of slope with rock type, presence or absence of earthquake epicentre, forest cover, proximity to a thrust/fault, rivers and landslides. The area has been classified into four classes of instability. To carry out landslide zonation in parts of Kumaon Himalaya, Anbalagan (1992) has developed a landslide hazard evaluation factor rating system considering the factors such as lithology, structure, slope, relative relief, landuse and ground water conditions. The ratings are assigned according to the proneness of the factors to landslide. Subsequently, Gupta and Anbalagan (1995) used this scheme in parts of Garhwal Himalaya.

Landslide hazard zonation mapping based on the relationship between landslides and the factors like dip slopes, distance from ridge top, geological formation, landcover and road density was carried out by Pachauri and Pant (1992). They computed the ratings for sub-categories of the factors and identified five hazard classes in the Aglar catchment of the Yamuna valley. Mehrotra et al. (1992; 1996) have carried out landslide hazard zonation in Tehri-Garhwal Himalaya and in parts of Sikkim Himalaya based on assignment of numerical rating to the factors; lithology, slope, distance from major thrust, landuse and drainage density

and on the relation between these factors and landslide. In similar way Sarkar et al. (1995) have produced a zonation map of Srinagar, Garhwal Himalaya. A statistical model for slope instability classification, based on information theory and regression analysis, has been developed and tested in parts of Alaknanda valley by Sridevi and Sarkar (1993).

Over the past few years there has been a significant contribution of Geographic Information System (GIS) to spatial data analysis. In India, Roy et al. (1992) have developed a Spatial Statistical Prognostic Modelling (SSPM) using USEMAP GIS package for landslide hazard zonation and applied it to parts of Himachal Pradesh. The USEMAP has also been used by Lakhera et al. (1992) for landslide hazard zonation mapping in parts of Chamoli district of Garhwal Himalaya by integrating selected geo-environmental variables. An integrated GIS approach was adopted by Garg et al. (1996) to generate landslide hazard zonation map around Tehri Dam, Garhwal Himalaya.

Apart from the regional landslide hazard zonation study, the site specific slope stability assessment using Slope Mass Rating technique has also been carried out by some workers. A modified Slope Mass Rating has been used by Anbalagan (1992) to study the stability of road cuts in Garhwal Himalaya. The technique was also used by Mehrotra et al. (1995).

The brief literature review reveals that there are several techniques for landslide hazard zonation. The most widely used approach is the factor overlay technique. The various overlay techniques differ in the choice of factors, the modes of rating assignment and the final hazard potential computation. During past few years several attempts have been made to undertake objective and quantitative analysis using different techniques. Although several landslide hazard zonation exercises, using different techniques, have been performed in the Himalaya, yet not much work has been done towards quantitative analysis. Further, the efficacy of these techniques and their applicability potentials have not been systematically studied.

1.4 OBJECTIVES AND SCOPE OF STUDY

The ongoing developmental activities in Himalaya call for identification of landslide susceptible zones. In order to achieve this goal the present study aims at developing regional landslide hazard zonation methodologies based on overlaying technique with subjective as well as objective criteria for rating assignment. The validation of zonation maps has been ascertained in terms of certain parameters defined for the purpose. The maps obtained using

different techniques have been compared to assess their degree of agreement. Further, in a part of the study area, a detailed landslide hazard zonation using another technique has also been carried out. This study enabled us to ascertain as to what details of the sub-area zonation map can be found in the regional zonation maps of the entire study area. Since from the results of regional zonation, it is difficult to assess stability of an individual slope, a technique for site specific slope stability assessment has also been evaluated for its applicability.

The objectives of the study have been achieved through following steps:

- (1) Identification of landslide slopes and preparation of landslide map of the area.
- (2) Preparation of terrain factor maps to assess their spatial variation in the area.
- (3) Study of relations between landslides and different terrain factors.
- (4) Development of methodologies for regional landslide hazard zonation and preparation of zonation maps of the study area.
- (5) Detailed regional landslide hazard zonation of the sub-area.
- (6) Comparative study of different zonation maps.
- (7) Slope stability assessment of individual slopes using Slope Mass Rating (SMR) technique.

1.5 AREA OF STUDY

The present study has been carried out in Srinagar-Rudraprayag area, which is a part of Alaknanda valley in Garhwal Himalaya (Fig. 1.1). It falls between the latitudes $30^{\circ}10'$ - $30^{\circ}20'$ and longitudes $78^{\circ}45'$ - $79^{\circ}0'$ and encompasses an area of 444 km^2 . The selection of study area was primarily governed by the need of hazard zonation in the area in view of the upcoming developmental projects and the necessity of keeping the strategically important Rishikesh-Badrinath road functional. The choice was facilitated by the fact that there exist a number of landslides as well as different terrain factors with their varied characteristics. To undertake the detailed regional zonation study, a sub-area has been selected from the study area. This sub-area falls between the latitudes $30^{\circ}10'$ to $30^{\circ}16'$ and longitudes $78^{\circ}49'$ to $78^{\circ}57'$ encompassing an area of 78 km^2 .

1.5.1 GENERAL PHYSIOGRAPHY OF THE STUDY AREA

In the study area, the Alaknanda river is flowing downstream from Rudraprayag to Srinagar in NE-SW to WSW direction with deep antecedent gorge. The river meanders before

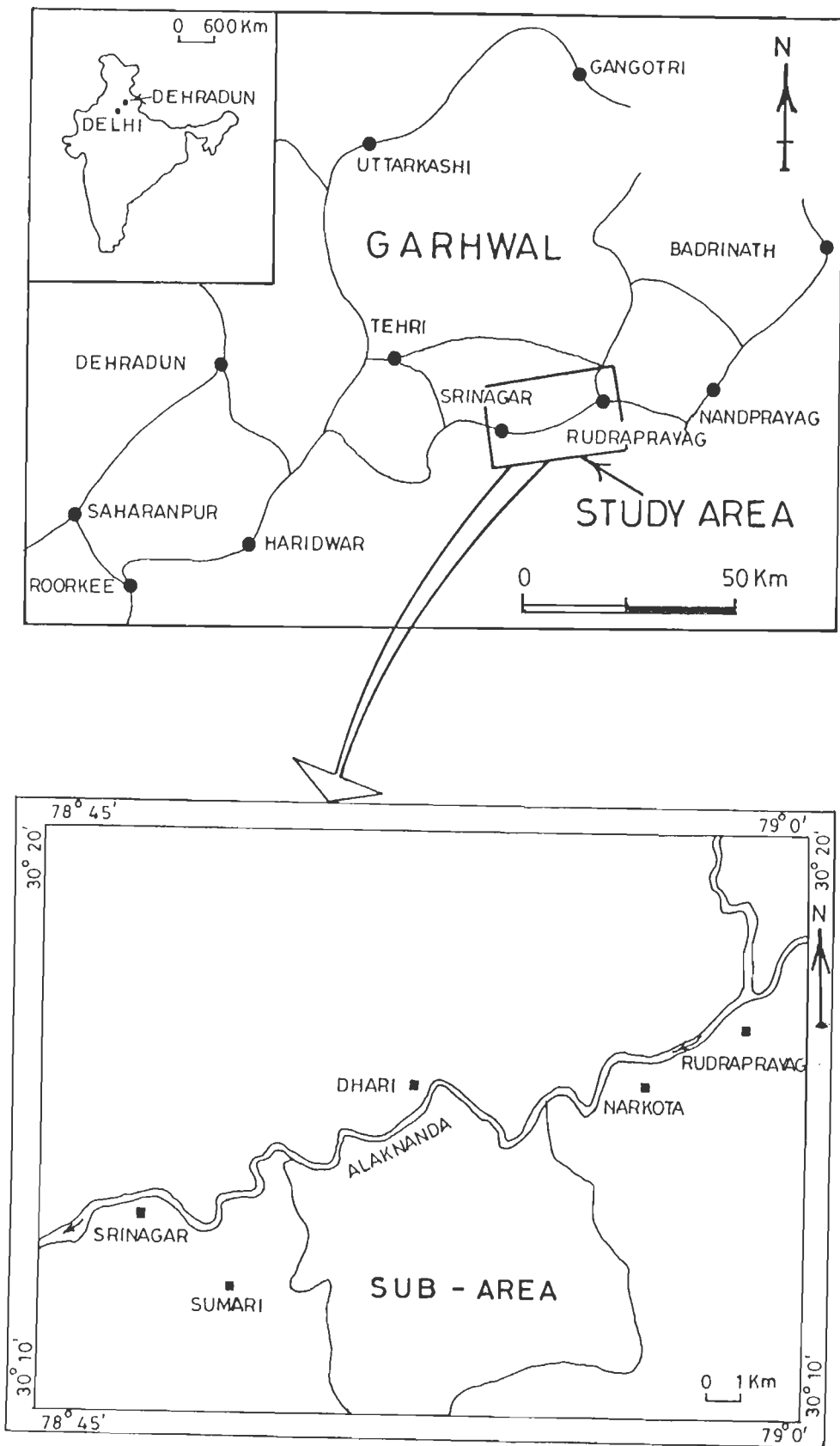


Figure 1.1 Location map of the study area

it reaches Srinagar valley with a wider shape and broader terrace deposits. The Alaknanda has shifted its course abandoning its old channel and is now flowing through a gorge (Pant, 1975). The abandoned channel is located near Kaliasaur, Supana and Srinagar. The terraces of Alaknanda valley are mainly of depositional type and are of fluvial and fluvioglacial origin. They have been dated to Quaternary and Holocene period (Khan et al., 1982).

During its course, Alaknanda river traverses through various geological formations and flows downstream from a height of about 1400m near Rudraprayag to 800m at Srinagar. At Rudraprayag, the river Mandakini meets with this river. The major tributaries, in the study area are Dhundsir, Badiyar, Bhardari, Neyal, Dewalgarh, Gostu and Bachchan. On the right bank of the Alaknanda, the Badiyar is flowing in NW-SE direction, whereas Dhundsir and Bhardari are flowing in N-S direction. On the left bank of Alaknanda the Neyal stream meets near Srinagar, flowing in NW-SE direction, while Dewalgarh and Gostu are flowing almost in N-S direction. These streams are all separated by ridges. Six major ridges are located to the north of Alaknanda while seven are marked on the southern part. The maximum elevation in the study area is about 2300 m in the south eastern corner near village Chuthani while the minimum elevation is about 700 m near Srinagar. Some of the peaks are around Dharpayankot, Murchunda and the north of Rudraprayag. The physiographic map of the area (Fig. 1.2) shows that the southern part presents a more dissected topography due to closely spaced ridges and streams in comparison to the northern part.

1.6 THESIS OUTLAY

The study is presented in six chapters including the present one. Chapter 2 deals with geology of the study area. Different rock types belonging to the different geological formations are shown in the prepared geological map. The major thrust and faults present in the area are described.

In Chapter 3, the existing landslides in the area are identified and a landslide map is prepared. Various terrain factor maps showing the spatial distribution of their categories are presented. The relationships between landslide frequencies and different factors are then derived.

Chapter 4 deals with the landslide hazard zonation study. Three different techniques for zonation are described and applied to the study area. The results obtained from the techniques

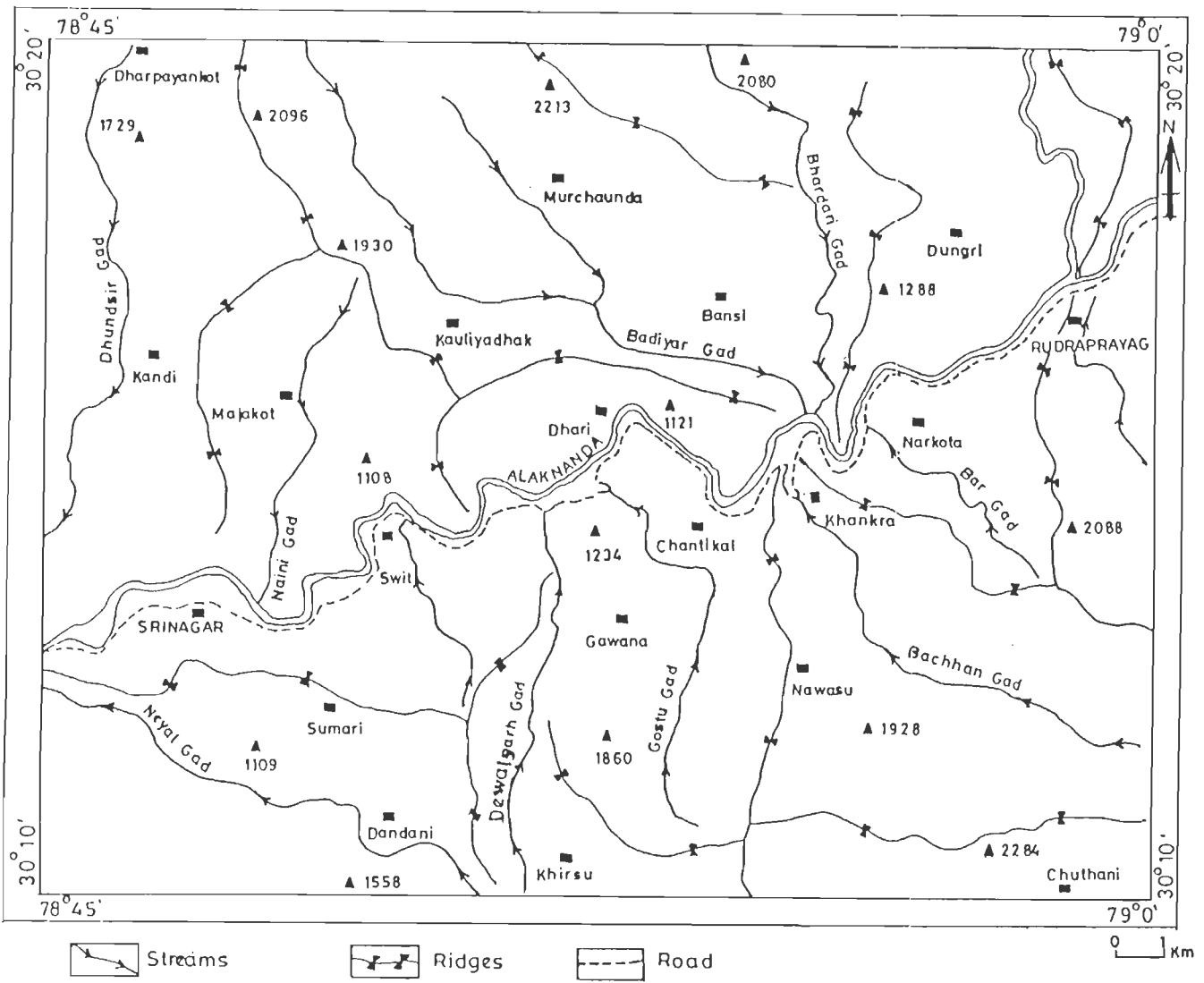


Figure 1.2 Physiographic map of the study area

are analysed and compared.

In Chapter 5, Slope Mass Rating technique for specific slope stability assessment is described in detail. The results of its application to various slopes along 34 km stretch of Srinagar - Rudraprayag road are presented.

Finally, in Chapter 6, findings of present study are summarized and a concluding discussion is presented.

GEOLOGICAL SETTING

The Himalayan mountain ranges, trending NW-SE, were formed by the collision of the Indian plate with the Eurasian plate. This collision resulted in uplift of the northern boundary of the Indian plate with the formation of a number of lofty peaks. The Himalaya has been divided into four longitudinal parts viz., the Sub-Himalaya, the Lower or Lesser Himalaya, the Higher or Greater Himalaya and the Tibetan or Tethys Himalaya (Gansser, 1964; Fig. 2.1). The Sub-Himalaya with average relief of 400-800 m has its southern boundary demarcating it from the alluvial plains of Ganga. This unit is full of dip-slopes and escarpments. It comprises Siwalik rocks, represented by sandstone, shale, siltstone and conglomerate in the southern foothills of the Himalaya. The boundary between the Sub-Himalaya and the Lesser Himalaya is marked by the Main Boundary Thrust (MBT). The Lesser Himalaya has a series of ridges and spurs divided by deep valleys. The average relief of the ridges ranges from 1500 to 3000 m. The Lesser Himalaya comprises low to medium grade metamorphic rocks like phyllites, quartzites, dolomites, schists and gneisses. The Main Central Thrust (MCT), which is characterised by a zone of intense shearing, separates the extremely deformed and transformed assemblage of Lesser Himalayan rocks from the high grade metamorphics of the Great Himalaya. The Great Himalaya has high mountain ranges with average relief of 4800 to 6000 m. The upper regions of this area are mostly blanketed by glaciers and snow. The high peaks in this region are separated by the transverse gorges of the major rivers of the area. The high grade metamorphic rocks of the Great Himalaya include gneisses, migmatites, granites, schists, and marbles. The Tibetan or Tethys zone comprises sedimentary rocks such as shale, sandstone, siltstone and conglomerate with limestone and quartzite interbeds. This is bordered

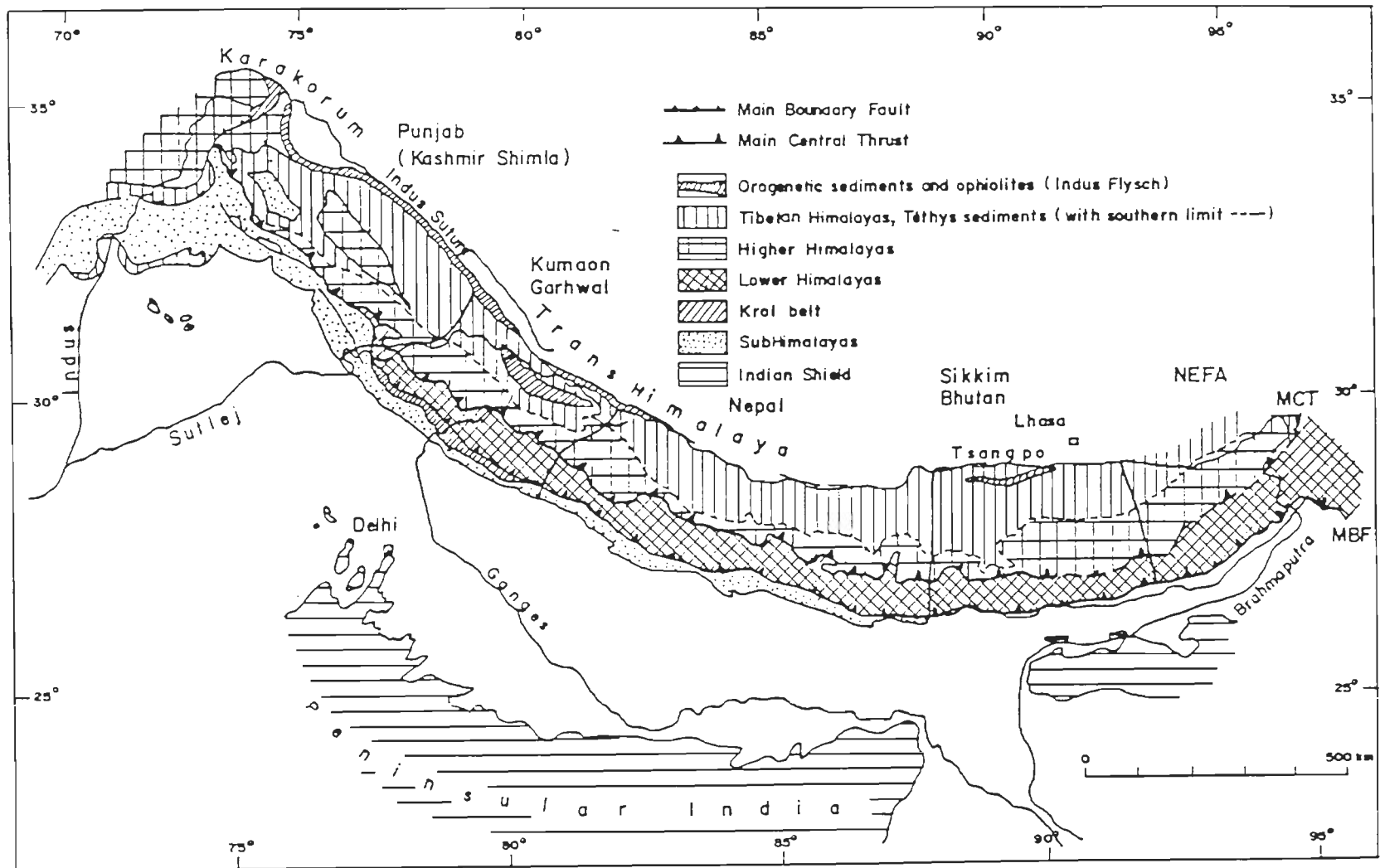


Figure 2.1 Longitudinal sub-divisions of the Himalaya (Gansser, 1964)

on the north by an ophiolite suite associated with Indus Tsangpo Suture Zone (Gansser, 1980; Stocklin, 1980). Further north lies the Trans Himalayan belt.

The present study area of Srinagar-Rudraprayag falls in the Garhwal Lesser Himalaya of Alaknanda valley. The first geological map of Garhwal Himalaya was prepared by Herbert (1842) followed by Middlemiss (1887), Heim and Gansser (1939) and Auden (1949). During the last two decades, several workers have carried out studies on geology, tectonic and stratigraphy of various parts of Garhwal-Kumaun Himalaya (Jain, 1971; Sakalani, 1971, 1972; Rupke, 1974; Kumar et al., 1974; Kumar and Agarwal, 1975; Valdiya, 1978, 1980; Fuchs and Sinha, 1978; Srivastava and Ahmad, 1979; Viridi, 1986; Roy and Valdiya, 1988; Thakur, 1993).

The chapter deals first with the regional geology of middle and lower parts of Alaknanda valley and then with the local geology of Srinagar-Rudraprayag area.

2.1 REGIONAL GEOLOGY OF ALAKNANDA VALLEY

Alaknanda river, during its course of journey, cuts across all the litho-tectonic units of Garhwal Himalaya, ranging in age from Precambrian to Neogene. There are significant facies variations from east to west and north to south, covering vast areas of Garhwal and adjoining Kumaun Himalaya. The three stratigraphic Groups, the Kumaun Super Group, the Garhwal Group and the Central Crystalline Group, constitute the three separate tectonic units. The Alaknanda valley has been traversed by three almost parallel major faults, Main Central Thrust (MCT), Alaknanda fault and North Almora Thrust (NAT), all trending NW-SE. The North Almora Thrust (NAT) and the Main Central Thrust (MCT) respectively mark the southern and northern boundaries of the Garhwal Group while the Alaknanda fault separates Rudraprayag Formation and Chamoli Formation of the Garhwal Group.

Mehdi et al. (1972) classified the litho-units occurring south of North Almora Thrust (NAT) into the Dudatoli Group. It was later sub-divided into Pauri phyllite, Marchula quartzite, Manila phyllite and Dudatoli-Almora crystalline by Kumar et al. (1974). They included Saknidhar Formation into Dudatoli Group and described the whole sequence as Kumaun Super Group.

Kumar and Agarwal (1975) prepared a geological map of Srinagar -Nandprayag area of Alaknanda valley and classified the rocks of the area into Central Crystalline, Garhwal and Dudatoli Groups forming the northern, central and southern parts of the area respectively. A

tectonic map of this area is shown in Fig. 2.2. The MCT separates Central Crystalline from the Garhwal Group and the NAT separates the Garhwal Group from the Dudatoli Group. The Central Crystalline Group in this area comprises kyanite schist, garnet-mica schist, quartzite and amphibolite of the Tungnath Formation and is intruded by tourmaline granite. The Garhwal Group, divided into the Rudraprayag, Lameri, Chamoli, Gwanagarh and Patroli Formations, shows a variety of rock assemblages like quartzite, dolomite, phyllite, slate and metavolcanic along with intrusion of granite and dolerite. The Dudatoli Group is represented by the Maithana and Pauri Formations in which the rocks are essentially phyllite and quartzite with basic flows.

Later, Ahmad (1976) suggested that all the Pre-Blaini Formations of Lesser Himalaya, occurring between MCT and MBT, may be classified as Garhwal Group. Srivastava and Ahmad (1979) classified the entire litho-tectonic succession of Alaknanda valley into two sub-heads; the Pre-Blaini sequence and the Post-Blaini sequence. The former is well exposed in the Inner Lesser Himalayan - Great Himalayan regions and the latter in the Outer Lesser Himalayan - Krol Belt region. The Garhwal Group in the upper, middle and lower parts of the Alaknanda valley is represented by the Rudraprayag, Pokhri, Chandpur and Simla Formations. It can be emphasized that similar formations and their members have been named differently by different workers.

2.2 GEOLOGY OF SRINAGAR-RUDRAPRAYAG AREA

A number of investigators have carried out geological and other related studies in the Srinagar-Rudraprayag area. The differences of opinion among different workers lie primarily in the stratigraphic succession. For the present study, the lithological characteristics and structure of the area are only of major concern and not their stratigraphic position.

The geological map of Srinagar-Nandprayag area, prepared by Kumar and Agarwal (1975), is used for the present field investigations in the study area of Srinagar-Rudraprayag. The reported contacts of various rock types and the presence of major structures are checked in the field and additional informations collected. In the north western and the south western part of the area, the contacts of different members are mapped and extended. The modified geological map prepared on 1:50,000 scale is shown in Fig. 2.3. The nomenclature, used in the present study, is essentially the same as used by Kumar and Agarwal (1975).

The litho-units of the study area belong to the Garhwal Group and Dudatoli Group of

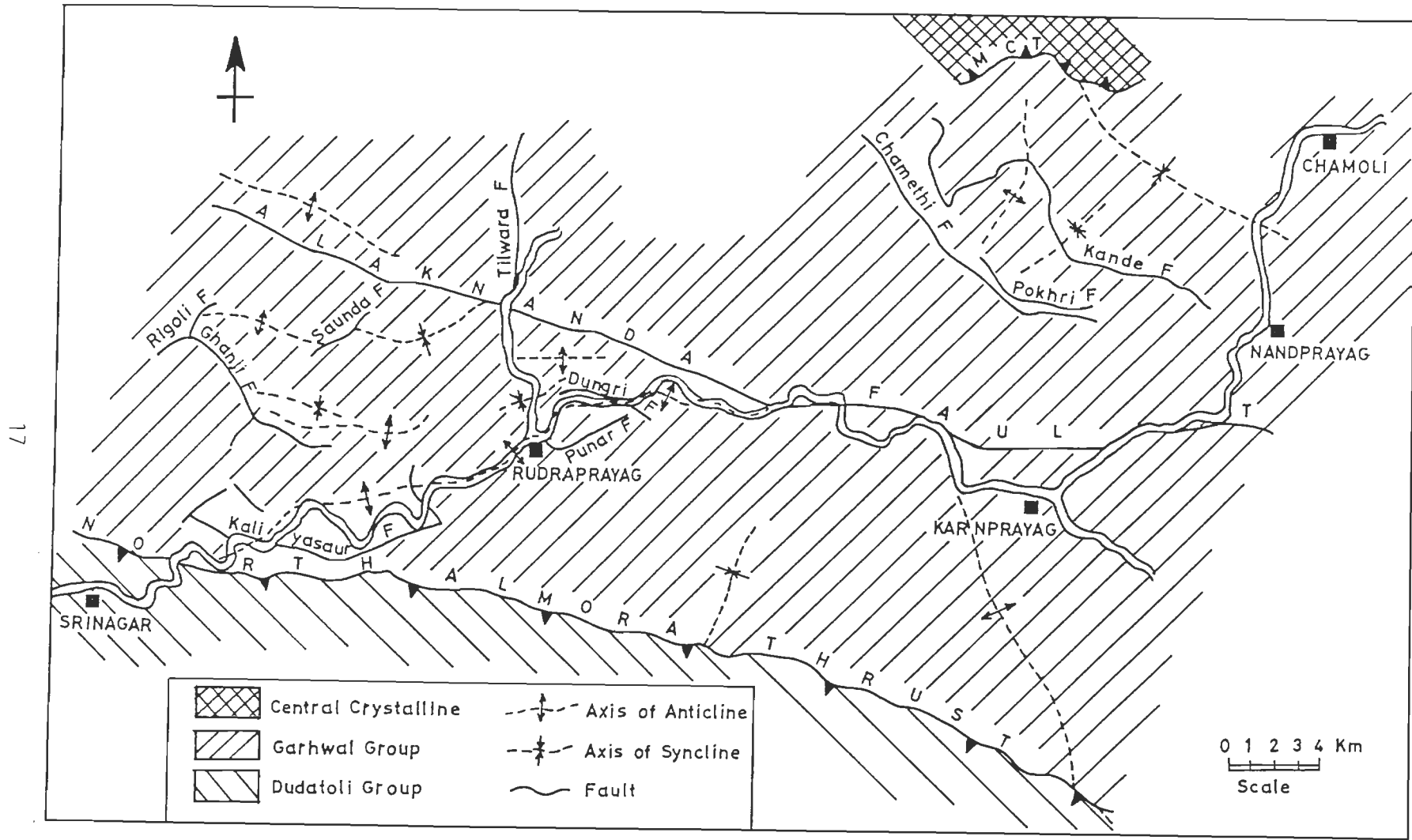


Figure 2.2 Tectonic map of Srinagar-Nandprayag area (Kumar and Agarwal, 1975)

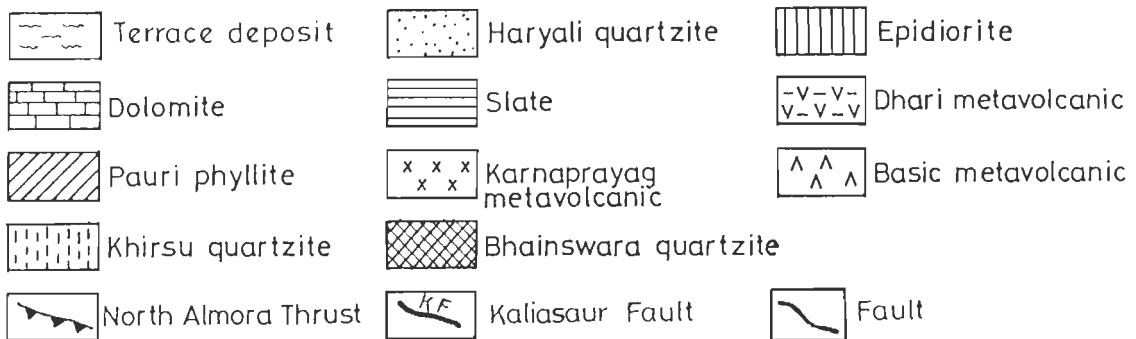
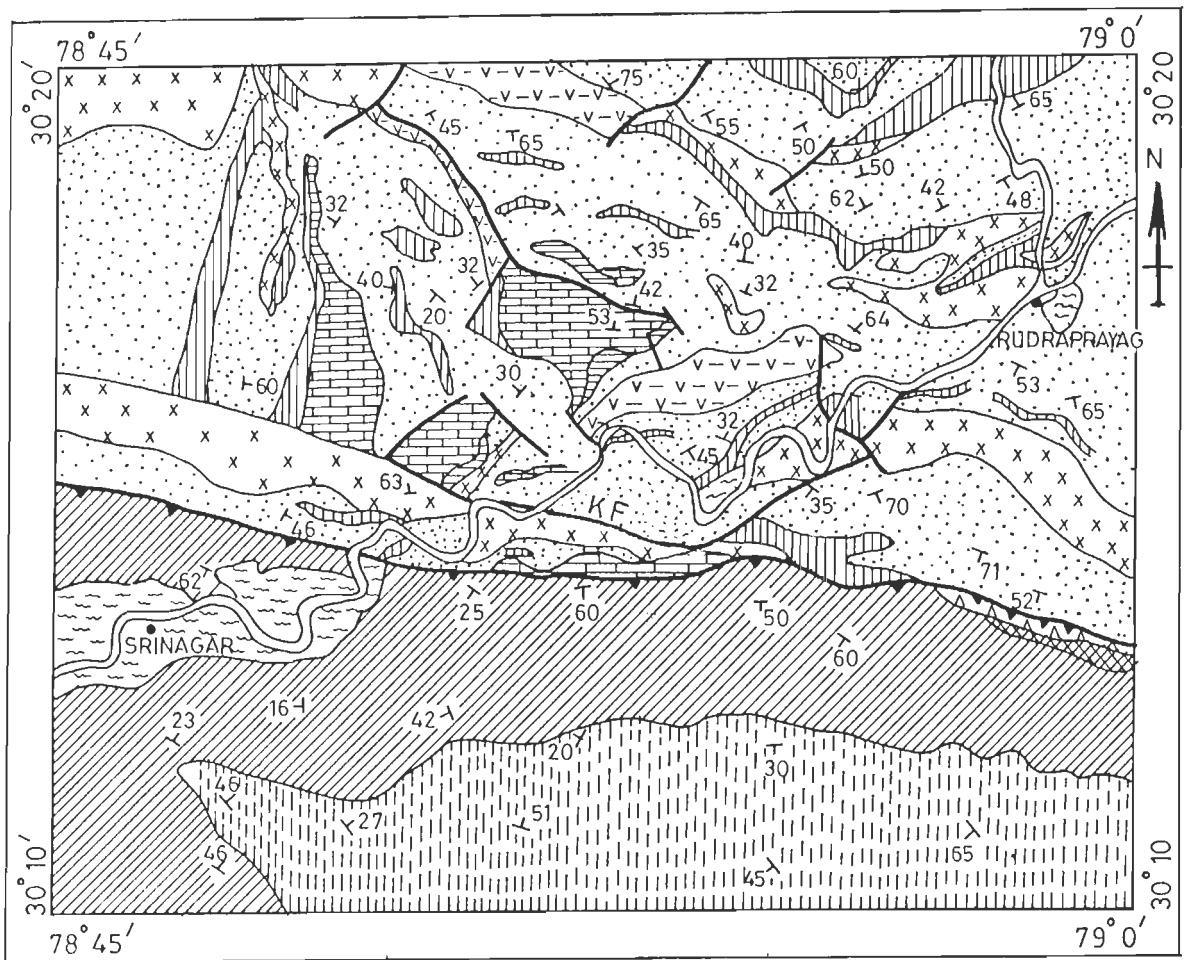


Figure 2.3 Geological map of Srinagar-Rudraprayag area (modified after Kumar and Agarwal, 1975)

rocks separated by the North Almora Thrust. The lithological succession of these two Groups in this area is given in the Table 2.1.

Table 2.1 Lithological succession in Srinagar-Rudraprayag area

Group	Formation	Member
Garhwal Group	Chamoli	Karnaprayag metavolcanic
	Formation	Haryali quartzite
		Dhari metavolcanic
-----North Almora Thrust-----		
Dudatoli Group	Maithana	Khirsu quartzite
	Formation	
	Pauri	Pauri phyllite
	Formation	Bhainswara quartzite

The members of all these Formations are not exposed in Srinagar-Rudraprayag area. Here a brief description only of the rock types present in the study area is given.

2.2.1 DUDATOLI GROUP

In the study area, the Dudatoli Group consists of Maithana and Pauri Formations lying south of NAT. The characteristics of different members of these Formations are briefly described here.

Bhainswara Quartzite occurs at the base of the Pauri Formation and is present in the study area for a small areal extent near Dongra. Here it is associated with basic metavolcanic, which is basaltic in nature and contains amygdules filled with chalcedony and quartz.

At Koteswar, North Almora Thrust brings the Haryali Quartzite of Chamoli Formation of Garhwal Group in juxtaposition with the Pauri Phyllite of Dudatoli Group. The Pauri phyllite is the eastward continuation of the phyllite exposed around Pauri. In the study area phyllite is grey and some times greenish grey with thinly bedded foliation planes. Fine compositional bandings and crenulation cleavages are characteristics of these rocks. These

phyllites show schistosity planes near Srinagar.

Khirsu Quartzite is found to the south of Pauri Phyllite around Khirsu and it forms the southern boundary of the study area. It is made up of fine grained quartz with sericite and chlorite sometimes making schistosity parallel to bedding.

2.2.2 GARHWAL GROUP

The Garhwal Group of rocks are well exposed in the Alaknanda valley. However, only few members of Chamoli Formation of the Group are present in the study area.

Dhari Metavolcanic is considered to be the oldest basic flow in the Chamoli Formation. It is named after the village Dhari where it is well exposed. The metavolcanic is composed of basic flows, some times associated with slates and minor quartzites. It is green coloured, vesicular and amygdoloidal in nature.

Haryali Quartzite is well developed in the study area and is named after the Haryali peak. It is white, purple or maroon coloured quartzite, thickly bedded and fine to coarse grained, occasionally gritty in nature. The gritty varieties have well rounded pebbles. In the study area, at some places, particularly near NAT, these quartzites are found associated with brown coloured shale. At some locations, the quartzite shows alternate dark and light colour banding. The dark bands are due to the presence of ferruginous and heavy minerals. At few locations, dolomite occurs in the basal part of Haryali Quartzite and is often associated with slates. Dolomite is siliceous in nature and grey in colour. Exposures of this dolomite is seen near east of Koteswar along NAT, around Sera and north east of Kauliyadhar.

Karnprayag Metavolcanic is a basic flow occurring within the Haryali quartzite and is named after Karnprayag where it is well developed. In Srinagar-Rudraprayag area, exposures of this volcanic can be seen in the western part which continues to Alaknanda river where it is cut off by the Kaliyasaur fault. Again it is exposed at Dungripanth, near Khankra and at Narkota. This volcanic is schistose in nature but at some places looks like a massive body and it is difficult to distinguish it from other volcanics. The metavolcanic at many places are altered and weathered to green coloured chlorite schist. At some locations it shows one or two sets of joint with irregular cracks.

Epidiorite in the study area is intrusive body in Chamoli Formation, in the form sills and dykes. In the study area, these intrusive bodies are scattered mostly in the form of

elongated bodies. Basically it is doleritic in composition and was subsequently metamorphosed and termed by different workers as epidiorite, metadolerite and amphibolite. In the present study, it is termed as epidiorite. This epidiorite is greenish grey coloured, fine to medium grained, weakly foliated in nature and is composed of green hornblende and feldspars.

2.3 STRUCTURES AND TECTONICS

The Garhwal Group of rocks has been sandwiched between the North Almora Thrust and the Alaknanda Fault. The major structural feature of the study area is represented by the NAT. In addition, there are several major and minor faults in the area.

The NAT, as already stated, separates the Pauri and Khirsu Formations of the Dudatoli Group from the Garhwal Group of rocks. It has been traced to the Bhagirathi and Yamuna valleys (Jain, 1971; Agarwal and Kumar, 1973) in the north west and to the Kali river (Mehdi et al., 1972) in the south east. The NAT is termed as Srinagar Thrust (Mehta, 1971) and Srinagar Shear (Bhargava, 1972) in Alaknanda valley and Dharasu Thrust in the Bhagirathi valley (Jain, 1972). This thrust is trending WNW-ESE and dipping southerly at high angle. According to Srivastava and Ahmad (1979) the North Almora Thrust in the study area hades northwards, but else where it dips southwards also. Thus, it is a sub-vertical zone of dislocation. As a result, it swings sometimes towards north and sometimes towards south. However, the southern side is down throw side of this thrust. In the study area the thrust cross cuts the Alaknanda valley at Koteswar and is characterised by wide shear zone. Fragments and pulverised materials of quartzites and phyllites, more like schists, have been seen along this thrust zone. The evidences of thrusting were found to the westward of Koteswar across the river, as reported by Doval and Sakalani (1980).

There are few other important faults present in the area. One of these is the Kaliasaur fault striking NW-SE in the eastern part but swinging NE-SW in the western part. In the area, this fault is offsetting the Karnprayag Metavolcanic and has been offset by the Narkota fault trending NW-SE at Narkota. The another major fault is the Ghanji fault trending NNW-NSE near Sera.

There are several anticlinal and synclinal structures in the area. The major anticline is the Rudrapryag anticline whose axis trends ENE-WSW. It is delimited by the NAT in the west and the Alaknanda fault in the east. It is a doubly plunging fold due to which the Dhari

Metavolcanic close on both sides (Kumar and Agarwal, 1975). Another anticline of doubly plunging nature is the Syari Anticline, the core of which is composed of slate and dolomite. The Syari anticline and the Satni syncline are truncated against the Ghanji fault.

2.4 SUMMARY

The rocks in the area of study belong to Garhwal Group and Dudatoli Group separated by the North Almora Thrust trending WNW-ESE and is, in general, a sub-vertical zone of dislocation. Main rock types belonging to the different members of the Garhwal and Dudatoli Groups are quartzite, phyllite, metavolcanic, dolomite and epidiorite. The major portion of the area is occupied by quartzites (Haryali Quartzite and Khirsu Quartzite) followed by phyllite. There are also river terrace deposits along the Alaknanda river, particularly in Srinagar. In addition to NAT, there is another major fault named Kaliasaur fault present in the area. Among several anticlines and synclines, the Rudraprayag anticline is the major one which almost follows the bed of Alaknanda river in the central portion of the study area.

LANDSLIDES AND TERRAIN FACTORS

Landslides are the natural processes, which occur and recur in specific geoenvironmental conditions. The term "landslide" is, in general, used to describe a wide variety of downward and outward slope mass movements, under gravitational influence, due to shear failure at the boundaries of moving mass of soil, rock and vegetation. The slope instability is a condition which gives rise to slope mass movements in the form of landslides. Although there are many components of the slope system which can change unilaterally to destabilise the slope, yet the significance of any change depends upon the aggregated effect of other components. Since the slopes are, for most of the time, stable or at least marginally stable, an actual landslide represents a transient condition infrequently attained by the slope. In a hill slope, some forces assist the movements, while some others resist. The stable slopes have a margin of stability, proportional to the excess of resistance over the sliding forces. On the other hand, the slopes at the point of movement have no such margin and the resisting and sliding forces, in these cases, are approximately equal.

Crozier (1986) grouped the destabilising factors into three categories. The **Preparatory factors** make the slope susceptible to movement without actually initiating it and thus pushing the slope into a marginally stable state. The **Triggering factors** set off the movement by shifting the slope from a marginally stable to an actively unstable state. The **Controlling factors** dictate the condition of movement, its form, rate and duration. A particular factor may take on any or all of these roles, depending upon its degree of activity and on the margin of stability within the slope. For example, the preparatory or passive factors, such as the weaknesses in composition or in structure of the rock or soil, progressively change, over a long period of time, to reduce the resistance/shear stress ratio. These are, however, incapable to

trigger movement which, in turn, can be initiated by the triggering factors like heavy rain, seismic activity, anthropogenic activity.

Among the various governing factors for slope instability, the few important ones are selected in the present study and the maps showing their variation in the study area are prepared together with the landslide map of the area. All the maps are prepared on 1:50000 scale using the pertinent data from aerial photos, topographic maps and field investigations. In the present chapter, the spatial distributions of the landslides and of the factors are studied in detail, with a view to determine the proneness of the factors to landslide occurrence and to establish the relationships between landslides and these factors.

3.1 LANDSLIDE STUDY

Several workers have described and classified different types of landslide and mass-movement. The important among these are Sharpe (1938), Ward (1945), Campbell (1951), Varnes (1958), Yatsu (1966), Hutchinson (1968), Zaruba and Mencl (1969), Crozier (1973), Hutchinson (1977) and Varnes (1978). The most generalised classification has been given by Hutchinson (1977) and Varnes (1978). Both these authors used the type of movement to establish the principal groups but they differ in sub-classification. The secondary grouping in Hutchinson's classification is based on the additional criteria like the depth, direction and sequence of movement with respect to the initial failure. On the other hand, in Varnes classification, the subgroups are based on the nature of source material (bed rock, debris and earth). In the present study, the term landslide is used in its generality, incorporating various types of slope mass movement.

3.1.1 TYPES OF LANDSLIDES IN THE STUDY AREA

The most common types of landslide observed in the study area are described below.

Rock slide refers to the movement of rocks along a distinct surface of rupture which separates the slide material from the more stable underlying materials. It consists predominantly of rock fragments of varying sizes as well as of blocks with associated soils. Rock slide occurs mainly due to planar and wedge failures.

Planar failure occurs along a discontinuity surface such as bedding or joint plane

dipping outward with respect to the slope. For planar failure the following geometrical conditions must be satisfied (Hoek and Bray, 1981).

- The plane on which sliding occurs must strike parallel or near parallel to the slope face.
- The failure plane must daylight on the slope face, i.e., its dip must be smaller than the dip of the slope face.
- The dip of the failure plane must be greater than the angle of friction of this plane.
- Release surfaces must be present in the rock mass to define the lateral boundaries of the slide.

This type of failure is very common in the study area and the failures are observed on prominent discontinuity surface. A typical rock slide due to planar failure in quartzite is seen near Khankra along Khankra-Kherakhal road (Plate 3.1). Another planar failure in phyllite is found near the village Gawana (Plate 3.2).

Wedge failure occurs when two discontinuities strike obliquely across the slope face and their line of intersection daylights on the slope face. The wedge of the rock resting on these discontinuities will slide down along the line of intersection, if the inclination of the line of intersection is significantly greater than the angle of friction. Such failures are also observed at many locations particularly in highly jointed quartzites and metavolcanics. An example of wedge failure is observed at 5.5 km upstream of Dhari along Srinagar-Rudraprayag road (Plate 3.3).

Toppling failure occurs in competent rock containing well defined bedding planes or joints dipping into the slope. This structure forms tall thin slabs and when the slope is excavated the slabs topple down because the line of action of centre of gravity lies outside the base. Toppling failure is less common in the study area.

Rotational slide is one in which the surface of rupture is curved concavely upward and the slide movement is rotational about an axis, parallel to the slope. These usually occur in soil or homogenous debris materials derived from deep weathering of parent rock. Some times it also occurs in highly crushed and fragmented rocks. Such slides are characterised by the backward tilting of head portion of the slided mass and by the presence of steep scarps and transverse cracks near the crown. The magnitude of rotational slide depends upon the depth of slip surface. Few slides of this nature are observed in the highly weathered phyllites near village Nawasu.

Debris Slide mainly consists of rock fragments with loose weathered material in which

some planar discontinuity surface may occur as remnant of the parent bed rock. The severity of sliding depends on the quantity of debris on the slope. This is the most common type of slide found in the area. Several debris slides are observed in the area. The evidence of a severe debris slide along a drain is found 4 km upstream of Dhari, damaging the road (Plate 3.4). The debris slide during heavy rains along the intersection of two discontinuity planes forming a wedge along the drain. There is another debris slide of small magnitude along near village Chamdhar (Plate 3.5).

Debris flow is a form of rapid mass movements in which water saturated debris or earth material flows downslope, restricted to a limited surface area, sometimes in the form of channels. A debris flow occurred recently near village Sakarta. due to a new road construction on the slope (Plate 3.6).

Falls are abrupt free fall of rock and earth materials that become detached from steep slopes or cliffs. Movement occurs by free fall, bouncing and rolling. Depending on the type of materials involved, the result is rock fall or debris fall. In the study area, rock falls are generally observed in quartzites and dolomites. The rock fall in quartzite is seen along Kirtinagar-Silkakhal road near village Kandi (Plate 3.7).

Complex slide is the combination of different type of movements. In real field condition, it is a very common type, such as planar slide with debris slide or rock slide involving planar and wedge failures. For this type of cases, the dominant mode of movement should be considered. A typical example of complex slide is Kaliasaur slide located 3 km upstream of Dhari along Srinagar-Rudraprayag road (Plate 3.8). The landslide shows debris slide along with the failure of small rock wedges. It also shows evidences of a deep seated rotational failure.

3.1.2 LANDSLIDE IDENTIFICATION AND MAPPING

The landslide slopes in the study area are identified from aerial photo interpretation. Several of these are confirmed during the field checks. Landslide detection on aerial photographs is based on the photo recognition elements such as tone, texture, pattern, shape, association and other physical features of the terrain. Although a landslide can be identified from an aerial photograph, yet it is difficult to decipher its detailed features.

Rib and Liang (1978) have listed the following features as discernible on aerial



Plate 3.1 Planar failure in quartzite



Plate 3.2 Planar failure in phyllite



Plate 3.3 Wedge failure in metavolcanic



Plate 3.4 Debris slide along a drain



Plate 3.5 Debris slide in metavolcanic



Plate 3.6 Debris flow due to recent road construction



Plate 3.7 Rock fall in quartzites



Plate 3.8 Panoramic view of Kaliasaur slide

photographs and helpful in identifying landslides.

- (a) Land masses undercut by stream
- (b) Steep slopes having large masses of loose soil and rock
- (c) Sharp line of break at the scarp or presence of tension crack or both
- (d) Hummocky surface of the sliding mass below the scarp
- (e) Unnatural topography, such as spoon trough in the terrain
- (f) Seepage zones
- (g) Elongated undrained depressions in the area
- (h) Accumulation of debris in drainage channels or valleys
- (i) Appearance of light tones where vegetation and drainage have not been reestablished
- (j) Distinctive change in vegetation indicative of changes in moisture
- (k) Inclined trees and displaced fences or walls due to creep.

However, not all these features are necessarily present in any individual slide.

The landslide map of the terrain is prepared in three steps. Firstly, the uncontrolled mosaics of the aerial photographs are prepared to obtain a synoptic view of the area. Secondly, a detailed stereoscopic study, using Zoom-Stereosketch is carried out. Finally, the informations from photo interpretation are transferred onto the topographic maps with the help of ground controlled points. The landslide map (Fig. 3.1) shows spatial distribution of all the existing landslides of the area. Few landslides which are not very clear in aerial photographs have been marked in the map after field investigations.

Overall 139 landslides are identified in the terrain and marked in the landslide map. The average density of landslide, i.e., the number of landslides per square kilometer, in the area is found to be 0.313. The map reveals higher concentration of landslides to the south of Alaknanda than to the north of it. It is particularly higher in the region between the two major streams, namely Dewalgarh and Bachchan flowing from south to north.

The most important and well known landslide in the study area is the Kaliasaur slide located on the left bank of river Alaknanda about 3 km upstream of Dhari. It has damaged the road for a 100 m stretch. The nature of this slide is of complex type, the predominant mode being the debris flow from the weathered and crushed rocks. The joint analysis shows several local wedge failures along two discontinuity planes. The presence of a large crack behind the

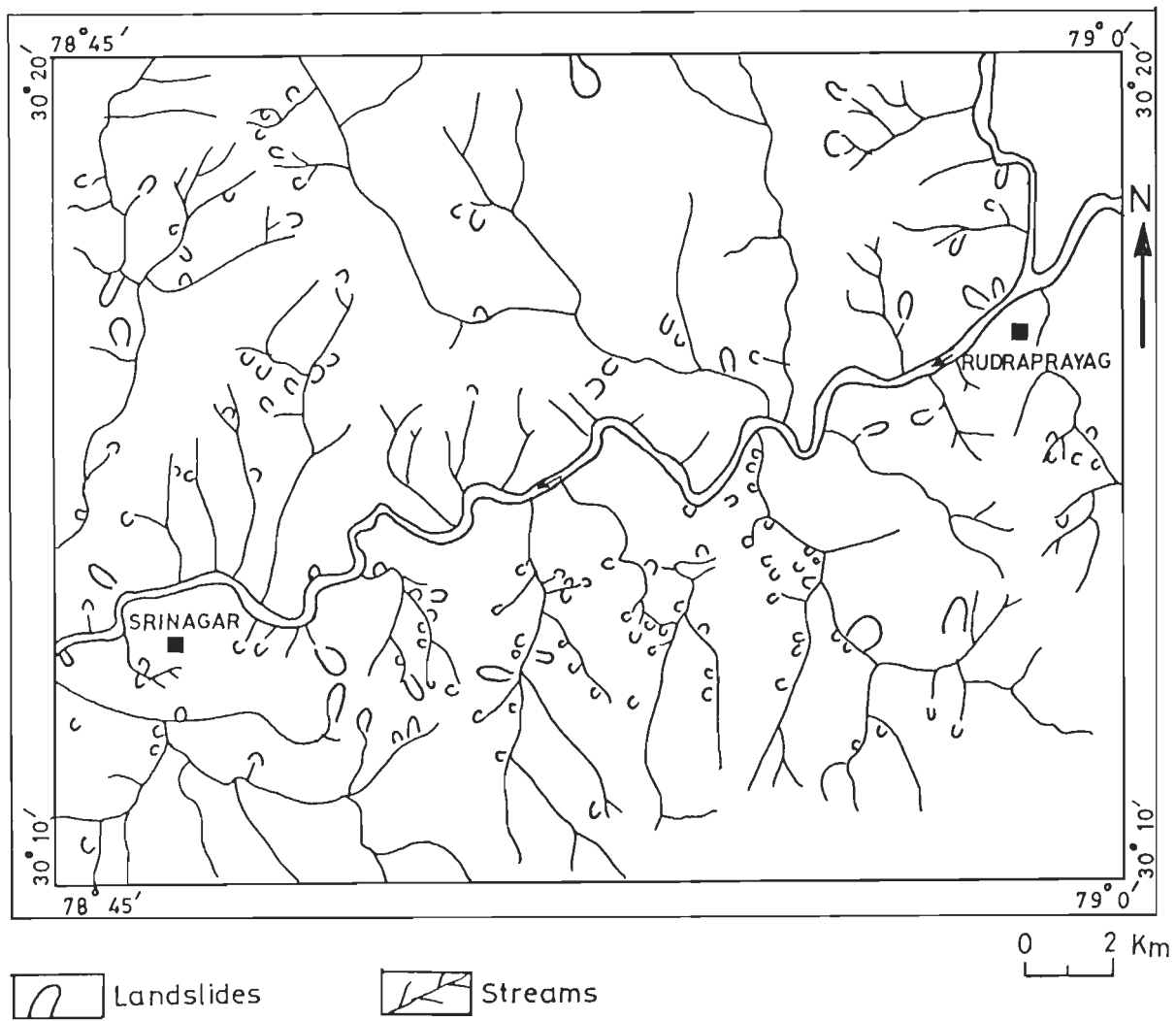


Figure 3.1 Landslide map of the study area

crown and heave at the toe indicate a deep seated rotational failure. The rocks exposed in the area are quartzites with thin beds of shales. The quartzites are highly fractured and jointed as well as pulverised, particularly in the central part. This condition of rocks could possibly have been due to the presence of Kaliasaur fault which is passing just behind the crown of the slide. In addition, the Alaknanda river takes a sharp turn, right at the toe of the slide, causing continuous toe erosion which is a major contributing factor for the slope instability.

3.2 TERRAIN FACTORS

Landslide can be triggered by both natural and man induced changes in the environment. Numerous factors control the stability of the slope. The major governing factors are lithology, geological structure, slope characteristics, topographic relief, drainage characteristics, landuse, anthropogenic activity, seismicity and climatic conditions. The adverse nature of any of these factors affects the existing equilibrium of stability. Of these factors, the anthropogenic factor, seismicity and climate, particularly rainfall, come under the class of triggering factors, while the remaining factors are essentially the preparatory factors. The triggering factors are difficult to gauge, because their magnitude as well as their temporal behaviour is unpredictable. Further, reliable data are not available all the time. On the contrary, the preparatory factors can be judiciously studied and the pertinent data can be collected from the existing field conditions. These factors, termed here as terrain factors, represent the inherent terrain characteristics. Carrara et al. (1992), while discussing the uncertainty in assessing landslide hazard, presented a list of the main contributing factors along with the uncertainty associated with their data collection (Table 3.1). It is evident from the table that the factors rock type, surface water condition, slope geometry and landuse, which are considered as the preparatory factors in the present study, possess less degree of uncertainty. The other factors showing intermediate or high uncertainty are the triggering factors, except the rock structure, the slope geomorphic processes and the geodynamic setting.

The six terrain factors selected in the present study are lithology, distance from the major thrust (North Almora Thrust), slope, relative relief, drainage density and landuse. It may be mentioned here that the uncertainties in procurement of these factor data are reasonably low. A detailed study of these factors is necessary to know the inherent condition of the study terrain. Lithology and major thrust of the area have already been described in chapter 2. The

other terrain factors are described below.

Table 3.1 Main factors controlling instability and degree of uncertainty (Carrara et al., 1992)

Factor	Uncertainty
Geodynamic setting	High
Rock composition	Low
Rock structure	Intermediate
Ground water conditions	High
Surface water conditions	Low
Slope geometry and angle	Low
Slope geomorphic processes	Intermediate/high
Landuse	Low
Human activity	Intermediate
Present climatic conditions	Intermediate
Past climatic conditions	Intermediate/high

3.2.1 SLOPE

The slope of a region can be defined as its upward or downward inclination to horizontal. Its variation in different parts of an area indicates the spatial distribution of the slope gradients. The distribution of slope categories depends on the geomorphological history and the geological set up of the area. The steep slopes, in general, develop in hard, compact and resistant rocks, while the gentle slopes develop in soft and less resistant rocks. The spatial distribution of various slopes and of ridges is studied.

The distribution of slope gradients in the area is inferred from the slope map, prepared from topographic maps. Initially, the area has been divided into a number of facets possessing more or less uniform slope direction with the natural topographic boundaries in the form of streams and ridges. These facets are further divided into different slope categories on the basis of number of contours and their spacings. For this, number of contour lines per cm of

horizontal distance is counted on the topographical map. The slopes are grouped into five categories representing escarpment ($>45^\circ$), steep slope ($35^\circ-45^\circ$), moderately steep slope ($25^\circ-35^\circ$), gentle slope ($15^\circ-25^\circ$) and very gentle slope ($<15^\circ$).

On the 1:50000 topographical map, the number of contour lines per cm with 20 m contour interval, for the different slope categories are as follows:

Slope categories	Number of contour lines
$>45^\circ$	>25
$35^\circ - 45^\circ$	19 - 25
$25^\circ - 35^\circ$	13 - 18
$15^\circ - 25^\circ$	8 - 12
$<15^\circ$	<7

The resulting slope map, shown in Fig. 3.2, reveals that very gentle slope ($<15^\circ$) exists mostly on the terrace deposits along Alaknanda river, while the moderately steep slope of $25^\circ-35^\circ$ is uniformly distributed in the area in association with the slope category of $15^\circ-25^\circ$. Broad zones of steep slopes of $35^\circ-45^\circ$ with small patches of very steep slopes ($>45^\circ$), are present primarily in the south eastern and north western parts of the area. These are also present as small area in other parts of the map. The area is maximum for the slope category $25^\circ-35^\circ$, followed by the categories $35^\circ-45^\circ$, $15^\circ-25^\circ$, $<15^\circ$ and $>45^\circ$. The area covered by the slope category of $25^\circ-35^\circ$ constitutes 50% of the total area.

3.2.2 RELATIVE RELIEF

Relative relief, the local height of a region, can be defined as the difference in height between the highest and the lowest points in a unit area. The low values of relative relief indicate that the area has undergone very little differential erosion and vice versa.

A relative relief map of the study area is prepared with the help of the topographic map. The data of difference between the highest and the lowest contours are collected for individual cells of 1 cm^2 size on the map. The contours of these values are drawn at 200, 300, 400 and 500 m to prepare the map with five classes of relief, i.e., <200 , 200-300, 300-400, 400-500 and >500 m. The map is shown in Fig. 3.3. From this map it is evident that the lowest

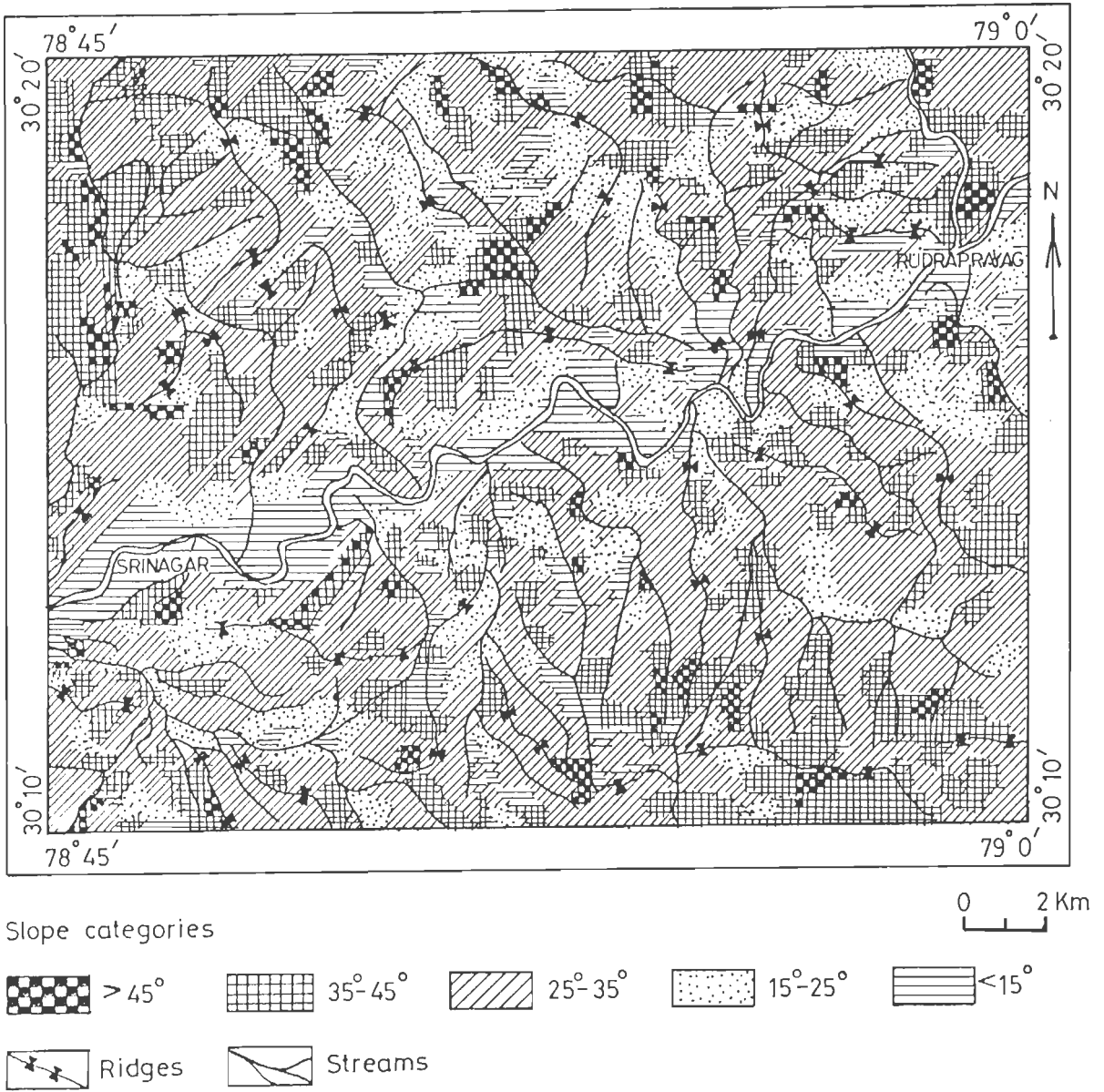
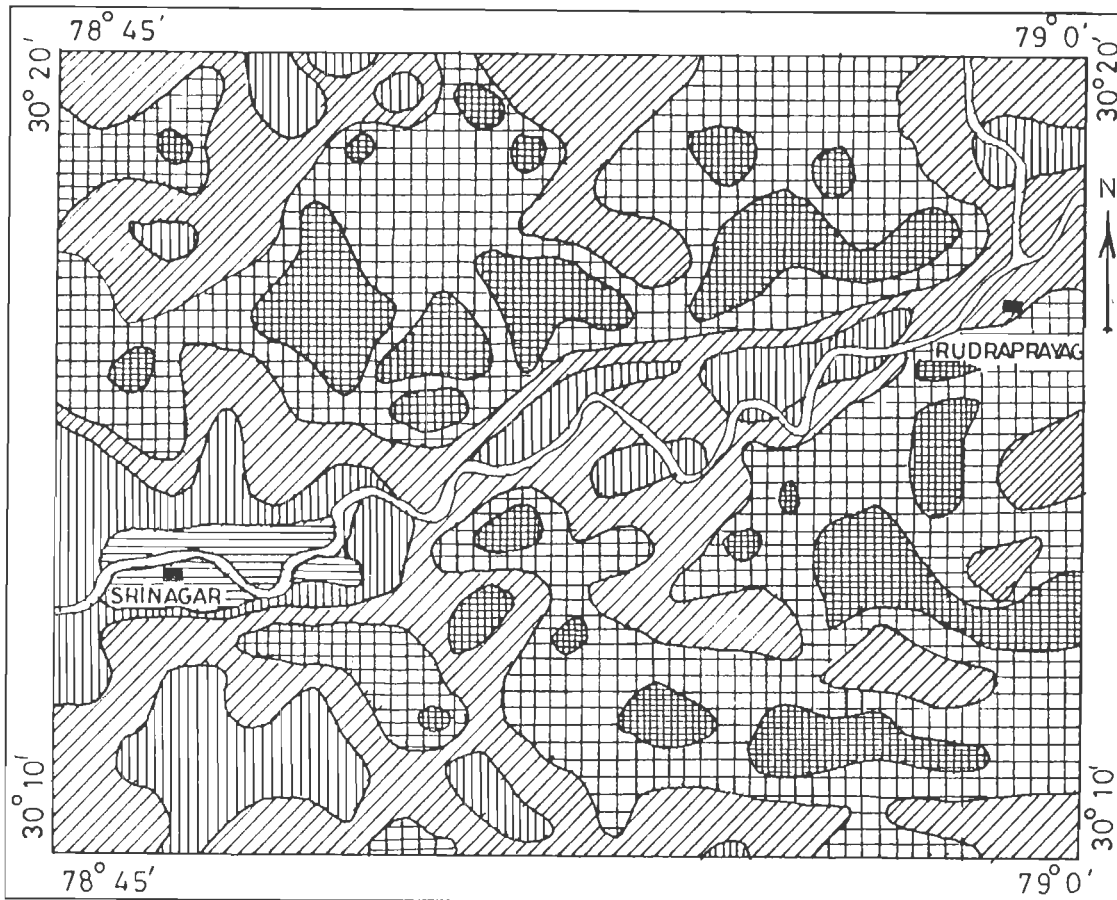


Figure 3.2 Slope map of the study area



Relative relief categories

0 2
Km



Figure 3.3 Relative relief map of the study area

relief of <200 m is present only in a small area around Srinagar town while the highest relief of >500 m exists in the south eastern part of the area and to the north of Alaknanda river. The area of each category of relief is calculated. It shows that the prominent ranges are 300-400m and 400-500m relief categories.

3.2.3 DRAINAGE DENSITY

Drainage represents the water courses of rivers and streams in the area. Alaknanda river represents the major basin in the area, in which there are several sub-basins of different orders. It has been observed in the field that most of the first order streams are the newly emergent streams at higher slopes and these gradually come down to join the higher order ones at lower slopes. A drainage map of the area is prepared on 1:50000 scale with the help of topographic maps and aerial photographs. All the streams starting from 1st order to higher orders are mapped. The major river Alaknanda and the major streams of higher order, like Dhundsir, Badiyar, Bhardari, Khanda, Dewalgarh, Gostu, Bachhan, are all perennial in nature, while most of the 1st and 2nd order streams are seasonal in nature. From the map it can be seen that drainage pattern of the study area is mostly dendritic to sub-dendritic. At some parts, however, trellis pattern is present.

The drainage map, shown in Fig. 3.4, depicts the boundaries of sub-basins. The major sub-basins of the area are, in general, 4th and 5th order. However, few small basins of 2nd order are also present. Altogether there are 34 sub-basins marked in the map. Only parts of the sub-basins numbered 32, 33, and 34 are falling in the area of study. At few places along Alaknanda, there exist small streams of 1st order having very small basin area. These streams are clubbed together to form a single sub-basin.

There are several drainage basin parameters, however, only drainage density is considered in the present study. Drainage density, defined as the ratio of the total length of streams to the area of basin, is an important parameter of a drainage basin. Lower drainage density means less surface runoff in the basin and more seepage. To obtain drainage density of each sub-basin, the length of all the streams are measured with the help of a rotometer and the cumulative length of streams in each sub-basin is calculated. Similarly, the area of all the 34 sub-basins are measured using a digital planimeter. Drainage density values of all the 34 sub-basins are computed (Table 3.2). It is observed that the drainage density values range from

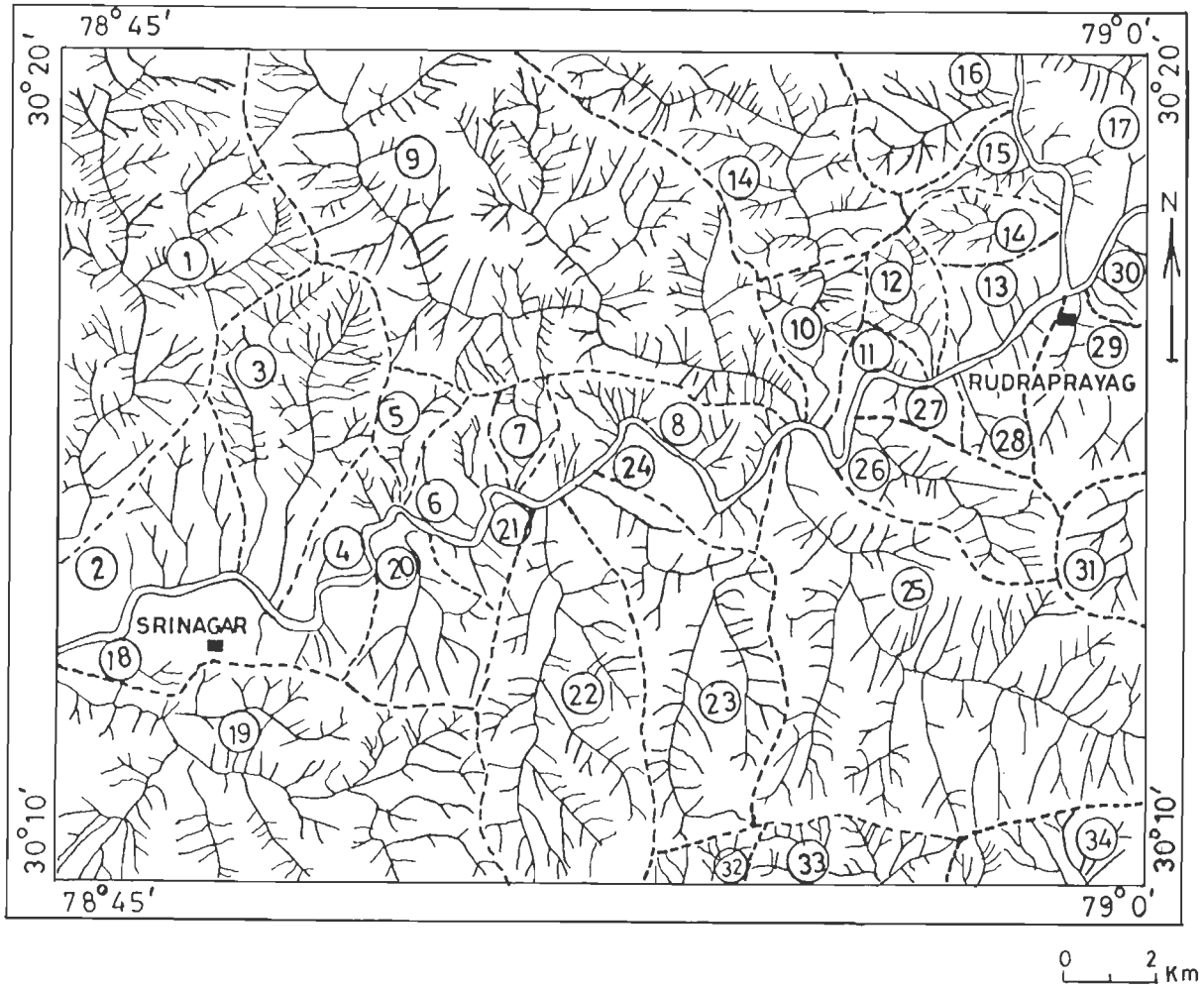


Figure 3.4 Drainage map showing sub-basins of the study area

Table 3.2 Drainage density of sub-basins

Basin No.	Area (sq.km)	Length (km)	Drainage density	Class
1	40.74	127.36	3.13	high
2	18.90	63.30	3.35	high
3	62.58	184.35	2.94	moderate
4	28.38	87.30	3.08	high
5	43.02	115.75	2.69	moderate
6	26.76	63.30	2.36	moderate
7	22.89	52.35	2.28	moderate
8	53.32	133.80	2.51	moderate
9	10.40	24.80	2.38	moderate
10	10.08	24.10	2.39	moderate
11	5.07	13.50	2.66	moderate
12	3.94	15.10	3.83	high
13	4.02	12.30	3.06	high
14	2.57	8.45	3.29	high
15	2.96	9.00	3.04	high
16	7.10	23.00	3.24	high
17	11.21	16.00	1.43	low

Contd...

Basin No.	Area (sq.km)	Length (km)	Drainage density	Class
18	4.00	7.00	1.75	low
19	4.44	11.00	2.47	moderate
20	8.40	25.00	2.98	moderate
21	2.11	5.00	2.37	moderate
22	4.20	7.00	1.67	low
23	3.30	10.00	3.03	high
24	9.30	18.00	1.93	low
25	10.00	13.00	1.30	low
26	9.32	19.00	2.04	moderate
27	2.80	6.00	2.14	moderate
28	4.30	4.00	0.93	low
29	2.30	4.00	1.74	low
30	2.30	5.00	2.17	moderate
31	2.20	4.50	2.04	moderate
32	2.10	9.00	4.28	high
33	5.40	20.00	3.70	high
34	6.60	19.00	2.88	moderate

1.3 to 4.28 km/km². The obtained values of drainage density are classified into three categories, i.e., low (<2 km/km²), medium (2-3 km/km²) and high (>3 km/km²). Maximum area has been found to possess moderate drainage density values.

3.2.4 LANDUSE

Landuse study deals with the pattern of landuse such as forest land, agricultural fields, urban land, water reservoir, roads, waste disposal etc. Landuse pattern in hill areas has been changing fast due to the expanding industrialization, mining activities and urbanization. The developmental activities in hilly terrains have a great impact on the natural eco-system due to the resulting deforestation, road construction and urbanization. Since the present study pertains to landslides, the most relevant landuse pattern is the vegetation cover.

The terrain is classified, depending upon the density of vegetation, broadly into three categories of landuse; forest land, agricultural land and barren land. Since density of vegetation under forest differs from place to place, the forest is further subdivided into thick forest, moderate forest and sparse forest. So, finally landuse study is carried out for spatial distribution of five categories, i.e., thick forest, moderate forest, sparse forest, agricultural land and barren land.

The landuse map of the study area is prepared from the aerial photographs of 1:25000 scale. Aerial photos provide a synoptic view of the area, where it becomes easier to recognise the categories of landuse. The different landuse categories, identified on the basis of photo-recognition elements are given in Table 3.3. The classification of forest cover into thick, moderate and sparse has been done qualitatively on the basis of approximate difference in tree densities.

The landuse map (Fig. 3.5) shows the geographical distribution of vegetation cover in the area of study. It is evident that most of the agricultural lands are located in valleys and at gentle slopes. The thick forests, in general, are developed on steeper slopes and the barren lands in most of the cases occupy the moderately steep slopes. The area of each category is calculated and it is found that maximum area is covered by the thick forest. The moderate forest, the sparse forest and the agricultural land cover almost equal areas.

Table 3.3 Photo recognition elements for landuse classification (Joshi,1987)

Landuse category	Tone	Texture	Pattern	Remarks
Thick forest	dark grey	fine	no definite pattern, irregular & sharp boundaries	dark tone due to thick tree density
Moderate forest	grey & white mix	coarse	no definite pattern, irregular boundaries sometimes sharp	light tone due to exposed land surface
Sparse forest	light grey to very light	coarse	scattered, no definite pattern	coarse texture due to scattered trees & shrubs
Agriculture land	light grey/white	fine	terraced fields with sharp boundaries	terraces & thin linear strips in the form of steps, grey tone when crop present, white tone when no crop
Barren land	white (bright)	fine	scattered, no definite pattern	white tone due to exposed rock surfaces or dry soil cover on surface

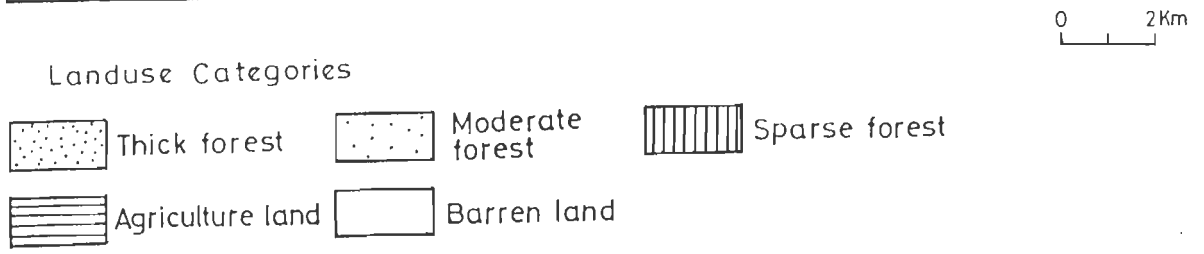
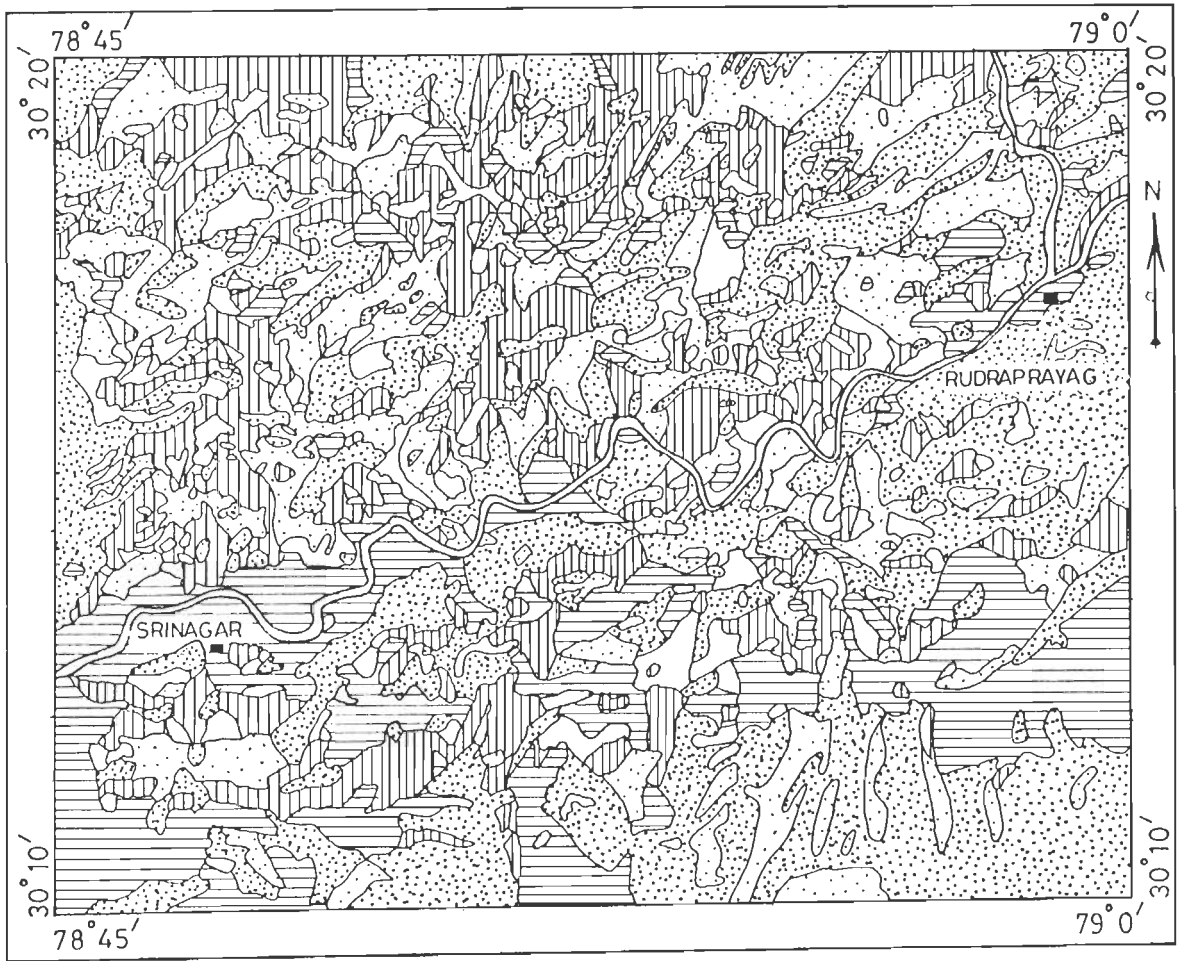


Figure 3.5 Landuse map of the study area

3.3 RELATIONSHIPS OF LANDSLIDES WITH TERRAIN FACTORS

A study has been performed to establish relationships between landslide occurrence in the area and its terrain factors. This study helps us in understanding how much the different factor categories influence landslide occurrence. For each factor category, the ratio of %landslides to %area, termed as relative density of landslide is calculated. This exercise is carried out by superimposing the landslide map on each factor map one by one and then counting the number of landslides in each category of the factor. Further, the density of landslides (DLS) is obtained by multiplying the relative density of landslide with the average density of landslide (0.313). The trends of DLS for the categories of different factors reveal the relationships.

3.3.1 LANDSLIDES IN RELATION TO LITHOLOGY

The rocks in the study area, as discussed in chapter 2, belong to six major lithologic group, i.e., quartzite, phyllite, metavolcanic, epidiorite, dolomite and terrace deposit. The slate, which is present locally is combined with the phyllite as both behave same so far as landslides are concerned. Density of landslides (DLS) in each rock type is calculated and the data is tabulated in Table 3.4 and the corresponding frequency distribution histogram is shown in Fig. 3.6. A trend can not be defined from this frequency histogram, as the rock types are nominal in nature. The data reveal that maximum DLS is in phyllite, followed by epidiorite, terrace deposit, dolomite and metavolcanic. The quartzitic terrain, though it has maximum number of landslides, has least DLS value.

This suggests that the phyllite in study area is more susceptible to landslides than other rocks, particularly the quartzite. This statement is very well justified by the field conditions, since the phyllites are generally weathered and thinly laminated making the slopes unstable, while the quartzites, although jointed and fractured in nature, are generally very strong and are exposed at steep slopes.

3.3.2 LANDSLIDES IN RELATION TO DISTANCE FROM NORTH ALMORA THRUST

Landslide distribution in relation to the major thrust of the area, North Almora Thrust, is studied by dividing the area into five zones with respect to the distance from NAT increasing at an interval of 2.5 km and then determining DLS of each zone. The DLS values for each

Table 3.4 Frequency distribution of landslide in relation to lithology

Lithology	% Area	% Landslide	Relative landslide density	Density of landslide (DLS)
Phyllite	22.67	46.76	2.06	0.64
Quartzite	51.67	24.46	0.47	0.15
Metavolcanic	12.83	12.95	1.01	0.32
Epidiorite	5.91	7.91	1.34	0.42
Dolomite	3.86	4.32	1.12	0.35
Terrace deposit	3.07	3.60	1.17	0.37

Table 3.5 Frequency distribution of landslide in relation to distance from NAT

Distance from NAT (km)	% Area	% Landslide	Relative landslide density	Density of landslide (DLS)
0 - 2.5	28.08	41.01	1.46	0.46
2.5 - 5.0	26.16	38.13	1.46	0.46
5.0 - 7.5	25.71	13.67	0.53	0.17
7.5 - 10.0	15.30	5.76	0.38	0.12
>10.0	4.74	1.44	0.30	0.09

Table 3.6 Frequency distribution of landslide in relation to slope

Slope category	% Area	% Landslide	Relative landslide density	Density of landslide (DLS)
>45°	3.21	1.44	0.45	0.14
35° - 45°	22.16	17.98	0.81	0.25
25° - 35°	53.23	58.27	1.09	0.34
15° - 25°	15.61	20.86	1.34	0.42
<15°	5.79	1.44	0.25	0.08

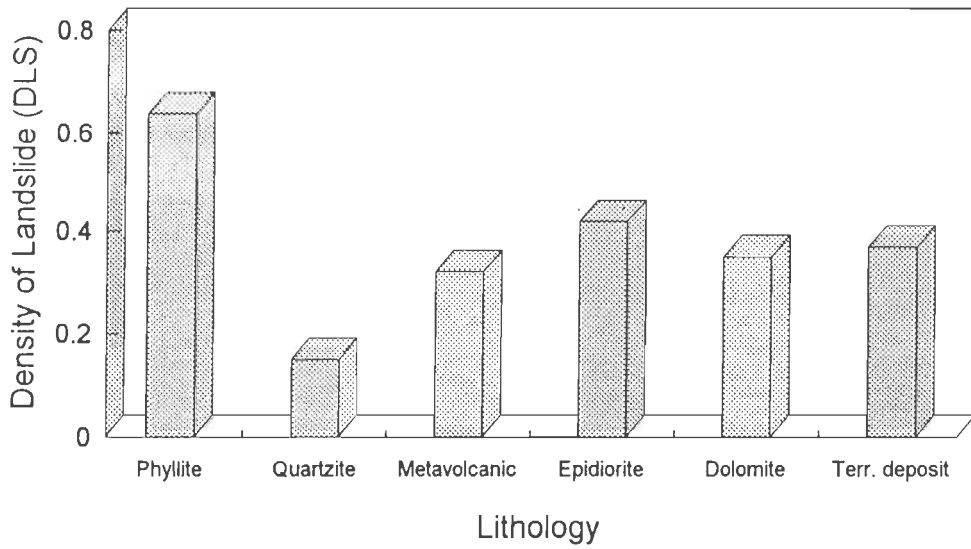


Figure 3.6 Density of landslide vs lithology

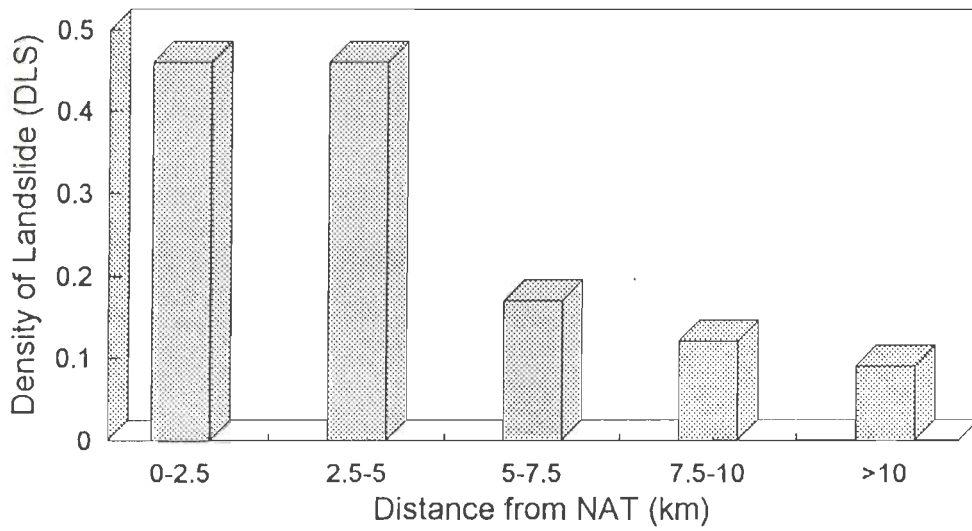


Figure 3.7 Density of landslide vs distance from NAT

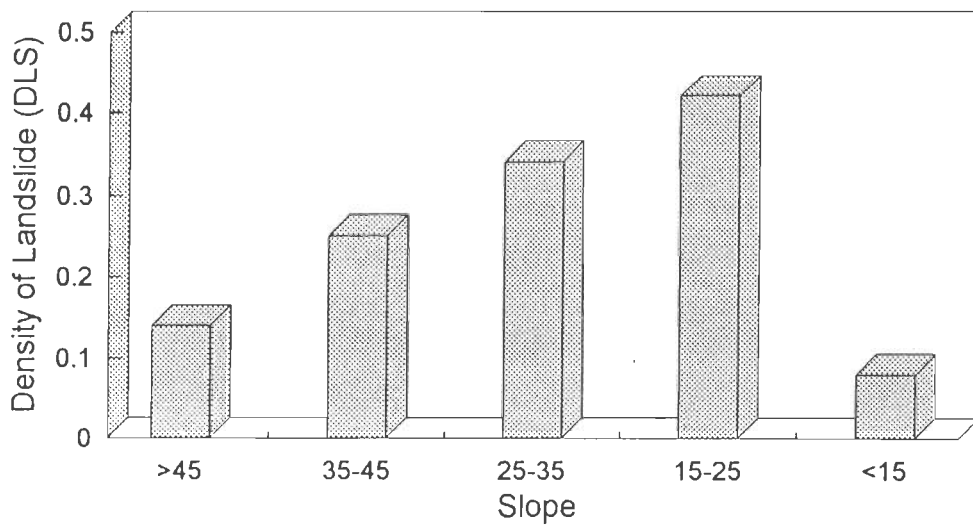


Figure 3.8 Density of landslide vs slope

zone are given in Table 3.5. A histogram showing the frequency distribution is also plotted (Fig. 3.7). The data reveals that DLS values are same for the first two zones, i.e., 0-2.5 km and 2.5-5 km and after 5 km, it decreases drastically (from 0.46 to 0.17) for the next zone, i.e., 5-7.5 km and the landslide density decreases still further as distance from the NAT increases. The frequency histogram is monotonically non-increasing in nature. From these findings it can be concluded that the landslide events are more frequent in the vicinity of a major tectonic zone. This is consistent with the observation that the areas close to the NAT are characterised by intense fracturing, shearing and shattering of the rocks. Similar inferences have been made by Valdiya (1985) and Joshi (1987).

3.3.3 LANDSLIDES IN RELATION TO SLOPE

The DLS values of different slope categories are given in Table 3.6 and the corresponding frequency histogram is shown in Fig. 3.8. A perusal of these data reveals that DLS is maximum in the slope category 15°- 25° and 25°-35°, followed by 35°-45°, >45° and <15°. The frequency histogram is of unimodal nature with a single peak at 15°-25°. Although the area covered by the category 15°-25° is much less, yet it has 20% landslides. As a result of this the DLS is maximum for this category. The DLS of 25°-35° is also high, although the area covered by this category is maximum, about half of the total area of study. So, it can be said that slopes of gentle to moderately steep (15°-35°) categories are more prone to landslides. The occurrence of more landslides in these slopes may be attributed to the presence of phyllites, which are highly susceptible to slope failures, generally having low angle slopes. On the contrary quartzites which are less prone to landslides form steep gradient due to its hard and more resistant nature. So, it can be said that slope gradients and rock types are inter-related as far as landslide events are concerned. This affirms that landslide is a result of complex interaction of multiple factors. Though slope is one of the most important factors for assessing instability of a region, yet, this inter-relation is not simple and some times steepest slopes may not be prone to landsliding (Varnes, 1984).

3.3.4 LANDSLIDES IN RELATION TO RELATIVE RELIEF

The landslides in relation to relative relief data (Table 3.7 and Fig. 3.9) show that the DLS is maximum at 400- 500m relative relief and drops down to almost half at 200-300 m

relief. Though the area covered by 300-400 m is maximum, yet it has less percentage of landslides (28.78%) than the category 400-500 m (50.36%). From the Table 3.7 it can be inferred that DLS is maximum for the relief category 400-500 m followed by 200-300 m, 300-400 m, >500 m and <200 m. Out of the five categories, the most vulnerable for landslides is the 400-500 m, i.e., higher relief, so far as the study area is concerned. The frequency histogram shows a bimodal trend with two peaks at 400-500m and 200-300m.

3.3.5 LANDSLIDES IN RELATION TO DRAINAGE DENSITY

Number of landslides in each sub-basin is determined and then the DLS values for the three drainage density categories are calculated as given in Table 3.8. The corresponding frequency histogram, drawn in Fig. 3.10, shows a monotonous decreasing trend from low to high drainage density.

The data indicates maximum DLS is in low drainage density category ($<2 \text{ km/km}^2$) followed by moderate ($2-3 \text{ km/km}^2$) and high drainage density ($>3 \text{ km/km}^2$). This finding may be explained in terms of the fact that in the areas of low drainage density, the surface runoff is less resulting, in turn, high seepage of water and generating pore pressure for landslide occurrences. This conjecture may be true because most of the 1st and 2nd order streams in the area of fine textured drainage (high drainage density), are seasonal in nature and these channelise rain water during monsoon. On the contrary, in coarse textured drainage (low drainage density), the rain water flow gets retarded and thus it saturates the slopes causing more instability.

3.3.6 LANDSLIDES IN RELATION TO LANDUSE

The DLSs for the five classes of vegetation, i.e., thick forest, moderate forest, sparse forest, agricultural land and barren land are calculated. The data are given in Table 3.9 and the frequency distribution is shown in Fig. 3.11. It is inferred from the table and the figure that the maximum DLS is in the category of barren land, though its areal extent is minimum. This is followed by sparse forest, moderate forest, agricultural land and thick forest. Thick forest, due to dense vegetation, has shown a low density of landslides, while sparse forest due to scanty vegetation, has shown high landslide density. In this case, frequency histogram is monotonically increasing from thick forest to barren land. So, the study reaffirms the trend that

Table 3.7 Frequency distribution of landslide in relation to relative relief

Relative relief (m)	% Area	% Landslide	Relative landslide density	Density of landslide (DLS)
<200	2.26	0.72	0.32	0.10
200-300	12.94	11.51	0.89	0.28
300-400	37.26	28.78	0.77	0.24
400-500	33.23	50.36	1.52	0.48
>500	14.31	8.63	0.60	0.19

Table 3.8 Frequency distribution of landslide in relation to drainage density

Drainage density (km/km ²)	% Area	% Landslide	Relative landslide density	Density of landslide (DLS)
Low (<2)	10.42	12.23	1.17	0.37
Moderate (2-3)	62.16	67.62	1.09	0.34
High (>3)	27.43	20.14	0.73	0.23

Table 3.9 Frequency distribution of landslide in relation to landuse

Landuse	% Area	% Landslide	Relative landslide density	Density of landslide (DLS)
Thick forest	37.32	24.46	0.66	0.21
Moderate forest	20.70	21.58	1.04	0.33
Sparse forest	18.27	28.06	1.54	0.48
Agriculture land	18.19	14.39	0.79	0.25
Barren land	5.51	11.51	2.09	0.65

247424

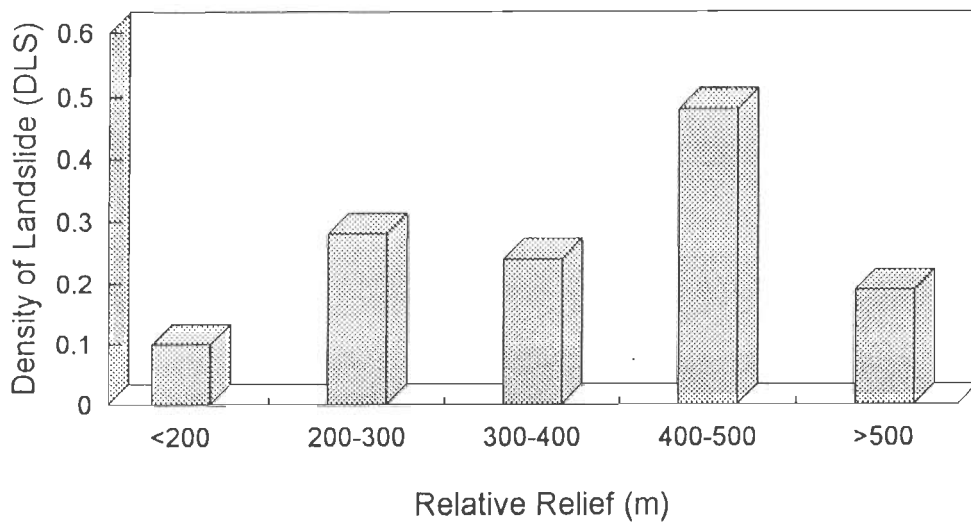


Figure 3.9 Density of landslide vs relative relief

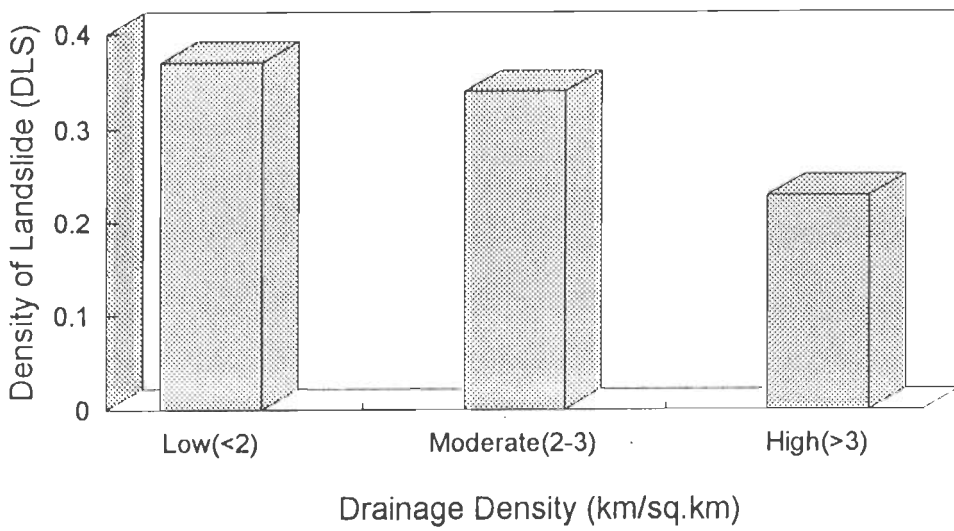


Figure 3.10 Density of landslide vs drainage density

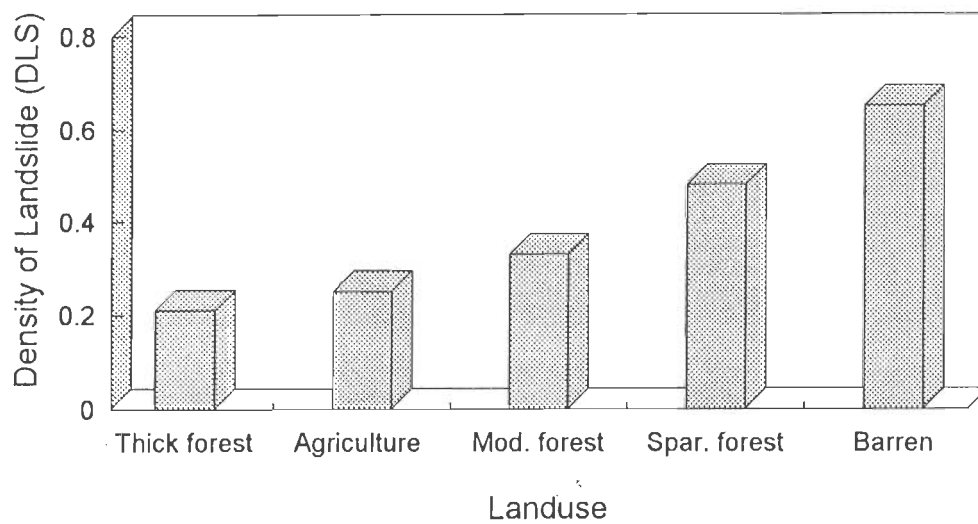


Figure 3.11 Density of landslide vs landuse

landslide events increase as vegetation density decreases. In the other words, one can say that vegetation growth provides stability to hill slopes.

3.4 SUMMARY

Several terrain factor maps together with the landslide map, are prepared for the study area. These maps show the spatial distribution of landslides and different categories of factors in the area. The relationship study between factors and landslides has been carried out on the basis of landslide density trend.

This study has provided important guidelines for assessing slope instability in the region. The lithology factor shows that the phyllite is much more prone to landslides than other rock types, particularly quartzite. It has been found that the landslides are mostly concentrated around North Almora Thrust indicating it to be a major contributing factor for landslide events in the terrain. The dependence of landslides on slope gradients reveals that the slopes in the range 15° - 35° are more susceptible to landslides. This can be attributed to the lithological control. When landslides are studied in relation to drainage density, it has been found that these are more frequent in low drainage density areas on account of more water seepage. Further, it has been found that the landslides are more frequent in high relative relief category of 400-500 m. The relationship between landslides and landuse confirms the fact that areas of barren and scanty vegetation are more susceptible to landslide occurrences.

The factors, slope and relative relief respectively show unimodal and bimodal distributions of landslides while all the other factors show a monotonous trend. The occurrence of more landslides in gentle to moderate slope ranges is an illustration of their complex dependence on various factors. The relationships established here have been used in the landslide hazard zonation study.

LANDSLIDE HAZARD ZONATION TECHNIQUES

The landslide hazard zonation study of an area aims at identifying the landslide potential zones and at ranking them in order of the degree of hazard from landslides. In other words, it is the spatial prediction of landslide potential areas. In regional landslide hazard zonation an appraisal of landslide potential areas can be made over a large terrain. The regional zonation is primarily based on the information procured from remote sensing data and available maps depicting topography, geology etc. Such studies, in general, do not call for intensive field study. In contrast to such schemes the detailed zonation is based on intensive field study and therefore can be meaningfully applied to a reasonably small area.

Several landslide hazard zonation schemes are available in the literature. The simplest one is to identify existing landslide areas in the field and to prepare the hazard zonation map accordingly. Some methods are based on analysis of terrain factors in relation to landslide. This analysis may be qualitative or quantitative. However, the most widely used technique is the factor overlay approach in which the maps of various factors, known to be promoting instability, are prepared and, by overlaying these maps, the zones with unfavourable conditions are identified to produce the hazard map. The present study deals with the techniques based on analysis of data pertaining to the factors conducive to landslide occurrence.

In the present study, two regional landslide hazard zonation schemes have been developed and applied to Srinagar-Rudraprayag area. Firstly, a method, based on subjective rating assignment to the factors, has been developed and termed as Subjective Regional Zonation (SRZ). To reduce the impact of subjective decisions, a second method, based on fuzzy set theory, has been developed and is named as Objective Regional Zonation (ORZ). After identifying the most vulnerable zones from the two zonation maps prepared using the

SRZ and ORZ techniques, a small region of interest (sub-area) has been selected for detailed zonation. For detailed zonation of this sub-area, a third method named as Detailed Regional Zonation (DRZ) has been employed. All these zonation maps are prepared on 1:50000 scale. Finally, a comparative analysis of the results of these zonation maps is performed.

4.1 BASIC STEPS FOR LANDSLIDE HAZARD ZONATION

Landslide hazard zonation is carried out in several steps. The first step is to select the factors considered to be governing stability of the terrain and then classify each of these into various categories. After selection of factors, selection of appropriate scale is an important issue in hazard zonation mapping program. Scale of 1:50000 is generally used for regional zonation, as used in the present study, while for a micro level zonation a scale of 1:10000 would be appropriate. Then the map unit for data collection is to be chosen. This may be a regular geometrical shape such as a square unit of selected size or a polygon depending on the scale of mapping and topography of the terrain. The data pertaining to the factors and their respective categories are then collected for the study area. This is followed by the preparation of relevant factor maps, depicting spatial distribution of the categories of factors contributing to landslide occurrences. The most important step in the zonation exercise pertains to the assignment of weightages to the factors and their categories. The various hazard zonation methods in literature primarily differ in the set of factors/parameters chosen and/or in the mode of assignment of numerical rating to each of them. The choice of factors and the degree of details to be considered is constrained by the goal of study, the areal extent, and the scale of mapping. The next step is assessment of landslide potential of each map unit. This is done by computing the score for landslide potential through integration of data pertaining to the different factors. These scores are then classified into various hazard classes following a classification criterion. In the end the landslide hazard zonation map is prepared, either by drawing contours on class boundaries, or by showing the hazard classes of individual map unit.

The zonation map prepared has to be tested/evaluated for its validity by means of analysis of map components. The measure used in the present study to evaluate the different hazard classes of a map, is the Hazard Index (HI) of a class which measures the relative density of landslides with respect to the mean landslide density of the study area. This can be obtained from the ratio of Class landslide density Index (CI) and the Mean landslide density

Index (MI). MI is the ratio of total number of landslides and the total area of study, i.e., $139/444 = 0.313$ for the present study. The CI is the ratio of number of landslides in the class and the area of the class.

$$HI = CI / MI$$

A hazard class with a HI value of 1.00 has a landslide density equal to the mean density over the whole study area. Hence, a good hazard zonation map is one which provides sufficient separation discriminating between different hazard classes.

4.2 SUBJECTIVE REGIONAL ZONATION (SRZ) TECHNIQUE

The Subjective Regional Zonation technique is based on the selection of terrain factors important for landslide study, their classification into different categories, preparation of factor maps, assignment of numerical ratings to the factors and their categories, computation of landslide potential scores and their classification into various classes of hazard. It may be added here that no external triggering factors like rainfall and seismicity are considered in the present study.

4.2.1 METHODOLOGY

In this technique the factors considered are lithology, distance from major thrust/fault, slope angle, relative relief, drainage density and landuse. Each factor is classified into various categories and the factor maps are prepared. The numerical ratings assigned to each factor, are then decided on the basis of relative importance of the factor in inducing landslides. In the present method, these ratings are termed as Landslide Susceptibility Ratings (LSR). The LSRs of the six factors have been chosen in such a way that their sum equals 100.

Slope, being the most important factor, has been accorded prime importance and is assigned an LSR of 30. The next important factor is lithology and for it LSR is 25. The landslides frequently occur along thrusts and faults, therefore an LSR of 20 is assigned to the distance from North Almora Thrust (NAT) which is a major thrust in the area. To each of the rest two parameters, i.e., landuse and relative relief, an LSR of 10 is assigned. The LSR for drainage density is 5.

After assigning the LSR to each factor, it is pertinent to determine the relative

weightages of different categories of each factor. This weightage is called here as Landslide Susceptibility Index (LSI) and is determined, on the basis of density of landslides (DLS) for each category of the factors. The LSI of a category is calculated from LSR of the corresponding factor and the normalised density of landslides (NDLS), which is the ratio of DLS of that category to the total DLS of all categories of the factor.

$$\text{LSI (x,y)} = \text{NDLS (x,y)} \times \text{LSR}$$

where, x - category
y - factor

In the next step, the study area is divided into small cells of appropriately chosen unit and the categories of the different factors belonging to each cell are noted. Finally, each cell is represented by a score obtained by adding the LSIs of the categories of factors of the cell. These scores, termed here as landslide potential scores, are divided into five classes for landslide hazard zonation.

4.2.2 DATA PROCUREMENT AND PROCESSING

The spatial data, pertaining to each factor, are obtained from the geological map, slope map, relative relief map, drainage map and landuse map of the area. The spatial distribution of existing landslides in the area is obtained from the landslide map. The mode of preparation and relevant characteristic features of these maps are already described in chapter 2 and chapter 3. The relation between landslides and the categories of the factors based on density of landslides (DLS) in each category of the factors is also reported in the previous chapter. Following this scheme, the LSI values of all the categories are computed from their DLS values and the LSRs of the corresponding factors. The LSIs calculated for all the categories of lithology, distance from NAT, slope, relative relief, drainage density and landuse are given in Tables 4.1 - 4.6 respectively.

The LSIs of the categories of lithology, tabulated in Table 4.1 show that the maximum LSI of 7.0 is for phyllite and the minimum is for quartzite (1.75). The LSIs, for the five categories of the factor distance from NAT, decrease from 7.0 for 0-2.5 km to 1.4 for >10 km (Table 4.2). However, the LSIs of the categories 0-2.5 and 2.5-5 kms are of the same order indicating same weightage within 5 km range of the North Almora Thrust. From Table 4.3, it can be seen that the LSI is maximum (10.2) for the slope category 15°-25°, which is followed

Table 4.1 LSI of lithology categories

Lithology	DLS	NDLS	LSI
Phyllite	0.64	0.28	7.00
Quartzite	0.15	0.07	1.75
Metavolcanic	0.32	0.14	3.50
Epidiorite	0.42	0.19	4.75
Dolomite	0.35	0.16	4.00
Terrace deposit	0.30	0.17	4.25

Table 4.2 LSI of distances from NAT

Distance from NAT (km)	DLS	NDLS	LSI
0 - 2.5	0.46	0.35	7.00
2.5 - 5.0	0.46	0.35	7.00
5.0 - 7.5	0.17	0.13	2.60
7.5 - 10.0	0.12	0.09	1.80
>10.0	0.09	0.07	1.40

Table 4.3 LSI of slope categories

Slope	DLS	NDLS	LSI
>45°	0.14	0.11	3.3
35° - 45°	0.25	0.20	6.0
25° - 35°	0.34	0.28	8.4
15° - 25°	0.42	0.34	10.2
<15°	0.08	0.06	1.8

Table 4.4 LSI of relative relief categories

Relative relief (m)	DLS	NDLS	LSI
<200	0.10	0.08	0.8
200 - 300	0.28	0.22	2.2
300 - 400	0.24	0.19	1.9
400 - 500	0.48	0.37	3.7
>500	0.19	0.15	1.5

Table 4.5 LSI of drainage density categories

Drainage density (km/km ²)	DLS	NDLS	LSI
Low (<2)	0.37	0.39	1.95
Moderate (2-3)	0.34	0.36	1.8
High (>3)	0.23	0.24	1.2

Table 4.6 LSI of landuse categories

Landuse	DLS	NDLS	LSI
Thick forest	0.21	0.11	1.1
Moderate forest	0.33	0.17	1.7
Sparse forest	0.48	0.25	2.5
Agriculture land	0.25	0.13	1.3
Barren land	0.65	0.34	3.4

by the slope categories 25°-35°, 35°-45°, >45°. The minimum LSI is 1.8 for the category <15°. For relative relief the maximum LSI 3.7 is for 400-500 m and minimum 0.8 for <200 m (Table 4.4). The LSIs, obtained for drainage density categories, show that the maximum of 1.95 is for low density while the minimum of 1.2 is for high density (Table 4.5). The last factor considered is the landuse for which the LSIs of the five categories show a maximum value of 3.4 for barren land and the minimum of 1.1 for thick forest area (Table 4.6). The data show an increase in LSI as the density of vegetation decreases. Since the LSIs for all the categories depend on the density of landslides, these follow the same trend as found in the relationship study.

For data integration, the whole area is divided into 1776 cells of 0.25 km² size (1 cm² on 1:50,000 scale map). The cell map of the area is shown in Fig. 4.1. The (0,0) is labelled at the left bottom corner of the map. Each cell can be identified by its co-ordinate on the map. In the next step, the categories of the factors of each cell are noted by superimposing the factor maps one by one on the cell map. In cases, where two or three categories of a single factor exist in the same cell, the category considered is the one covering the maximum portion of the cell. Finally, the LSIs of all the categories of the six factors in a cell are added to get the score of the cell for landslide potential. The minimum score obtained in 1776 cells is 9.6 while the maximum is 33.63. The higher score implies that the cell is more prone to landslide.

4.2.3 HAZARD CLASSES AND ZONATION MAP

The scores for landslide potential obtained above, are classified into five classes of landslide hazard, depicting the relative degree of instability. The boundaries for these five classes are drawn at 19, 23, 27 and 31 so that each class has uniform interval of 4 and the predicted hazard zones match with the prevailing field conditions.

Hazard class	Score
Very low	<19
Low	19-23
Moderate	23-27
High	27-31
Very high	>31

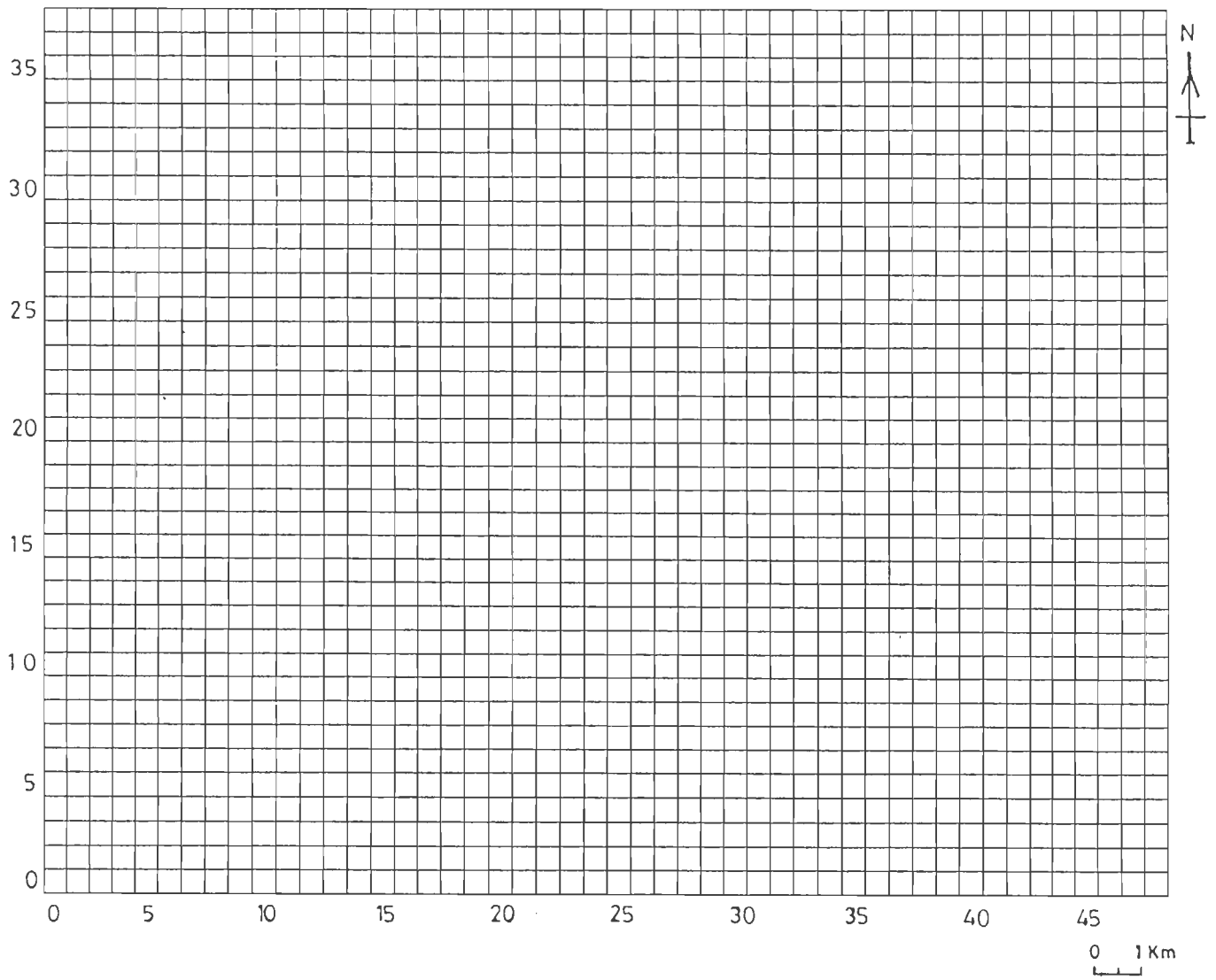


Figure 4.1 Cell map of the study area

To prepare the landslide hazard zonation map, the scores of the 1776 cells are contoured at the class boundaries. The zonation map, prepared using the SRZ technique, is shown in Fig. 4.2.

The landslide hazard zonation map shows that there is a prominent high hazard zone, lying to the south of Alaknanda river, extending in E-W direction. There are few very high hazard zones of very small area lying within this high hazard zone. Most of these very high and high hazard zones belong to the Dudatoli Group where phyllite is the predominant rock. These zones lie in close proximity to NAT. The villages situated in the high hazard zone are Sumari, Nawasu, and Gawana. The Srinagar and Rudraprayag towns fall in low and very low zones. The southern extreme of the area is bounded by the low and very low hazard zones. To the north of the Alaknanda, mainly moderate, low and very low hazard zones are present. In the northern part, the area around Rudraprayag is all in very low hazard zone and the area towards Srinagar side, i.e., around Kandi, is mainly in moderate hazard zone with scattered patches of high hazard zones. Overall, it can be said that in the study area, the regions close to NAT and lying to the south of the Alaknanda river have relatively more potential for landslide hazards. It is significant to note that the most important and major landslide, the Kaliasaur slide, located on the left bank of Alaknanda river, 3 km upstream from Dhari, is lying in the moderate hazard zone. This is due to the moderately stable zone around the slide area where the categories of factors are not conducive to landslide. However, for a small part, where sliding is active, some factors are locally unfavourable such as highly crushed quartzitic rocks with barren slope. So, it can be said that by regional zonation small part of a zone may not be predicted precisely.

The percentage area of each hazard class when determined, reveals that 1.91% is in very high, 14.3% in high, 25.17% in moderate, 29.62% in low and 29.11% in very low hazard class.

4.2.4 VALIDATION OF MAP

After preparing the zonation map, its validity is evaluated by calculating the Hazard Index (HI) values following the procedure as described earlier. The HI values calculated for the SRZ map are tabulated in the Table 4.7.

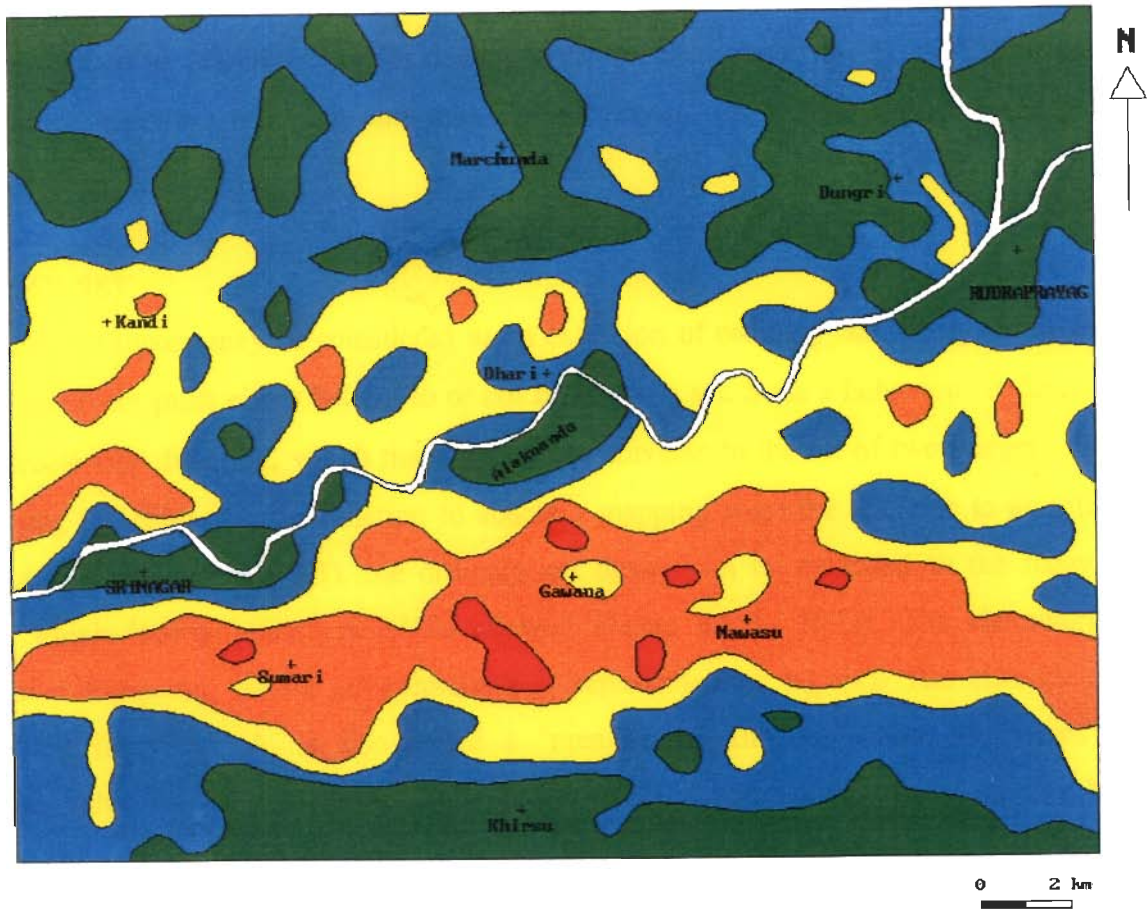
Table 4.7 Hazard Index for SRZ map

Hazard class	Area (km ²)	Number of landslides	Class landslide density Index (CI)	Hazard Index (HI)
Very low	129.25	17	0.13	0.42
Low	131.50	20	0.15	0.48
Moderate	111.75	47	0.42	1.34
High	63.50	44	0.69	2.20
Very high	8.50	11	1.29	4.12

From the table it can be seen that the HI for the very high hazard class is 4.12 while for the very low hazard class it is 0.42. The differences between the very high, high and moderate hazard classes are considerably larger than that between the low and very low hazard classes. Since our main aim is to identify the zones of high hazard, whose HIs are reasonably different from the other hazard classes, the quality of the map can be considered as good. Further, it can be seen that the HIs increase as the degree of hazard increases. This validates the zonation map since the zones of high degree of hazard coincide with the areas with larger landslide concentrations.

4.3 OBJECTIVE REGIONAL ZONATION (ORZ) TECHNIQUE

In the previous section we have seen that the subjective decisions have been made at several places. These steps are the choice of factors contributing to landslides, classification of these factors into different categories, the assignment of ratings to the factors and the classification of landslide potential scores into different hazard classes. To induce some amount of objectivity, the Objective Regional Zonation (ORZ) technique is developed. Here the ratings of categories of factors are derived directly from the frequency distribution of landslides. It is observed that, in most of the zonation methods, the boundaries of the categories of factors which are on ordinal scale are not crisply defined. In view of the diversified nature of the data,



Hazard Class

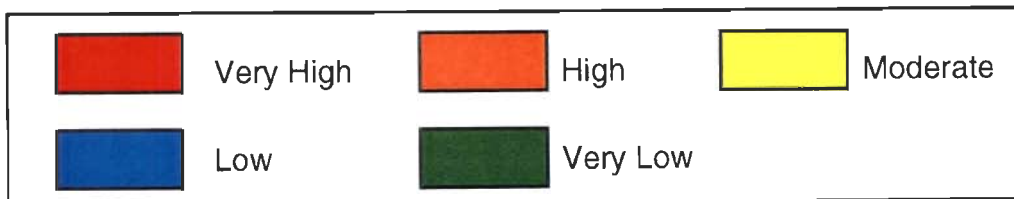


Figure 4.2 SRZ map of the study area showing landslide hazard zones

of cells with category x (NC).

$$\text{LSG (x,y)} = \frac{\text{NCL (x,y)}}{\text{NC (x,y)}}$$

This LSG may be interpreted as the contribution of a particular category in promoting landslide. For the different factors, different fuzzy sets are defined with categories as members and respective LSGs as membership grades.

In order to study the holistic contribution of the factors, a composite fuzzy set has to be derived. This can be achieved through the cartesian product of different fuzzy sets as discussed by Zimmermann (1991). A cartesian product set is a set whose individual member is itself a small set, comprising one member each from the different fuzzy sets of which the product is being taken. The membership grade of the members of the cartesian product set can be obtained by various means like taking maximum or minimum or an average of the membership grades of the individual fuzzy set member (Klir and Folger, 1988). In our study, we have chosen the arithmetic mean so as to uniformly account for all the factors.

The cartesian product of the n fuzzy sets, A_1, \dots, A_n belonging to the universes X_1, \dots, X_n is the fuzzy set in the product space $X_1 \cdot X_2 \cdot \dots \cdot X_n$ with the membership function

$$\mu_{(A_1 \cdot A_2 \cdot \dots \cdot A_i \cdot \dots \cdot A_n)}(x_1, x_2, \dots, x_i, \dots, x_n) = \sum_{i=1}^n \mu_i(x_i)$$

where $x_i \in A_i$ with $i=1, 2, \dots, n$

The elements of the cartesian product set are the collection of individual categories of each factor. The membership grade (μ) of this set is the score for landslide potential and higher the score more is the tendency for landslide occurrence. These scores are then suitably classified and the landslide hazard zonation map is prepared.

4.3.3 DATA PROCUREMENT AND PROCESSING

The factors and their categories, used in this technique are the same as considered in the SRZ technique. The cell map with same cell size of SRZ technique is used here for data collection. The data regarding factors and their respective categories, collected for the 1776 cells of the study area in the SRZ method, is appended with the presence or absence of landslide in each cell. Then by determining the values of NCL and NC for each category, the

i.e., to say the data can be on nominal (e.g., rock type), ordinal (e.g., landuse) or ratio scale (e.g., slope), a method is to be chosen which can systematically deal with such data. Of the several possible techniques, the fuzzy set theory is used in the present study. It has been since long established as an effective tool for dealing with linguistic data (Zadeh, 1975). Further, a more judicious approach has been employed for identifying the class boundaries for hazard classes.

4.3.1 FUZZY SET

Fuzzy set theory may be considered as an extension of ordinary set theory. In ordinary set theory an object must either belong to or not belong to a set. Such a behaviour is described by the characteristic function, which maps the whole universe to the set of two integers, (0,1). By modifying the characteristic function to enable a mapping from the universe to an infinite set of points in the interval (0,1), the ordinary set theory can be extended to the fuzzy set theory in which 'partial membership' is allowed (Juang et al., 1992). The characteristic function of a fuzzy set, A, for its member x is represented as $\mu_A(x)$. The characteristic function of a fuzzy set, A, is also called a "membership function" since it defines the membership value for each member of the fuzzy set. The membership function may be a discrete function or a continuous one.

If X is a collection of objects, x, then a fuzzy set A in X is a set of ordered pairs.

$$A = \{ x, \mu_A(x) ; x \in X \}$$

Hence, it can be said that a fuzzy set is a generalization of the classical set and its membership function is a generalization of the conventional characteristic function.

4.3.2 METHODOLOGY

The factors selected for landslide hazard zonation are first classified into various categories. The numerical weightages for these categories, called Landslide Susceptible Grades (LSG) in this technique, are determined from the landslide frequency for that category. To account for the areal coverage of the categories, the number of cells (map units) having that category is taken into account. The LSG of the category x, belonging to the factor y, is computed from the number of cells with category x having landslides (NCL) and the number

of cells with category x (NC).

$$LSG(x,y) = \frac{NCL(x,y)}{NC(x,y)}$$

This LSG may be interpreted as the contribution of a particular category in promoting landslide. For the different factors, different fuzzy sets are defined with categories as members and respective LSGs as membership grades.

In order to study the holistic contribution of the factors, a composite fuzzy set has to be derived. This can be achieved through the cartesian product of different fuzzy sets as discussed by Zimmermann (1991). A cartesian product set is a set whose individual member is itself a small set, comprising one member each from the different fuzzy sets of which the product is being taken. The membership grade of the members of the cartesian product set can be obtained by various means like taking maximum or minimum or an average of the membership grades of the individual fuzzy set member (Klir and Folger, 1988). In our study, we have chosen the arithmetic mean so as to uniformly account for all the factors.

The cartesian product of the n fuzzy sets, A_1, \dots, A_n belonging to the universes X_1, \dots, X_n is the fuzzy set in the product space $X_1 \cdot X_2 \cdot \dots \cdot X_n$ with the membership function

$$\mu_{(A_1 \cdot A_2 \cdot \dots \cdot A_i \cdot \dots \cdot A_n)}(x_1, x_2, \dots, x_i, \dots, x_n) = \sum_{i=1}^n \mu_i(x_i)$$

where $x_i \in A_i$ with $i=1, 2, \dots, n$

The elements of the cartesian product set are the collection of individual categories of each factor. The membership grade (μ) of this set is the score for landslide potential and higher the score more is the tendency for landslide occurrence. These scores are then suitably classified and the landslide hazard zonation map is prepared.

4.3.3 DATA PROCUREMENT AND PROCESSING

The factors and their categories, used in this technique are the same as considered in the SRZ technique. The cell map with same cell size of SRZ technique is used here for data collection. The data regarding factors and their respective categories, collected for the 1776 cells of the study area in the SRZ method, is appended with the presence or absence of landslide in each cell. Then by determining the values of NCL and NC for each category, the

Landslide Susceptibility Grades (LSG) of all categories of each factor are calculated. These represent their partial contribution to landslides. The grades of the categories of all factors are given in the Tables 4.8 - 4.13.

It is significant to note that the landslide affected cells are more than the number of landslides because a single landslide can extend to more than one cell, depending upon its size. So, indirectly we are accounting for the size of the landslides also. The total number of landslide affected cells is 204 (out of the total 1776 cells).

The Table 4.8 shows that for lithology, maximum LSG of 0.23 is for phyllite while minimum of 0.07 is for quartzite. For the factor, distance from NAT, LSG is maximum (0.15) for the categories 0 - 2.5 and 2.5 - 5.0 km and it progressively decreases as the distance increases (Table 4.9). For slope, LSG is maximum for 15°-25° category followed by 25°-35° and is minimum for <15° category (Table 4.10). The relative relief category of 400-500m has the maximum grade of 0.14 and <200m has the minimum grade of 0.03 (Table 4.11). The LSGs of drainage density are 0.13 for low density and 0.09 for high density (Table 4.12). Lastly, the grades for landuse decrease as the density of vegetation increases (Table 4.13). The maximum grade is for barren land, i.e., 0.16 and minimum is for thick forest, i.e., 0.09. When these grades are compared with the LSIs of the SRZ technique, it becomes evident that the trend of weightages is almost similar. As an example, the fuzzy set of the factor lithology is given below.

(phyllite,0.23), (quartzite,0.07), (metavolcanic,0.12), (epidiorite,0.08), (dolomite,0.09),
(terrace deposit,0.16)

The parameter Landslide Susceptibility Grade of a factor, equivalent to the LSR value in SRZ method, is defined as the sum of LSGs of its categories. To compare this parameter with LSR values, % normalized LSG of the factor is obtained in terms of the ratio of the grades of factors to the sum of grades of all the six factors.

Table 4.8. LSG of lithology categories

Lithology	NC	NCL	LSG
Phyllite	380	89	0.23
Quartzite	929	65	0.07
Metavolcanic	235	27	0.12
Epidiorite	106	8	0.08
Dolomite	69	6	0.09
Terrace deposit	57	9	0.16

Table 4.9 LSG of distances from NAT

Distance from NAT (km)	NC	NCL	LSG
0 - 2.5	494	75	0.15
2.5 - 5	489	76	0.15
5 - 7.5	455	33	0.07
7.5 - 10	258	16	0.06
>10	80	4	0.05

Table 4.10 LSG of slope categories

Slope	NC	NCL	LSG
>45°	54	5	0.09
35° - 45°	341	37	0.11
25° - 35°	970	112	0.12
15° - 25°	291	42	0.14
<15°	120	8	0.07

Table 4.11 LSG of relative relief categories

Relative relief (m)	NC	NCL	LSG
<200	30	1	0.03
200 - 300	231	24	0.10
300 - 400	627	76	0.12
400 - 500	621	84	0.14
>500	267	19	0.07

Table 4.12 LSG of drainage density categories

Drainage density (km/km ²)	NC	NCL	LSG
0 - 2	224	29	0.13
2 - 3	1070	133	0.12
>3	482	42	0.09

Table 4.13 LSG of landuse categories

Landuse	NC	NCL	LSG
Thick forest	622	56	0.09
Moderate forest	383	40	0.10
Sparse forest	336	46	0.14
Agriculture land	337	46	0.14
Barren land	98	16	0.16

Factors	% Normalized LSG in ORZ	LSR in SRZ
Lithology	23.96	25
Distance from NAT	13.42	20
Slope	16.93	30
Relative relief	14.67	10
Drainage density	10.86	5
Landuse	20.13	10

This shows that, in case of the factors distance from NAT, slope and landuse there exists a considerable difference in the computed factor LSGs and the assigned LSR. This highlights the inevitable bias introduced as a result of a priori subjective assignment of weightages in SRZ technique.

The score for landslide potential is determined by the grade of the members of cartesian product set. The cartesian product set of the six fuzzy sets (corresponding to the six factors) with 6, 5, 5, 5, 3 and 5 members will have in total 11250 (6x5x5x5x3x5) elements. However, there exist 962 combinations in the study area. Since the categories of different factors belonging to a particular cell are known, the membership grade for the cell is obtained from the cartesian product set membership grade value. For example, the typical cell comprising the factor categories given below has a membership grade of 0.78.

Item	Category	LSG	Membership Grade
Lithology	phyllite	0.23	0.78
Distance from NAT	0-2.5 km	0.15	
Slope	25°-35	0.12	
Relative relief	200-300m	0.10	
Drainage density	>3 km/km ²	0.09	
Landuse	thick forest	0.09	

This cell corresponds to the member of the cartesian product set ((phyllite, 0-2.5 km, 25-35°, 200-300m, thick forest, >2.5 km/km²), 0.78). The cell membership grade 0.78 is the score of landslide potential which points to the proneness of landsliding. The scores for all the 1776

cells are thus determined. The minimum score is 0.496 for the cell with co-ordinate (33,30) while the maximum is 0.953 for the cell with co-ordinate (19,11).

To carry out all the computational work, a computer program is written, whose input parameters are the number of cells, the number of factors, the number of categories in each factor and the cell data comprising its co-ordinates, categories of factors and presence or absence of landslides. The program outputs the LSGs of categories of each factor and the score of each cell. The scores of all the cells obtained using the program are contoured with 0.05 contour interval (Fig. 4.3). The contour map, shows the spatial trend of the degree of landslide proneness in which the contour of higher value shows more chances of landslide occurrence.

4.3.4 HAZARD CLASSES AND ZONATION MAP

The zonation map can be prepared, by partitioning the scores of the cells into different landslide hazard classes. The classification should be based on the trend of score frequency curve. For this, the simplest procedure can be "local boundary hunting" where one searches for the abrupt changes in average values or equivalently for the steepest gradients in the sequence (Davis, 1986).

Since the results of this method are to be compared with those of the other methods, before developing a classification scheme, the initial cell scores ranging from 0.496 to 0.953, are normalized on a scale 0 to 99 . The formula used for normalization is :

$$\text{Normalized score} = \frac{\text{Score} - \text{Score}_{\min}}{\text{Score}_{\max} - \text{Score}_{\min}} \times 99$$

Now the minimum and maximum normalized scores are 0 and 99 respectively.

The score frequencies are calculated next and a graph is plotted between the score and its frequency. It was observed that there existed severe oscillations in this graph. In order to reduce the intensity of these oscillations, instead of plotting the frequency of each score value, the score frequency of a 2 unit class, is plotted at the mid point of the class (Fig. 4.4a). This graph also shows several peaks at different scores. Since we intend to partition the score range into five classes, it is desirable to reduce the number of peaks. For this purpose, three more graphs with window lengths 3, 5 and 7, are plotted between frequency and scores (Figs. 4.4b,

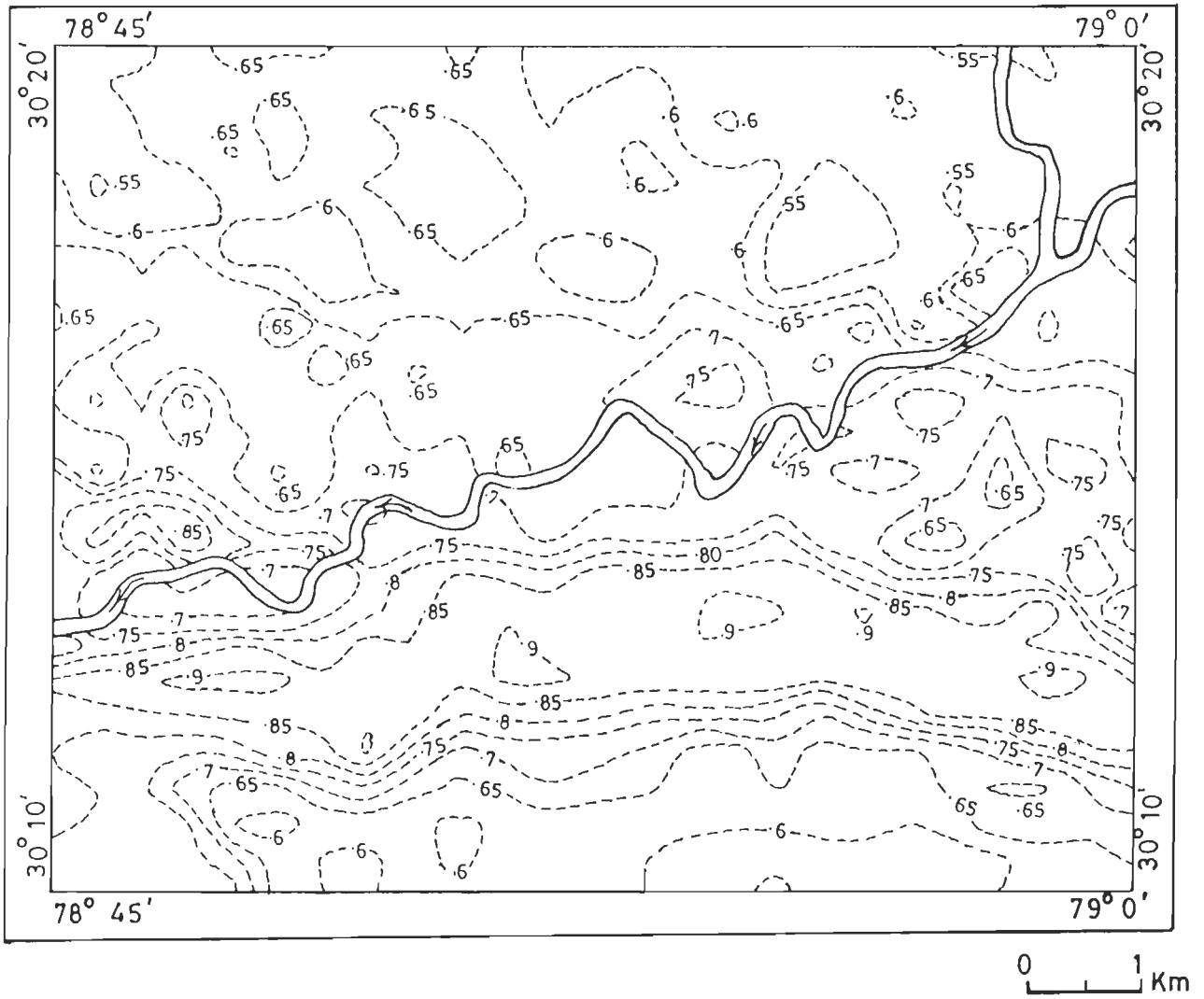


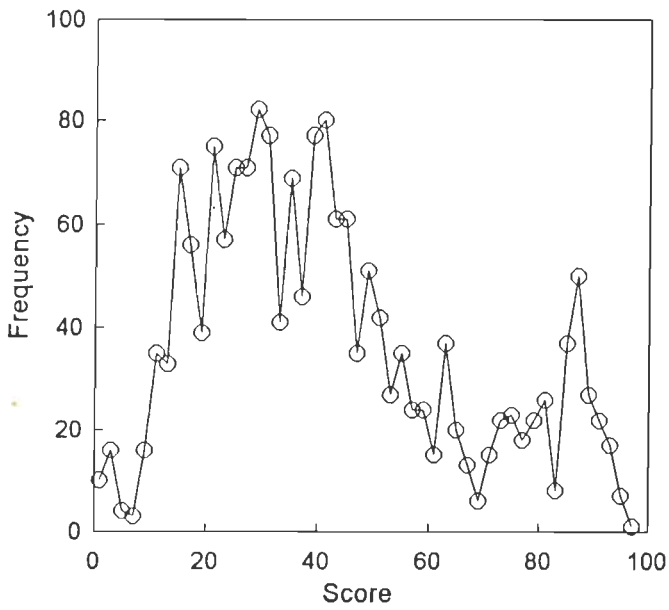
Figure 4.3 Contours of landslide potential scores of ORZ technique

4.4c and 4.4d). It may be alluded here that the window length 3 means that the frequency value, in the corresponding graph, at any point is an average of the three consecutive values centred at that point. These plots show that with increase in window length, the number of peaks is indeed reduced, in other words, the graphs get smoothed. Further, a composite graph (Fig. 4.5) is plotted by superimposing all the four plots. After scrutinizing the graphs carefully, the boundaries for classes are selected at scores 17, 46, 72 and 90. The boundaries are selected in such a manner that these coincide with significant change in gradient. With these score intervals, a contour map is prepared.

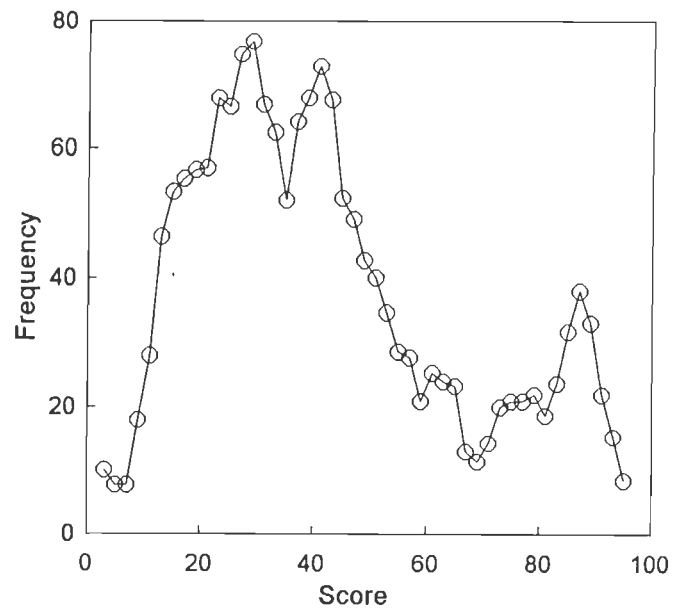
Further, to see how the zonation is affected when the boundaries are shifted by a given distance, a shifting width of 1.6, corresponding to 10% of the minimum score interval (0 to 16), is selected. Then the class boundaries are shifted in both directions by +1.6 and -1.6. The contour maps are prepared for these two cases with contour intervals 18.6, 47.6, 73.6, 91.6 and 15.4, 44.4, 70.4, 88.4 respectively. It is observed that there is practically no difference in the zones when these maps are compared with the original one. This confirms that our classification scheme is not very sensitive to a small change in the class boundaries. The hazard classes, defined on the basis of this classification are given below.

Hazard class	Score
Very low	0-16
Low	17-45
Moderate	46-71
High	72-89
Very high	90-99

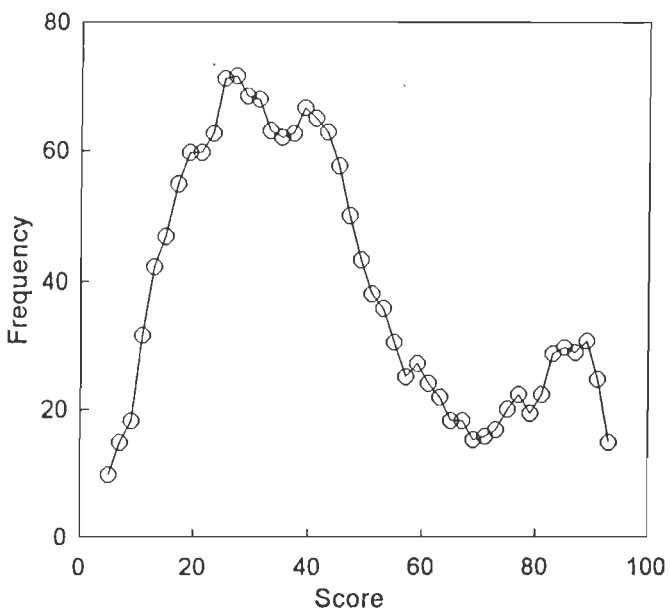
The different zones are marked in the contour map on the basis of these hazard classes. The resulting landslide hazard zonation map, the ORZ map, is shown in the Fig. 4.6. In this map, the area, to the south of Alaknanda, shows a large zone of high hazard. Within this zone, there are scattered zones of very high hazard. The villages falling in high hazard zones are Sumari, Gawana and Nawasu. In this map also the high hazard zone is falling in the Dudatoli Group and lying close to the North Almora Thrust. The extreme south is marked by a low hazard zone containing a very low hazard zone also. The area to the north of Alaknanda is almost completely in low hazard zone with few zones of very low hazard. The Srinagar and



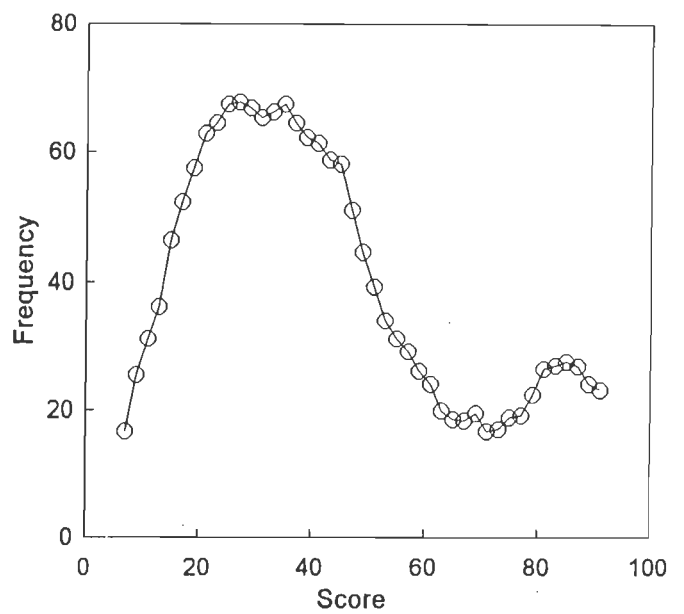
(a) without averaging



(b) averaged over window length 3



(c) averaged over window length 5



(d) averaged over window length 7

Figure 4.4 Frequency plots of landslide potential score

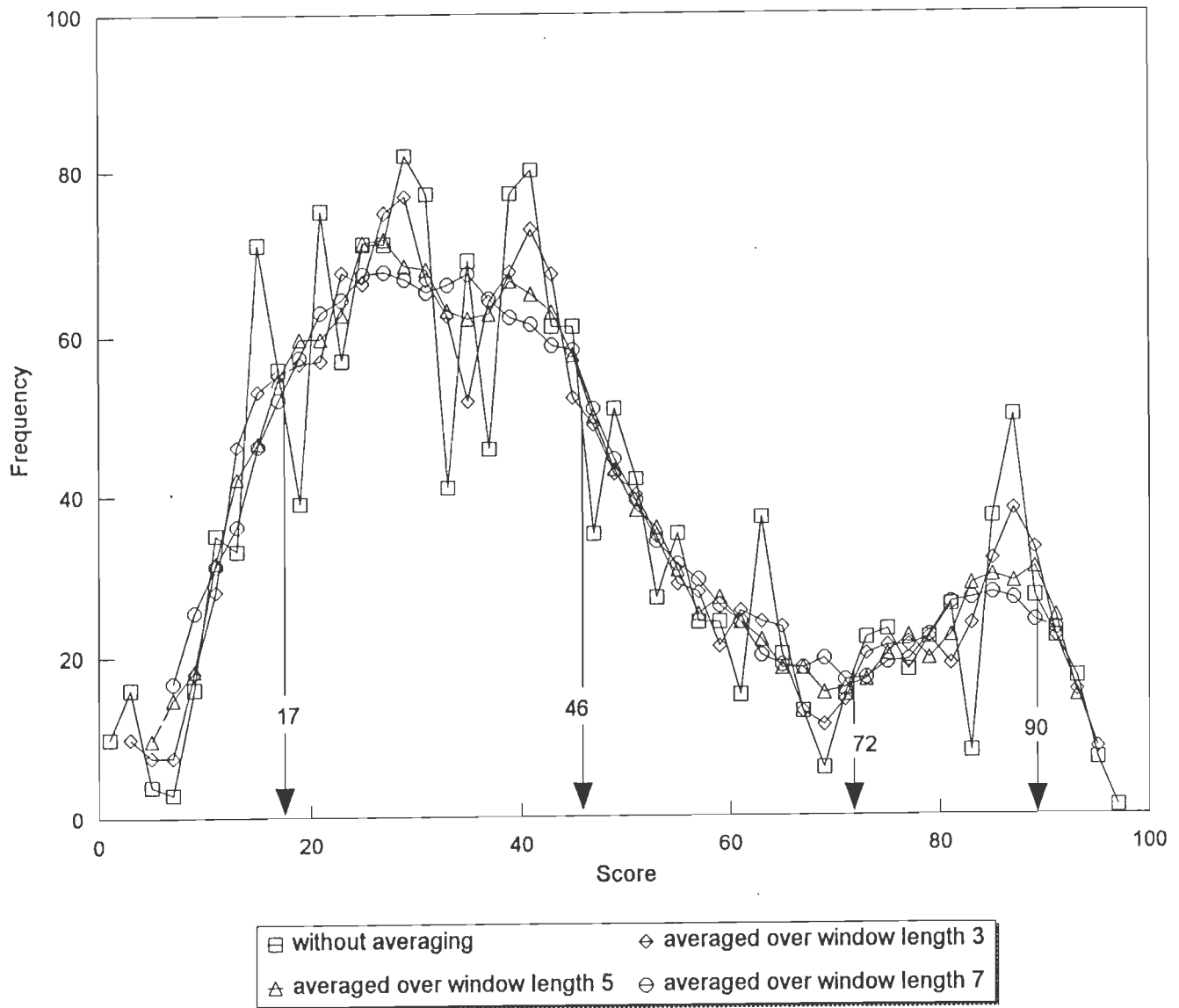


Figure 4.5 Composite graph obtained after superposing the curves (a), (b), (c) & (d) of figure 4.4.

Rudraprayag towns fall in low hazard zones. The zone along Alaknanda river falls in moderate hazard class but on the right bank of the river opposite to Srinagar, a zone of high hazard is visible. This map indicates that the region to the south of Alaknanda is more prone to landslides than the northern part. In this map also, the Kaliasaur slide is lying in the moderate hazard zone. The percent area of different hazard zones are, 2.65% in very high, 13.06% in high, 19.59% in moderate, 52.48% in low and 12.22% in very low hazard class.

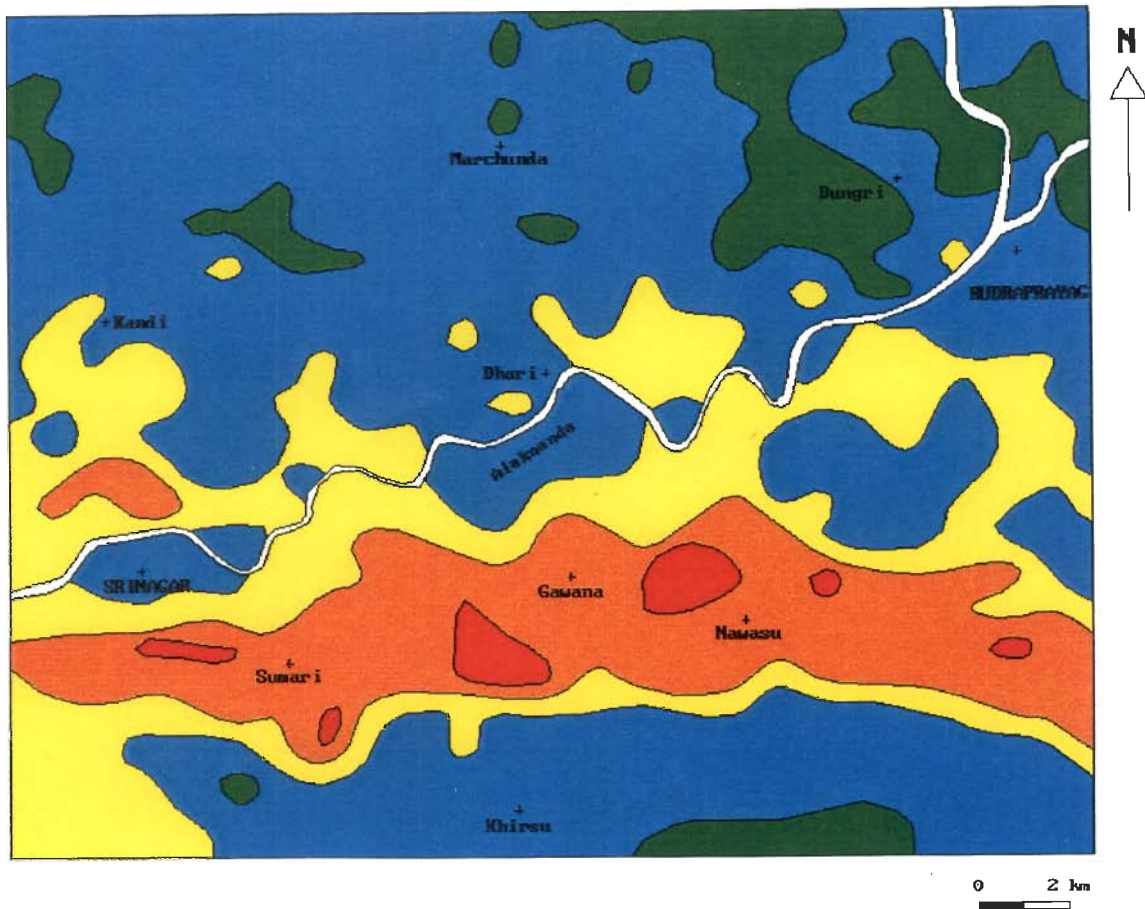
4.3.5 VALIDATION OF MAP

The prepared ORZ map is evaluated quantitatively to check the results obtained. The computed HIs for each hazard class of the zonation map, are given in the Table 4.14

Table 4.14 Hazard Index for ORZ map

Hazard Class	Area (km ²)	Number of landslides	Class landslide density Index (CI)	Hazard Index (HI)
Very low	54.25	4	0.07	0.22
Low	233	43	0.18	0.58
Moderate	87	33	0.38	1.21
High	58	45	0.78	2.49
Very high	11.75	14	1.19	3.80

The HI for the very high hazard class is found to be 3.8 while for the very low hazard class it is 0.22. The separation between the classes as shown by the HI values are quite significant. This map also shows an increase in HI, as the degree of hazard increases. Thus the high hazard zones correspond to higher landslide density.



Hazard Class

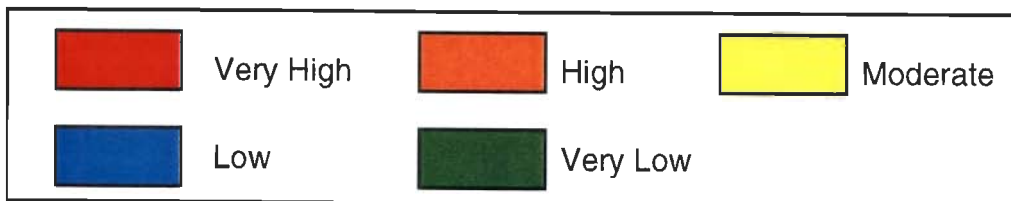


Figure 4.6 ORZ map of the study area showing landslide hazard zones

4.4 DETAILED REGIONAL ZONATION (DRZ) TECHNIQUE

The detailed regional landslide hazard zonation is carried out with a view to obtain finer details of the hazard zones. The Land Hazard Evaluation Factor (LHEF) rating scheme of Anbalagan (1992) is used for this purpose and is termed here as Detailed Regional Zonation (DRZ) technique. This DRZ method of zonation calls for more detailed field data collection than the earlier methods.

From the two zonation maps, i.e., SRZ and ORZ maps, a small sub-area of interest, is selected to carry out detailed hazard zonation. The sub-area selected shows large variation in hazard classes and includes the high and very high hazard zones already identified by the previous methods. The area lies to the south of the Alaknanda river between the latitudes 30°10' to 30°16' and longitudes 78°49' to 78°57'. Its northern boundary is demarcated by the river while the southern boundary almost coincide with the boundary of the complete study area. The eastern and western boundaries are close to the Dewalgarh and Bachchan streams respectively. The sub-area encompasses an area of about 78 km². The details of the scheme are described below.

4.4.1 METHODOLOGY

The LHEF scheme uses the facet concept as the map unit for data collection. The facets, defined by the topographical boundaries and the major break in slope, facilitates easy identification of the slopes under consideration. In this scheme, the factors considered are lithology, structure, slope, relative relief, landuse and surface water condition. However, some of these differ in their nature and/or categories from those of the earlier methods. The rating, for different categories of factors, is assigned on the basis of their estimated significance in causing instability. The various factors and their categories with respective ratings are given in Table 4.15. The various factors and their categories are described below.

Lithology : The main criteria for awarding ratings to the lithology categories, is their response to the process of weathering. The hard rocks quartzite, limestone and igneous rocks are massive and resistant. The terrigenous sedimentary rocks are vulnerable to erosion and hence are susceptible to landslides. In comparison, the phyllites and schists weather quickly and hence are more prone to sliding. Accordingly, the LHEF ratings have been awarded. Further, a correction factor, accounted for degree of weathering of rocks has also been defined.

Table 4.15 Landslide Hazard Evaluation Factor (LHEF) rating scheme

Factor	Category	Rating
LITHOLOGY		
Rock type	Type-I	
	Quartzite and limestone	0.2
	Granite and Gabbro	0.3
	Gneiss	0.4
	Type-II	
	Well cemented terrigenous cemented rocks, dominantly sandstone with minor beds of clay stone	1.0
	Poorly cemented terrigenous sedimentary rocks, dominantly sandstone with minor clay shale beds	1.3
	Type-III	
	Slate and phyllite	1.2
	Schist	1.3
Shale with interbedded claye and nonclayey rocks	1.8	
Highly weathered shale, phyllite and schist	2.0	
Soil type	Older well compacted fluvial material (alluvial)	0.8
	Clayey soil with nturally formed surface (eluvial)	1.0
	Sandy soil with naturally formed surface (alluvial)	1.4
	Debris comprising mostly rock pieces mixed with clayey/sandy soil (colluvial)	
	Older well compacted	1.2
	Younger loose material	2.0

Contd...

Factor	Category	Rating
--------	----------	--------

STRUCTURE

Relationship of structural discontinuity with slope

Relationship of parallelism between slope and discontinuity	>30°	0.20
	21°-30°	0.25
	11°-20°	0.30
	6°-10°	0.40
Planar ($\alpha_j - \alpha_s$)	<5°	0.50
Wedge ($\alpha_i - \alpha_s$)		

Relationship of dip of discontinuity and inclination of slope	>10°	0.3
	0°-10°	0.5
	0°	0.7
Planar ($\beta_j - \beta_s$)	0°-(-10°)	0.8
Wedge ($\beta_i - \beta_s$)	(-10°)	1.0

Dip of discontinuity	<15°	0.20
Planar - β_j	16°-25°	0.25
Wedge - β_i	26°-35°	0.30
	36°-45°	0.40
	>45°	0.50

Depth of soil cover	<5m	0.65
	6-10m	0.85
	11-15m	1.30
	16-20m	2.0
	>20m	1.20

SLOPE MORPHOMETRY

Escarpment/cliff	>45°	2.0
Steep slope	36°-45°	1.7
Moderately steep slope	26°-35°	1.2
Gentle slope	16°-25°	0.8
Very gentle slope	<15°	0.5

Contd...

Factor	Category	Rating
--------	----------	--------

RELATIVE RELIEF

Low	<100m	0.3
Medium	101-300m	0.6
High	>300m	1.0

LANDUSE AND LAND COVER

Agricultural land	0.65
Thickly vegetated forest area	0.80
Moderately vegetated area	1.2
Sparsely vegetated area	1.5
Barren land	2.0

SURFACE WATER CONDITIONS

Flowing	1.0
Dripping	0.80
Wet	0.5
Damp	0.2
Dry	0.0

NOTE: The correction factor C_1 (highly weathered), C_2 (moderately weathered) and C_3 (slightly weathered) should be multiplied with the fresh rock to get the corrected rating.

For rock type-I, $C_1 - 4$, $C_2 - 3$ & $C_3 - 2$

For rock type-II, $C_1 - 1.5$, $C_2 - 1.25$ & $C_3 - 1$

α_j - dip direction of joint, β_j - dip of joint
 α_i - direction of line of intersection of two joints β_i - plunge of line of intersection of two joint planes
 α_s - direction of slope β_s - inclination of slope

If the rocks are weathered, the correction factors C_1 , C_2 or C_3 , depending on the extent of weathering, should be multiplied to the ratings of rock types (Table 4.15).

Structure : The stability of slopes is greatly influenced by the disposition of the structural discontinuities, such as joints, beddings, foliation planes, in relation to slope. In the present method, three types of relations are considered.

- (i) The extent of parallelism between the slope direction and the direction of discontinuity or of the line of intersection of two discontinuities. This is determined from $\alpha_j - \alpha_s$ or $\alpha_i - \alpha_s$.
- (ii) The steepness of the dip of the discontinuity (β_j) or of the plunge of line of intersection of two discontinuities (β_i).
- (iii) The difference between the inclination of the slope and the dip of discontinuity or plunge of the line of intersection of the two discontinuities.

This is determined from $\beta_j - \beta_s$ or $\beta_i - \beta_s$.

The chances of failure enhance as the discontinuity, or the line of intersection of two discontinuities, tends to be parallel to the slope. Where the dip of the discontinuity or plunge of the line of intersection of two discontinuities increases, the chances of failure increases, because the angle of friction for the discontinuity surface may be reached. Based on these observations, the LHEF ratings have been assigned for the above described structural relation with slope.

Slope morphometry : This is the same slope parameter as used in the earlier schemes. The slope categories are escarpment/cliff ($>45^\circ$), steep slope ($35^\circ-45^\circ$), moderately steep slope ($25^\circ-35^\circ$), gentle slope ($15^\circ-25^\circ$) and very gentle slope ($<15^\circ$).

Relative relief : As already defined, the relative relief is the local relief of maximum height between the highest point and the lowest point in unit area. Under LHEF approach, three categories of relative relief have been chosen namely low ($<100\text{m}$), medium ($101-300\text{ m}$) and high ($>300\text{m}$).

Landuse and landcover : Land cover is an indirect indication of the stability of hill slopes. As in the previous two methods, five categories of landuse have been considered, i.e., agricultural land, thickly vegetated forest area, moderately vegetated area, sparsely vegetated area and barren land. The barren and sparsely vegetated areas show faster erosion and greater instability in comparison to the thickly vegetated land which is less prone to mass wasting

processes. Forest cover, in general, reduces the action of climatic agents on the slopes and protects them from the effects of weathering and erosion. Agricultural land has been considered as stable land. So based on the density of vegetation cover, the LHEF ratings have been awarded.

Surface water condition : The evaluation of behaviour of the hydrological condition on hill slopes is not possible over large areas. However, the nature of surface indication of the behaviour of sub-surface water provides valuable information on the stability of hill slopes for hazard mapping purposes. Surface indication of water, such as flowing, dripping, wet, damp and dry have been considered and LHEF ratings have been assigned.

After assigning the weightages, the total estimated hazard (TEHD) is calculated facet wise, depending on the categories of the factors present. The TEHD (earlier described as score) indicates the degree of instability and is obtained by adding the ratings of the individual categories of factors considered in the LHEF rating scheme.

TEHD = sum of ratings of the categories of lithology, structure, slope, relative relief, landuse and surface water in a facet

The computed TEHD is classified into the five classes, given below, of landslide hazards - very low hazard (VLH), low hazard (LH), moderate hazard (MH), high hazard (HH) and very high hazard(VHH).

Hazard class	TEHD values
Very low hazard	<4
Low hazard	4 - 5
Moderate hazard	5 - 6
High hazard	6 - 7
Very high hazard	>7

4.4.2 DATA PROCUREMENT AND PROCESSING

In this method the different facets are considered as map unit in terms of which the landslide hazard assessment is carried out. Hence, a facet map of the sub-area is prepared with natural topographical boundaries (Fig. 4.7). The sub-area is divided into 121 facets and each facet is referred by a number. The facet map shows average slope inclination of each facet. For all these facets, the data of each factor considered are collected.

The lithological data is collected from the geological map. The degree of weathering is noted during the field investigation and is classified into high, moderate, low and nil. Similarly, the slope, relative relief and landuse data are generated facetwise from the already prepared factor maps (chapter 3) and the detailed field study. The surface indications of damp, wet, dripping and flowing conditions are judged in the field and data are accordingly recorded. The most important data, i.e., the disposition of discontinuities on the slope and measurements of attitude of beds and joints are taken. With these data, a structural map, shown in Fig. 4.8, is prepared. It represents the prominent bedding and joint directions of the rock beds present in each facet. To establish the relation between slope face and discontinuity planes, these structural data along with the slope data are analysed in stereo net. From this analysis, the values of $\alpha_j - \alpha_s$, $\beta_j - \beta_s$, $\alpha_i - \alpha_s$, $\beta_i - \beta_s$, β_j and β_i are determined.

After collecting these data, the numerical weightages, following the rating scheme (Table 4.15), are assigned to each facet according to the categories of the factors present in the facet. Finally the weightages are added to arrive at a total estimated hazard (TEHD) which is the score for landslide potential for each facet. It is found that the minimum TEHD is 3.4 for the facet number 60 while the maximum TEHD is 8.1 for the facet number 47.

4.4.3 HAZARD CLASSES AND ZONATION MAP

The landslide hazard zonation map of the sub-area is prepared by ranking the TEHD of each facet into different classes of hazard as described earlier. The hazard zonation map, DRZ, prepared using this scheme is shown in Fig. 4.9. It shows all the facets with their classes of hazard. It is found that out of the 121 facets, 49 facets are in moderate hazard class, 31 in high hazard, 24 in low hazard, 11 in very high hazard and 5 in very low hazard class. A percent area calculation of hazard zones revealed 13.36% in very high, 25.36% in high, 35.41% in moderate, 20.05% in low and 5.28% in very low hazard class.

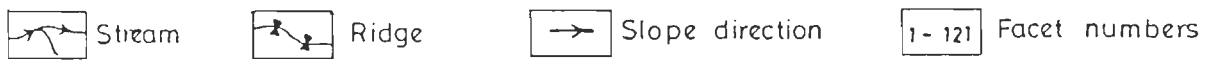
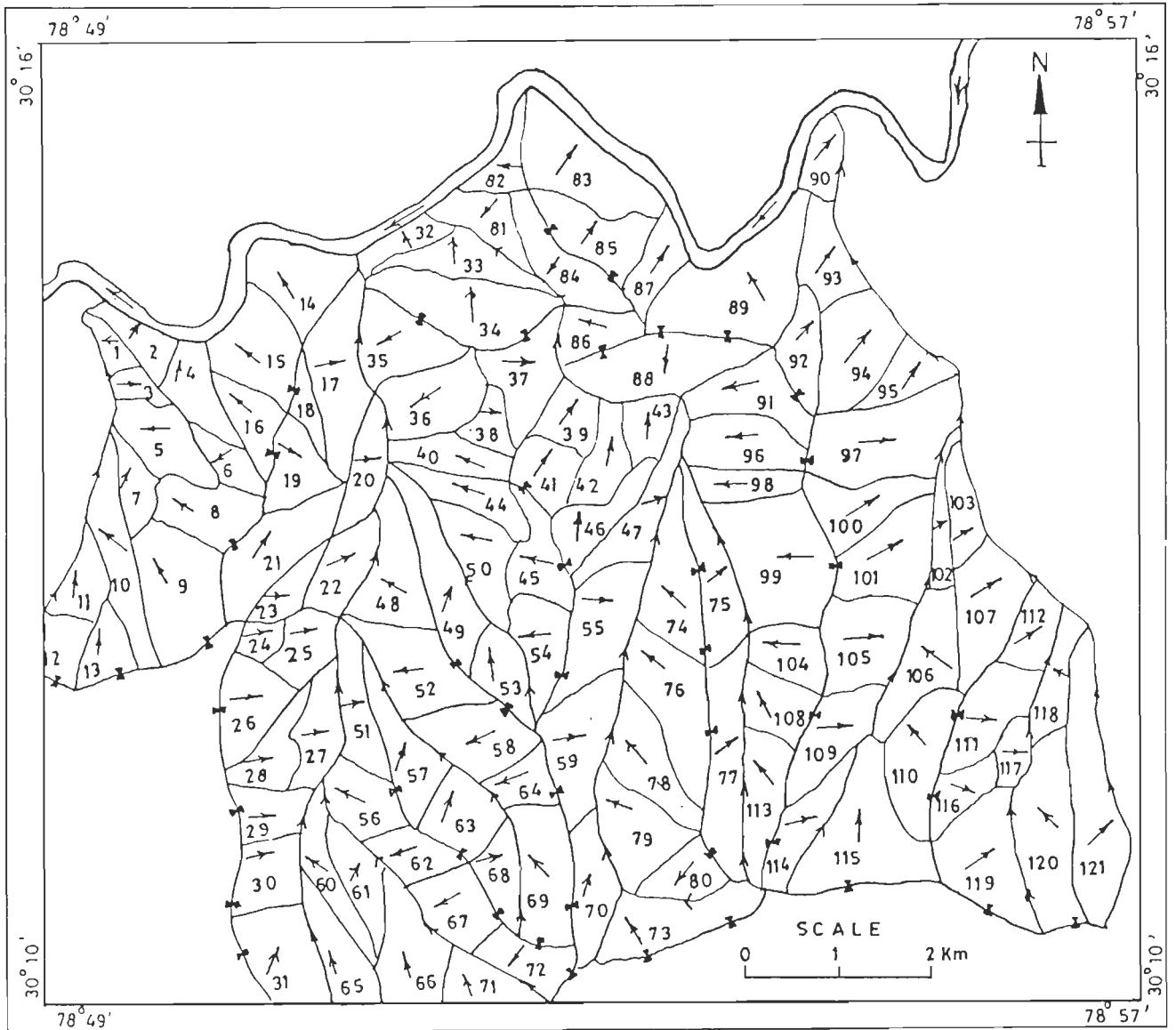


Figure 4.7 Facet map of the sub-area

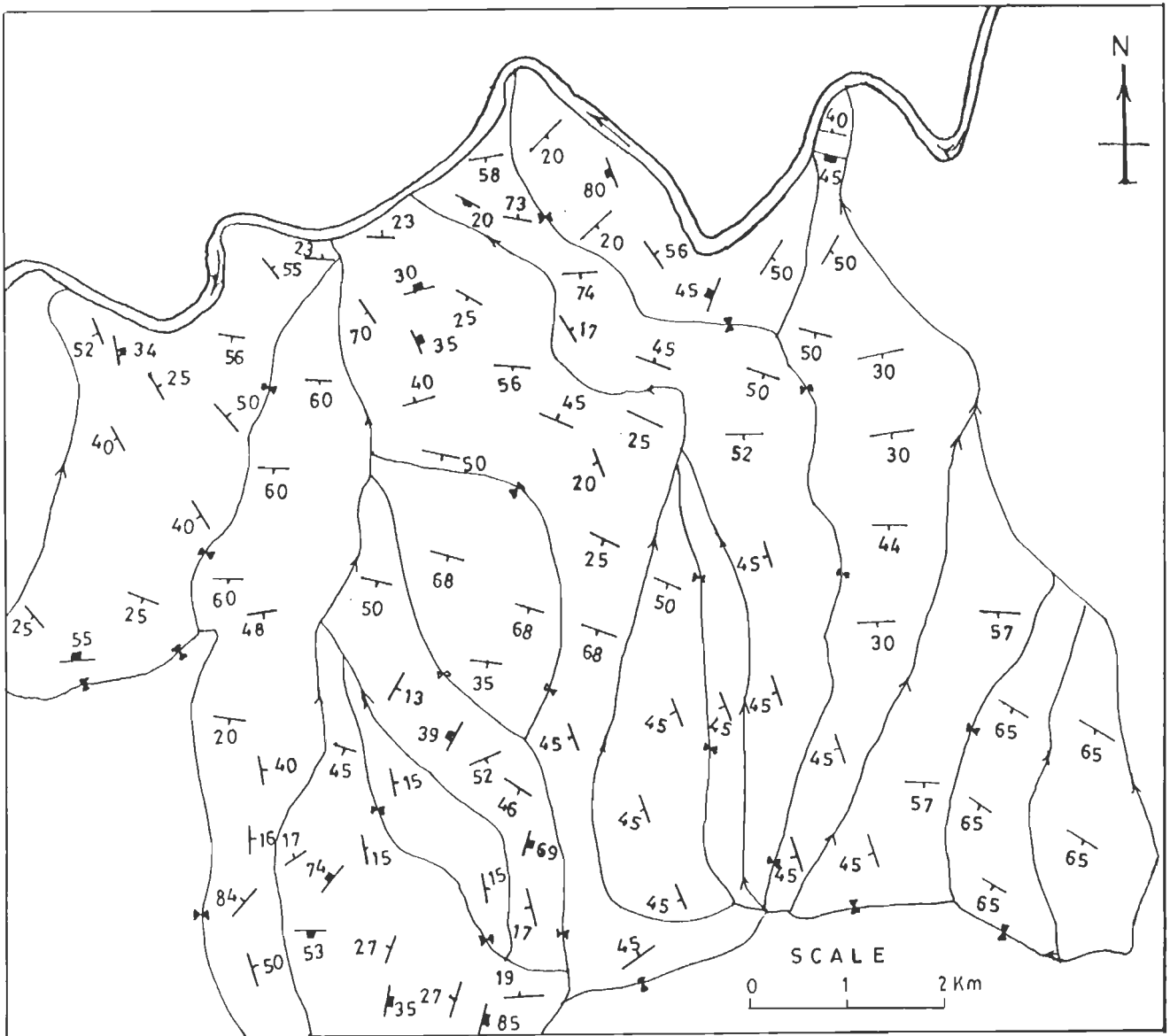


Figure 4.8 Structural map of the sub-area showing attitude of discontinuities

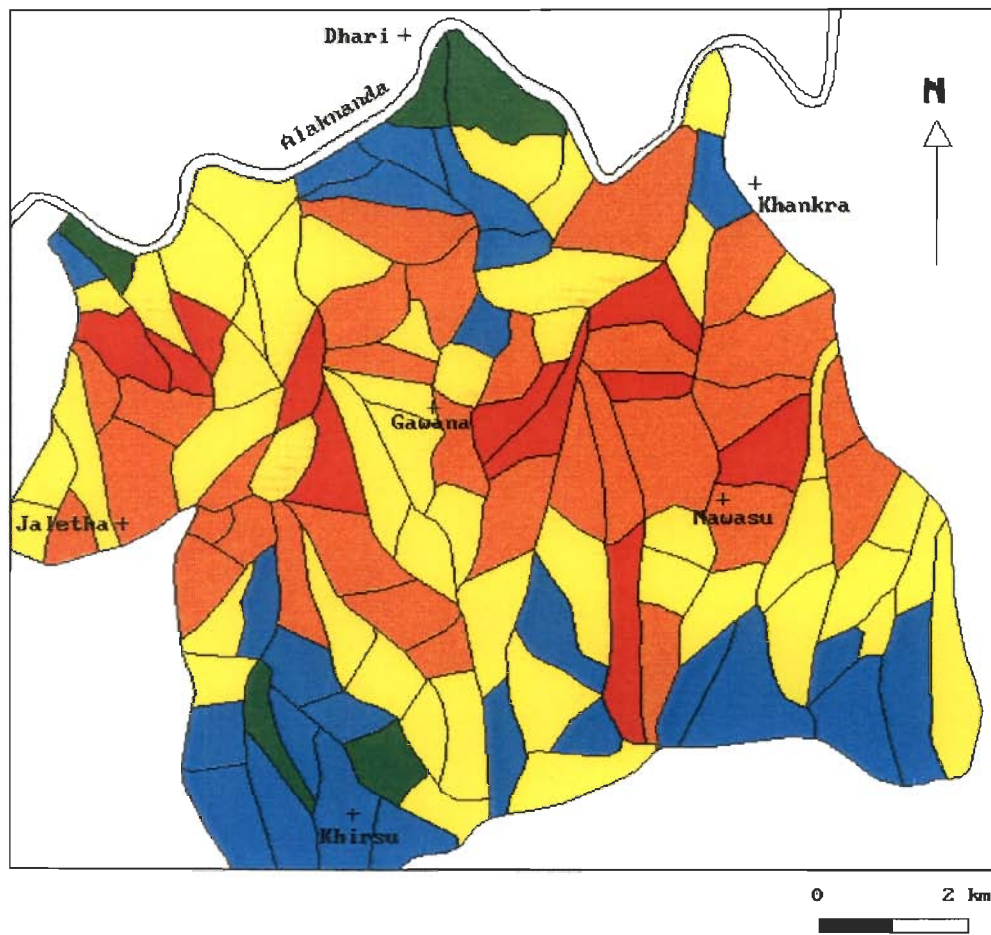
The very high hazard zone in DRZ map, comprising the few facets in the middle of the area such as east and west of Gawana village, north and south-west of Nawasu village and south east of Swit village. The high hazard zones are surrounding the facets of very high hazard class. Near Dhari, along the Alaknanda, there is a big facet of very low hazard zone adjacent to which are moderate and high hazard zones in upstream direction. The extreme south of the map has facets of low hazard class with two facets of very low hazard. Overall, it indicates that the middle part is more prone to landslide activities than the southern and northern parts. The significant point to note here is that, the facet number 89 in which the Kaliasaur landslide is located is coming in high hazard class in this map. However, the landslide is positioned near the boundary of moderate and high hazard zone. Further, the score obtained for this facet is 0.62 which is very close to the boundary of moderate and high hazard class (0.6). So, it is inferred that the area around the Kaliasaur slide is lying in moderate to high hazard class. Since in this method more field data are collected, it has been possible to demarcate the hazard classes of small parts.

4.4.4 VALIDATION OF MAP

The DRZ map is also evaluated for its validation and the values of HI are tabulated in the Table 4.16. The table shows that the HI for very high hazard is 4.28 and that for the very low hazard it is 0. Here also not only the trend of HI values shows an increasing trend as the degree of hazard class increases but there also exist reasonably good separations between the various classes. Hence, this map also shows a good quality.

Table 4.16 Hazard Index for DRZ map

Hazard Class	Area (km ²)	Number of landslides	Class landslide density Index (CI)	Hazard Index (HI)
Very low	4.54	0	0.00	0.00
Low	15.64	2	0.13	0.42
Moderate	27.62	20	0.72	2.30
High	19.78	23	1.16	3.71
Very high	10.42	14	1.34	4.28



Hazard Class

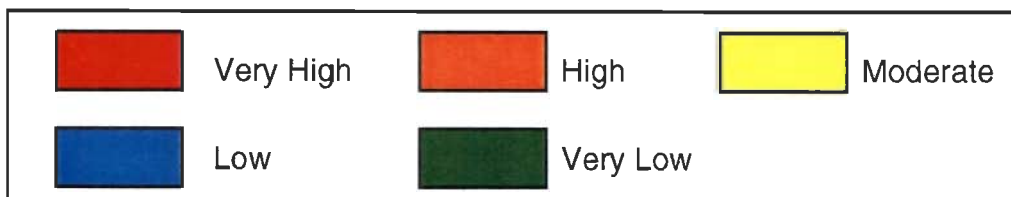


Figure 4.9 DRZ map of the sub-area showing landslide hazard zones

4.5 COMPARATIVE STUDY OF ZONATION MAPS

A comparative study of the zonation maps prepared by the three techniques is carried out to estimate the degree of similarity in them. First, the SRZ and ORZ maps for the entire study area are compared. The sub-area maps obtained using the three techniques are then compared with a view to identify how much detailed information contents of the DRZ map can be inferred from the SRZ and ORZ maps.

4.5.1 PARAMETER FOR COMPARISON

The comparative study of any two maps is initiated by a qualitative comparison of trends of various zones in the two maps. Since there are five hazard classes in all the maps, a parameter number of cells differing in hazard class (NCD) is obtained by determining the number of cells that are deviating by one or more hazard classes. The maximum hazard class difference possible is of four classes. For example for a particular cell, the hazard class difference of 1 means that if the cell lies in the moderate hazard class in one map then it will lie either in low or in high hazard class in the other map. It is to be noted that hazard classes in all the maps prepared are ordinal in nature, therefore it is quite likely that the adjacent classes in two maps overlap. Hence, an NCD value of 1 should not be treated as depicting significant difference between the two maps. Further, from the NCD values Mean Deviation per Cell (MDC) can be obtained as the weighted average of NCD values.

$$MDC = \sum_{i=1}^{n-1} [i \times NCD(i)] / (\text{number of cells})$$

where, i - hazard class difference
NCD - number of cells differing
 n - number of class

From the value of MDC the degree of similarity between the maps can be gauged.

4.5.2 COMPARISON BETWEEN SRZ AND ORZ MAPS

The SRZ and ORZ maps show very similar trends, particularly in the zones of very high and high hazards. In both the maps these zones fall to the south of the Alaknanda and close to the NAT. There is a little difference on the north-west part of the area where low hazard

zones of ORZ map has been replaced, to some extent, by moderate hazard zones in the SRZ map. The data pertaining to NCD and MDC of these two maps are given in the Table 4.17.

Table 4.17 Comparison of cells for SRZ and ORZ maps

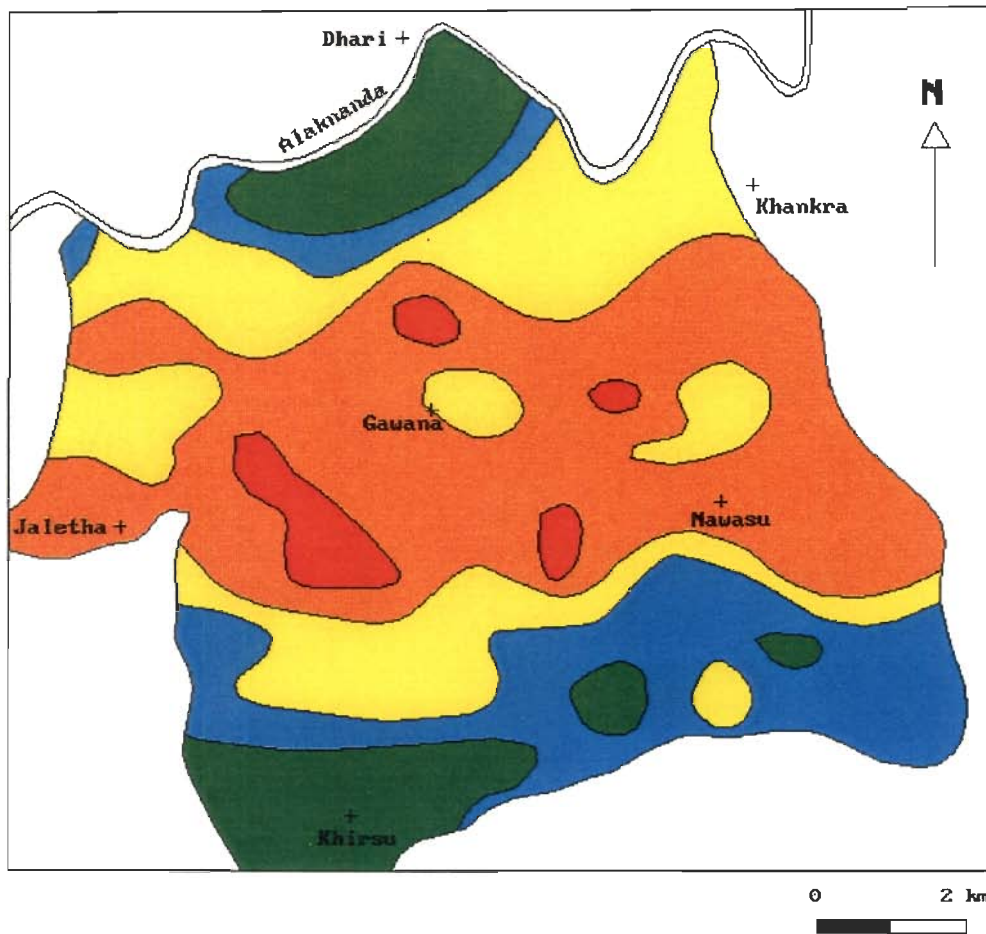
Hazard class difference (i)	Number of cells differing (NCD)	Mean Deviation per Cell (MDC)
1	779	0.48
2	32	
3	7	
4	0	

Out of 1776 cells, 818 cells (46.06 %) differ in their hazard classes. Of these, 779 cells (43.86 %) differ only by one class which should not be treated as a significant difference. The difference of one class could be due to the difference in class boundaries. This suggests that the two maps are in close agreement. The MDC computed for these maps is 0.48.

4.5.3 COMPARISON OF SUB-AREA MAPS FROM THREE TECHNIQUES

In order to compare the sub-area zonation in SRZ and ORZ maps with the DRZ map, the sub-area parts of the two maps are enlarged to the same scale of DRZ map and are named as SRZ1 map (Fig. 4.10) and ORZ1 map (Fig. 4.11). Since in DRZ map, the different zones of hazards are in the form of facets, it is contoured, for the comparison purposes, after obtaining, the scores for each cell of the sub-area (as used in other two techniques) from the scores of the facets in DRZ map. In the process it is found that at few locations a single cell contains parts of two facets, in such cases the average score of the two facets is considered. The scores are then contoured at class boundaries of DRZ technique to get the zonation map which is named as DRZ1 map (Fig. 4.12). This is the same map as DRZ, however, due to interpolation for contouring, shapes of zones are changed a little.

A glance at these three maps reveal broadly similar trends for zonation. However, the



Hazard Class

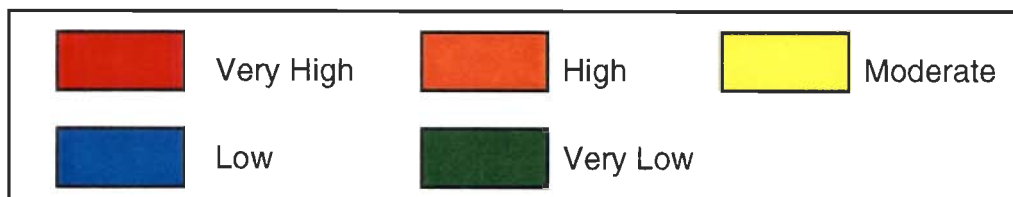
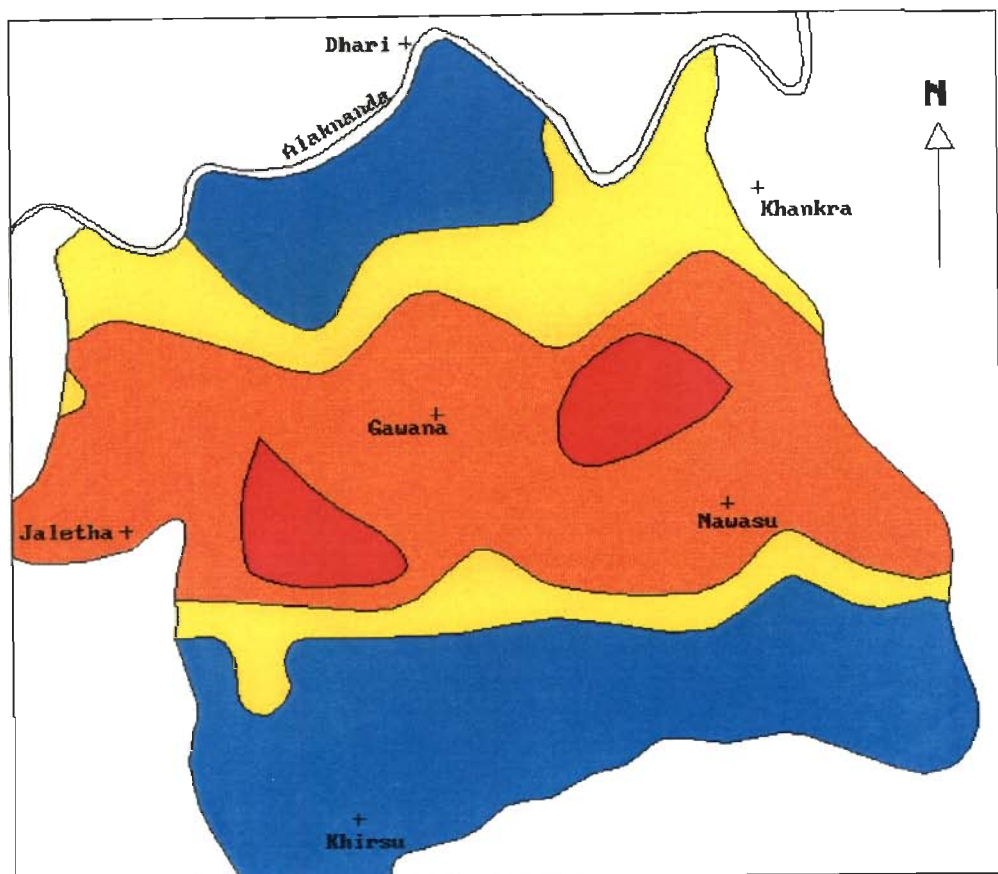


Figure 4.10 SRZ1 map of the sub-area showing landslide hazard zones



Hazard Class

0 2 km

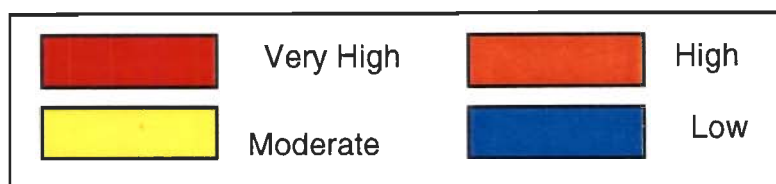
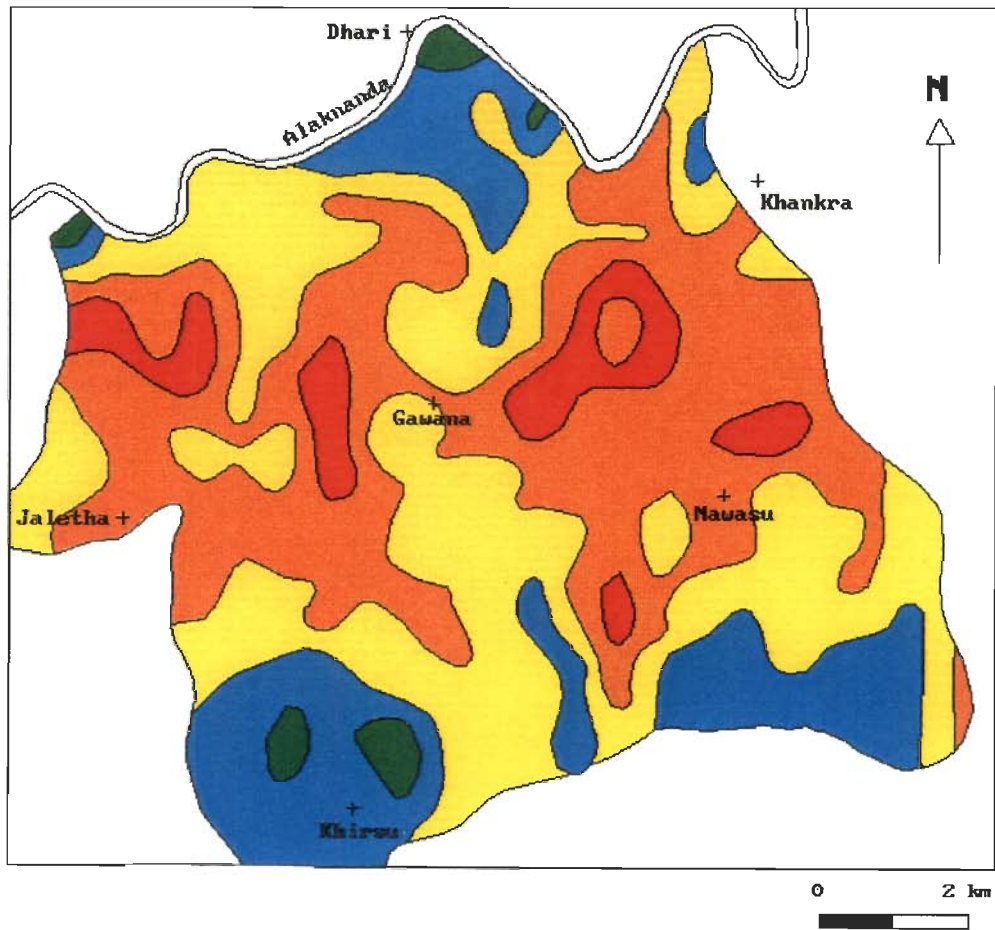


Figure 4.11 ORZ1 map of the sub-area showing landslide hazard zones



Hazard Class

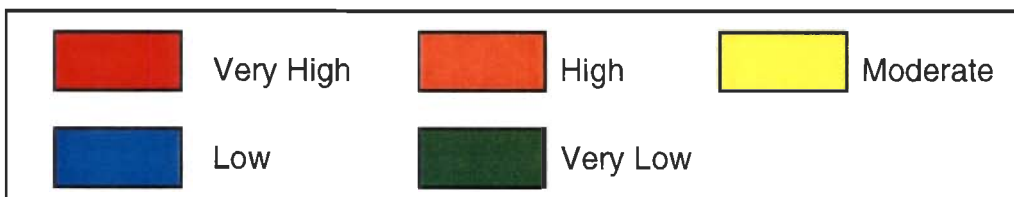


Figure 4.12 DRZ1 map of the sub-area showing landslide hazard zones

DRZ1 map has more detailed zonation than the SRZ1 and ORZ1 maps. The broad trend of high hazard zone as seen in the DRZ1 map can be easily identified in SRZ1 and ORZ1 maps. In DRZ1 map, some portion of the high hazard zone in the central part has got replaced with the moderate hazard zone. Further, there is a little extension of high hazard towards the river bank where the Kaliasaur slide is located. So it can be said that the maps produced by SRZ and ORZ techniques contain considerable detailed information as found from the map produced by the DRZ technique.

The comparison of these maps are then analysed with the number of differing cells in hazard classes. For this, the data pertaining to NCD and MDC for different pairs of maps are tabulated in the Table 4.18.

Table 4.18 Comparison of cells for sub-area maps

Hazard class difference (i)	SRZ1 - ORZ1		ORZ1 - DRZ1		SRZ1 - DRZ1	
	NCD	MDC	NCD	MDC	NCD	MDC
1	142	0.537	155	0.680	166	0.735
2	20		35		37	
3	1		3		3	
4	0		0		1	

The data for SRZ1 - ORZ1 maps show that out of the 344 cells, 163 cells (47.38%) are differing in hazard classes. In this case also it is observed that the majority of cells, i.e., 142 cells (41.28%) are differing by one hazard class implying that good agreement still exists between these maps. When ORZ1 - DRZ1 maps are compared it is found that out of the 193 differing cells (56.1%), 155 cells (45.06%) are differing by one hazard class. Hence, there exists a close agreement between these maps but comparatively less than that in the previous pair. The NCD values for SRZ1 - DRZ1 maps reveal that 207 cells (60.17%) are differing in total and out of these 166 cells (48.26%) are differing by one class. In this case the degree of agreement is quite reasonable but lower than that in the previous two cases. Since, in all the

cases, majority of NCD values differ only by one hazard class, it can be said that all the maps broadly show a good agreement with each other. However, the results of ORZ1 - DRZ1 are more compatible than of the SRZ1 - DRZ1 case.

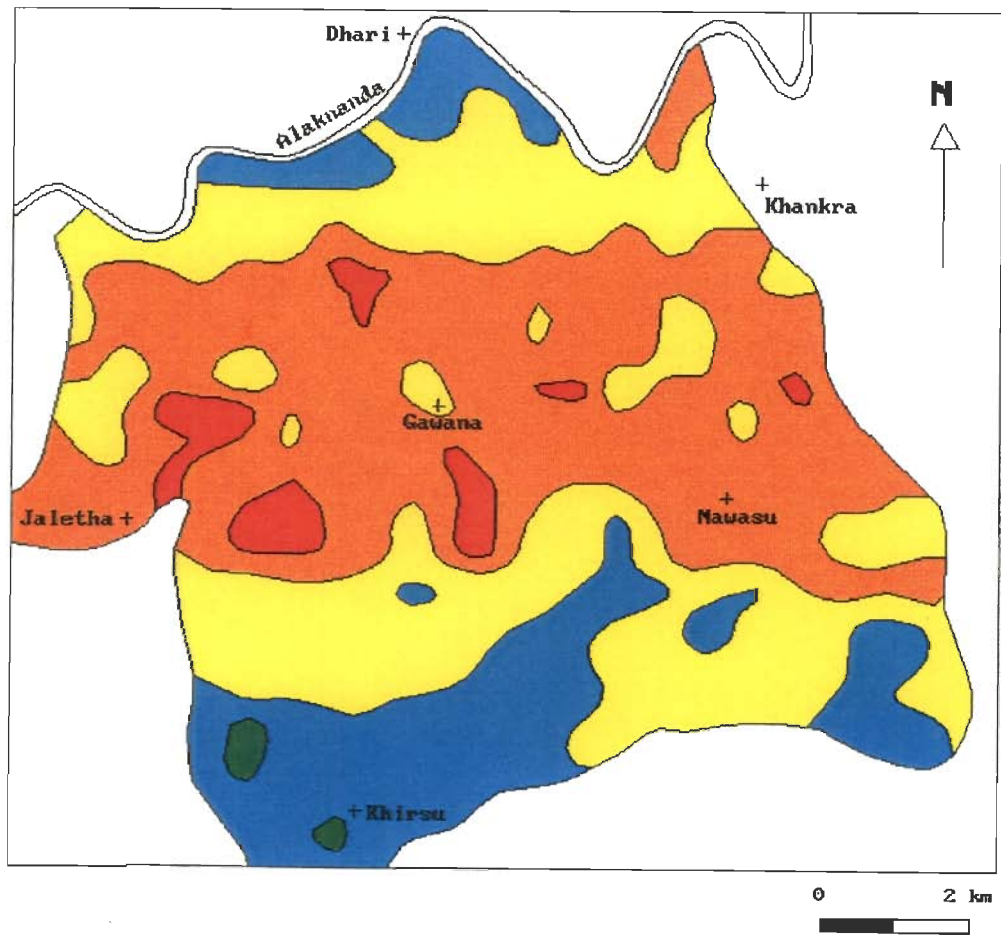
When the values of MDC are compared for the three pair maps, same inference is reached at. The MDC (0.537) is least for SRZ1 - ORZ1 and largest (MDC = 0.735) for SRZ1 - DRZ1. So, for the sub-area, here it can be stated that the SRZ1 and ORZ1 maps show close match and the DRZ1 map is closer to the ORZ1 map than to the SRZ1 map. Since the same set of factors and categories have been used in both SRZ1 and ORZ1 maps, the disagreement between the two can be attributed to the different modes of defining the ratings and the class boundaries of hazard zones. The larger disagreement between SRZ1 - DRZ1 and between ORZ1 - DRZ1 is because of the additional difference in the choice of factors and their categories.

4.5.4 COMPARISON OF MAPS WITH IDENTICAL CLASS BOUNDARIES

In order to reduce the impact of different classifications for hazard classes, an attempt is made to view the zonation maps of the sub-area with same class boundaries. To achieve this, it is necessary to convert the scores of different techniques on to one scale. Since an effort has been made for objective classification in ORZ technique, the class boundaries of ORZ map are selected as standard for the scaled scores. Hence, the scores of SRZ1 and DRZ1 are scaled to 0-99 scale to bring the three maps on to the same scale. The two zonation maps SRZ2 and DRZ2 are then prepared by employing scaled scores and the ORZ class boundaries. These are shown in Fig. 4.13 and Fig. 4.14 respectively.

In SRZ2 map the central portion of the area falls in high hazard class at same locations as in the SRZ1 map. There are few zones of very high hazard within the high hazard zone. The northern and the southern boundaries of the area are marked by low hazard zones which are separated from the high hazard zone by moderate hazard zones. So, although the classification boundaries have been changed, yet the trends of the various zones are broadly similar to those in the SRZ1 map barring the minor differences in areal extent of different zones.

The DRZ2 map shows a very wide zone of moderate hazard class in which there are several zones of high hazard class. There are zones of low hazard at the northern and southern boundaries of the area. The hazard zones of this map are at variance with those of the DRZ1



Hazard Class

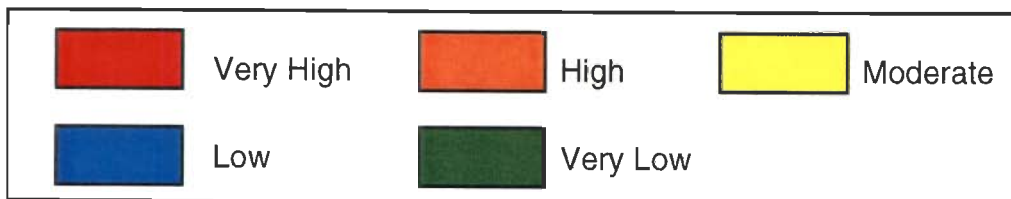
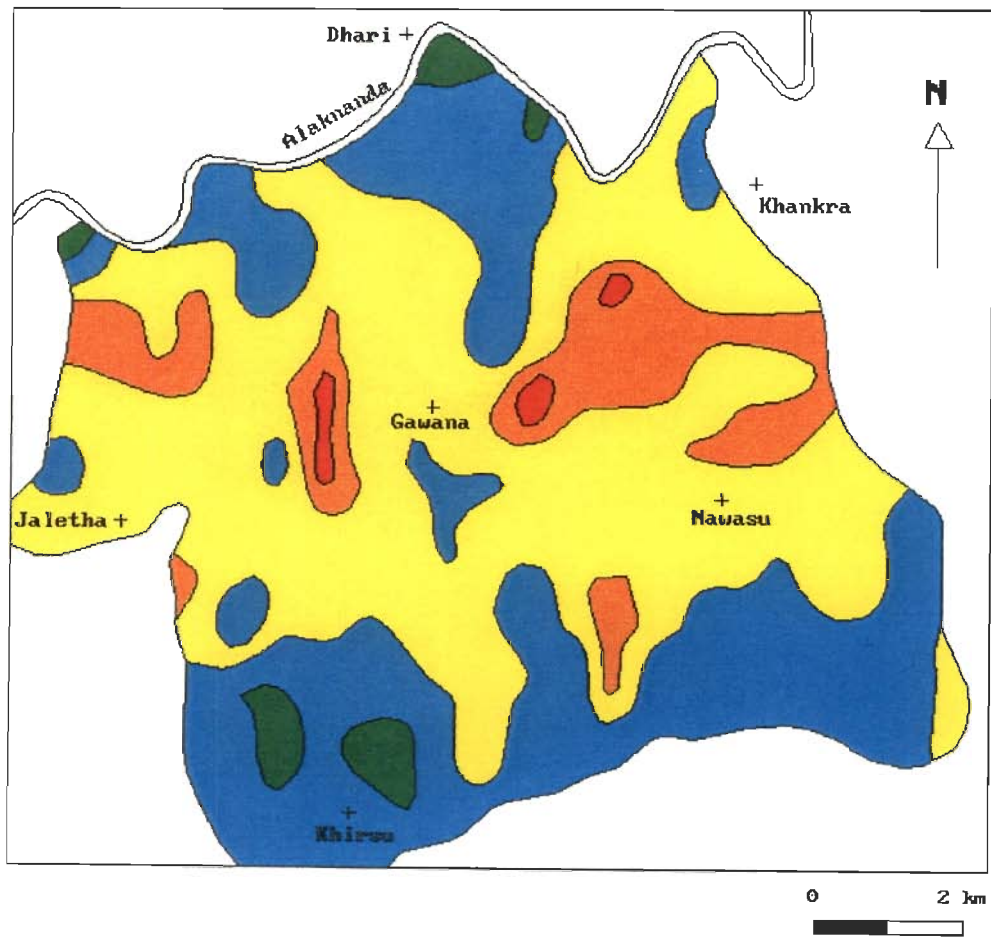


Figure 4.13 SRZ2 map of the sub-area showing landslide hazard zones when class boundaries of ORZ map are used



Hazard Class

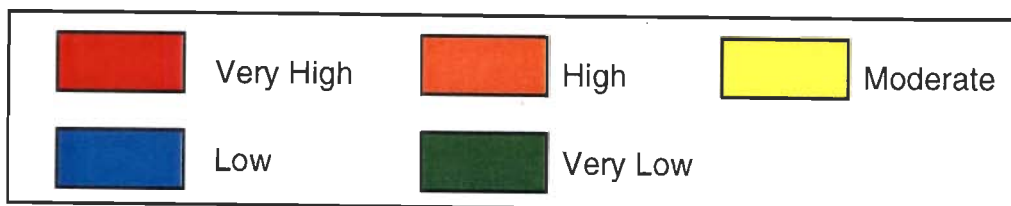


Figure 4.14 DRZ2 map of the sub-area showing landslide hazard zones when class boundaries of ORZ map are used

map. The very high hazard zones of DRZ1 map get transformed into high hazard zones in DRZ2 map and the zones of high hazard are merged into moderate hazard class. So, it can be said that the changes in the classification has resulted in changes in the zones of hazard. By imposing the class boundaries of ORZ map on the scores of DRZ map, the resulting level of degree of hazard has been somewhat lowered.

The three zonation maps, SRZ2, ORZ1 and DRZ2, when observed carefully reveal close similarity of zonation trends between SRZ2 and ORZ1 but the DRZ2 map shows considerably different trends of zones. For the three pairs of maps the data of number of cells differing in hazard class are given in the Table 4.19.

Table 4.19 Comparison of cells for sub-area maps with similar classification

Hazard class difference (i)	SRZ2 - ORZ1		ORZ1 - DRZ2		SRZ2 - DRZ2	
	NCD	MDC	NCD	MDC	NCD	MDC
1	134	0.436	149	0.688	189	0.770
2	8		41		35	
3	0		2		2	
4	0		0		0	

The table shows that for the pair SRZ2 and ORZ1, out of the 344 cells only 142 cells (41.28%) are differing in hazard class and of these, 134 cells (38.95%) are differing by one hazard class. The MDC for this pair is 0.436. So these maps show a closer agreement than the SRZ1 and ORZ1 maps where different class boundaries are used. The total NCD of the ORZ1 - DRZ2 and SRZ2 - DRZ2 maps are 192 (55.81%) and 226 (65.7%) respectively. The cells having class difference of 1 are 149 (43.31%) for ORZ1 - DRZ2 and 189 (54.94%) for SRZ2 - DRZ2. The NCD values suggest a broad general similarity as found in the earlier ORZ1 - DRZ1 and SRZ1 - DRZ1 maps. However, DRZ2 map has better agreement with ORZ1 map than with SRZ2 map. This could again be confirmed by looking at the MDC values which is more for SRZ2 - DRZ2 pairs.

From this study, it is evident that the use of identical class boundaries improves the agreement only if the two techniques have identical set of factors and categories. This exercise exhibits the importance of judicious choice of class boundaries for zonation.

4.6 SUMMARY

Landslide hazard zonation study has been carried out by three different techniques. The SRZ technique, though based on several subjective steps, has produced a good quality map. The ORZ technique has been developed to induct some amount of objectivity and the resulting hazard zones are found to match with existing landslide hazards. The DRZ technique, based on detailed field study, when applied to a small part of the area, has provided more detailed information about the hazard zones. These maps can be very useful for planning any hill development programs.

The three methods are compared at different levels. The SRZ and ORZ maps for the area have shown similar zonation trends, particularly in case of very high and high hazard zones which are lying to the south of Alaknanda river. From these maps it is found that the area to the north of Alaknanda lies mainly in moderate to low hazard zones. The comparison has also been made by analysing the number of cells differing in hazard class and its mean deviation.

When SRZ1, ORZ1 and DRZ1 maps for the sub-area are compared pairwise, it is found that all the three maps show a broadly similar trend of zonation and considerable amount of information present in the DRZ1 map can be obtained from the SRZ1 and ORZ1 maps. A more detailed analysis based on the number of cells differing in hazard class has shown higher degree of agreement between ORZ1 and DRZ1 maps than between SRZ1 and DRZ1 maps. Further, the SRZ2 and DRZ2 maps are produced using the ORZ class boundaries. SRZ2 has zonation trend similar to SRZ1 but DRZ2 trends differ from DRZ1. This highlights the importance of selecting class boundaries.

At the end, it can be concluded that the aim of regional zonation, i.e., an appraisal of landslide hazard zones, can be achieved by the SRZ and ORZ techniques in a short duration based on subjective and objective methodologies respectively. The detailed zonation can be carried out for small area using the DRZ technique which involves intensive field study.

SLOPE STABILITY ASSESSMENT USING SMR TECHNIQUE

Landslide hazard zonation map provides a regional assessment of slope failure and can be used for identification of landslide potential zones. The broad hazard classes of the map represent gross-characteristics of a region and in general, do not reflect stability conditions of any individual slope. For the study of an individual slope, the site specific slope stability assessment techniques have to be employed.

The conventional limit equilibrium methods determine the stability of slopes by evaluating the factor of safety. These methods are based on analysis of slopes, incorporating several engineering parameters of the slope material. This involves collection of samples, evaluation of shear strength properties under field conditions and subsequent slope stability analysis. Obviously, this is a detailed investigation process and hence requires significant amount of time and resources. However, there is always a need for a method which can be carried out rapidly for preliminary assessment of slope stability. One such method is the Slope Mass Rating (SMR) technique developed by Romana (1985). This technique is primarily based on field data and is comparatively fast. Hence, the SMR technique is used here for stability assessment of individual slopes.

This method has been applied mainly for identifying unstable slopes along Srinagar-Rudraprayag road. Thirty slopes, each numbered for reference, shown in the Fig. 5.1, are considered for stability assessment. The slopes are selected in such a way that these represent different stability conditions. In this chapter, the SMR technique is described in detail, followed by the stability assessment of slopes.

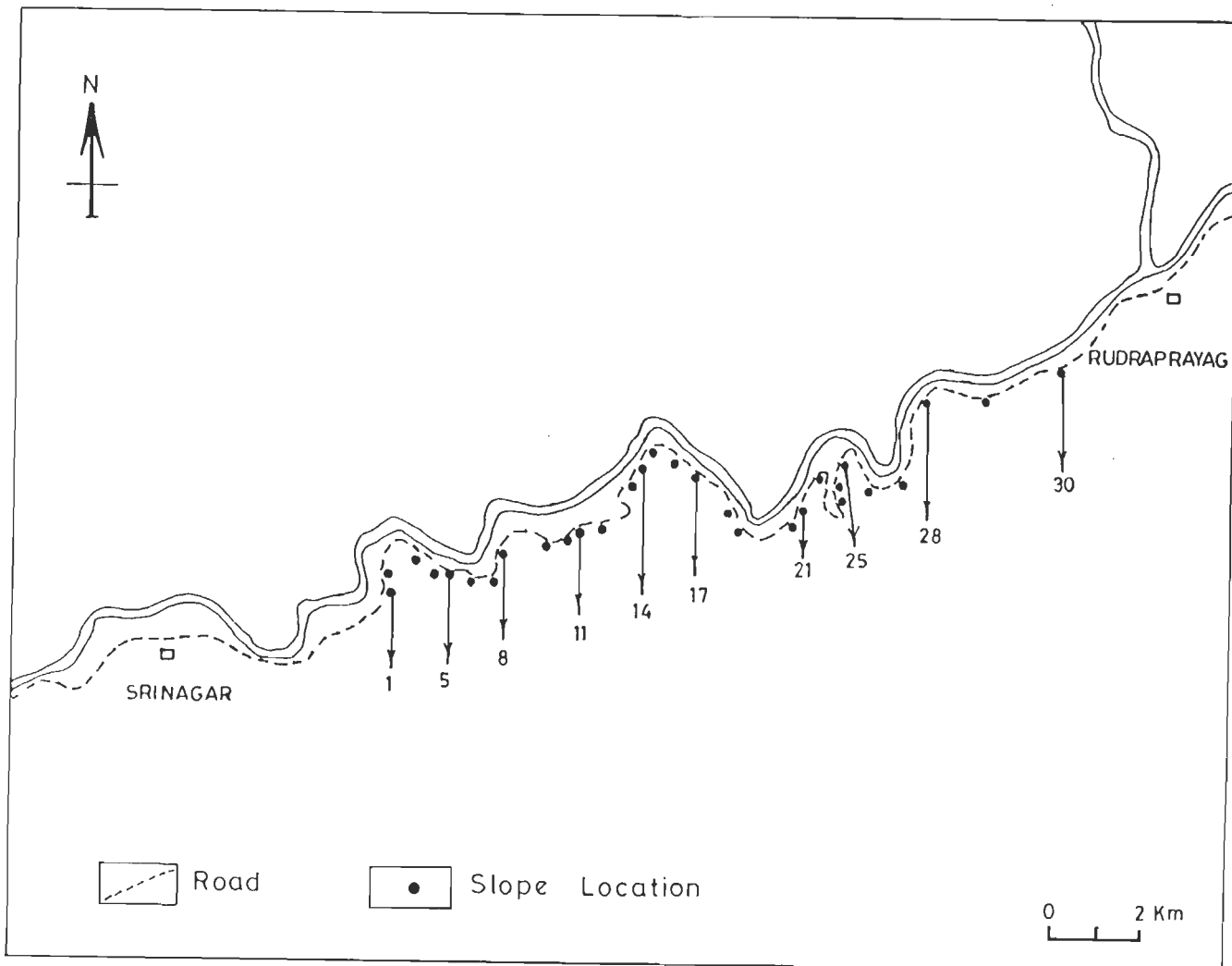


Figure 5.1 Slope locations along Srinagar-Rudraprayag road

5.1 SLOPE MASS RATING TECHNIQUE

Romana (1985) developed the Slope Mass Rating technique for stability assessment of the rock slopes. The method is primarily based on the application of Rock Mass Rating (RMR), developed by Bieniawski (1979). Recognizing that the rock slope stability is governed by the behaviour of discontinuities and that in the original Rock Mass Rating system (Bieniawski, 1979) the specific guidelines for favourability of joint orientations were lacking, Romana developed a factorial approach to rating adjustment based on the field data. This approach is suitable for preliminary assessment of slope stability in the rocks, including the very soft or heavily jointed rock masses (Bieniawski, 1989). Romana obtained the SMR from the RMR_{basic} by subtracting the newly proposed adjustment factor for joint orientation and adding a new adjustment factor for the method of excavation. Operation of subtraction is an explicit manifestation of the fact that the adjustment factor of joint orientation is negative. However, in the present study the negative sign of this factor is accounted algebraically, as a result, the SMR is obtained from RMR_{basic} as follows:

$$SMR = RMR_{basic} + (F_1 \times F_2 \times F_3) + F_4$$

where, F_1, F_2, F_3 - adjustment ratings for joints
 F_4 - adjustment rating for excavation method

The SMR values range from 0-100. This range has been classified into five different stability classes as discussed in section 5.8.

5.1.1 ROCK MASS RATING SYSTEM

The Rock Mass Rating (RMR) system, also known as Geomechanics Classification, was developed by Bieniawski (1973) and has since been modified over the years as more and more case histories became available (Bieniawski, 1979). There are modifications and extensions of RMR in different fields such as mining application, dam foundations, tunneling and hill slope stability. Romana (1985) has considered the RMR_{basic} for slope stability assessment which depends on the following five basic parameters of Rock Mass Rating system.

1. Uniaxial Compressive Strength (UCS) of rock mass
2. Rock Quality Designation (RQD)



3. Spacing of discontinuities
4. Condition of discontinuities
5. Groundwater condition

Each of these five parameters has been partitioned into five ranges of values. Since the various parameters are not equally important in overall classification of a rock mass, importance ratings are assigned to the different value ranges of the parameters, a higher rating indicating better rock mass condition (Beiniawaski, 1989). The ratings for different range values of each parameter are given in Table 5.1. The ratings for these five parameters are summed to yield the RMR_{basic} ranging between 0 -100.

5.1.2 ADJUSTMENT RATING FOR JOINT ORIENTATIONS

Romana (1985) introduced the adjustment rating for joints depending on the orientation of joints in relation to the slope. He used plane and toppling failure modes for the analysis. No special factors have been considered for wedge mode of failure, different from applied plane mode of failure. However, the present study considers plane and wedge failures as different cases, following the modifications incorporated by Anbalagan et al. (1992). The adjustment rating for joints is the product of the three following factors.

F_1 is a measure of parallelism between the slope face and the joint plane or the line of intersection between two joint planes, i.e., the difference between dip direction of joint or plunge direction of line of intersection between two joint planes and the slope direction. This rating ranges from 1.00, when these are near parallel, to 0.15, when the angle between them is greater than 30° .

F_2 depends on the dip of the joint plane or the plunge of the line of intersection between two joint planes. Its rating value varies from 1.00 for a joint plane dipping more than 45° to 0.15 for a joint plane dipping less than 20° .

F_3 depends on the relation between the dip of the slope face and dip of the joint plane or plunge of the line of intersection of two joint planes. This rating value ranges from 0, when slope dips less than 10° to joint plane or the line of intersection of two joint planes, to -60, when slope dips more than 10° to joint plane or the line of intersection of two joint plane.

The rating values for F_1 , F_2 and F_3 are given in Table 5.2.

Table 5.1 Rock Mass Rating of Bieniawski, 1979

Parameters		Ranges of values						
Strength of intact rock material	Point load strength index	>10 MPa	4-10 MPa	2-4 MPa	1-2 MPa	For this low range UCS test is preferred		
	Uniaxial compressive strength	>250 MPa	100-250 MPa	50-100 MPa	25-50 MPa	5-25 MPa	1-5 MPa	<1 MPa
Rating		15	12	7	4	2	1	0
RQD		90-100%	75-90%	50-75%	25-50%	<25%		
Rating		20	17	13	8	3		
Spacing of discontinuities		>2m	0.6-2m	200-600 mm	60-200 mm	<60mm		
Rating		20	15	10	8	5		
Condition of discontinuities		Very rough, not continuous, no separation, unweathered wall	Slightly rough, separation <1mm, slightly weathered walls	slightly rough, separation <1mm, highly weathered walls	slickensided or gauge <5mm thick or separation 1-5mm, continuous	soft gauge >5mm or separation >5mm, continuous		
Rating		30	25	20	10	0		
Ground water condition		completely dry	damp	wet	dripping	flowing		
Rating		15	10	7	4	0		

Table 5.2 Adjustment ratings for joint orientations (Romana, 1985)

Case	Very favourable	Favourable	Fair	Unfavourable	Very unfavourable
P $\alpha_j - \alpha_s$ W $\alpha_i - \alpha_s$ T $\alpha_j - \alpha_s - 180^\circ$	30°	30°-20°	20°-10°	10°-5°	<5°
P/W/T F_1	0.15	0.40	0.70	0.85	1.00
P β_j W β_i	<20°	20°-30°	30°-35°	35°-45°	>45°
P/W F_2	0.15	0.40	0.70	0.85	1.00
T F_2	1	1	1	1	1
P $\beta_j - \beta_s$ W $\beta_i - \beta_s$	>10°	10°-0°	0°	0°-(10°)	<-10°
T $B_j + \beta_s$	<110°	110°-120°	>120°	----	----
P/W/T F_3	0	-6	-25	-50	-60

P - Plane failure, W - Wedge failure, T - Toppling failure

α_s - slope direction,

β_s - slope angle,

α_j - joint dip direction,

β_j - joint dip,

α_i - plunge direction of line of intersection,

β_i - plunge of line of intersection

5.1.3 ADJUSTMENT RATING FOR METHOD OF EXCAVATION

The methods of excavation for slopes have been categorised into the following five classes by Romana(1985).

Natural slopes are more stable, because of the longtime erosion and built-in protection mechanisms.

Presplitting increases slope stability for half a class.

Smooth blasting, when well done, increases slope stability.

Mechanical excavation of slopes is often combined with some preliminary blasting. The plane of slope is difficult to finish. The method neither increases nor decreases slope stability.

Deficient blasting often with too much explosives, no detonation timing and/or non parallel holes, decreases stability.

The ratings (F_4) assigned to the excavation methods range from +15 (natural slope) to -8 (deficient blasting) and are given in Table 5.3.

Table 5.3 Adjustment rating for methods of excavation of slopes (Romana, 1985)

Method	Natural slope	Pre-splitting	Smooth blasting	Blasting/mechanical	Deficient blasting
F_4	+15	+10	+8	0	-8

5.2 FIELD DATA COLLECTION

The term discontinuity is, in general, used for any plane of weakness in a rock mass, along which there exists no or at most low tensile strength. It is a collective term commonly used to denote joints, bedding planes, foliation planes, shear zones and faults. In the present work the word 'joint plane' is used to imply discontinuities like bedding plane, foliation plane and joint plane. A detailed field investigation for these discontinuities is carried out for the 30 slopes selected for stability assessment. The parameters studied are the uniaxial compressive strength, the rock quality designation, the spacing of discontinuities, the condition of discontinuities, the ground water condition and the joint orientations. These parameters are briefly described here.

5.2.1 ROCK QUALITY DESIGNATION (RQD)

The Rock Quality Designation (RQD) is an index of rock quality, first introduced by Deere et al. (1967). It is based on the core recovery percentage in which all the pieces of sound core, 10 cm or greater in length, are counted as recovery and are expressed as a percentage of the total length drilled. This quantitative index has been widely used to identify the low quality rock zones. The small core pieces result from closely spaced discontinuities, faulting or weathering and these cause a decrease in rock quality. The following correlation between the RQD index and the engineering quality of the rocks was proposed by Deere (1968).

RQD%	Rock Quality
<25	Very poor
25-50	Poor
50-75	Fair
75-90	Good
90-100	Excellent

In the field, it is not always possible to get the drilled core for RQD. Palmstrom (1982) has suggested that if core is not available, the RQD may be estimated from the number of joints per unit volume, in which number of joints per meter for each joint set is added. The relation is as follows:

$$\text{RQD} = 115 - 3.3 J_v$$

where, J_v - number of joints per cubic meter

During field investigation, the number of joints per m^3 are counted at several locations in each slope. For a particular slope, the maximum number of joints per m^3 is considered for the analysis. The estimated RQD for each slope is tabulated in column 2 of Table 5.4. The highly jointed quartzite showing low RQD is shown in Plate 5.1.

Table 5.4 Joint parameters for RMR of the studied slopes

Slope No.	RQD (%)	Spacing (cm)	Condition of joints					Water condition
			Roughness	Weathering	Opening (cm)	Filling	Continuity (m)	
1	45.7	6.5-20	slickenside	high	0.4-0.5	present	>10	damp
2	75.4	8-19	smooth	high	0.3-0.5	absent	>10	dry
3	45.7	4-25	rough	slight	0.1-0.3	absent	<10	dry
4	75.4	27-50	slight	moderate	0.1-0.5	absent	>10	dry
5	68.8	5-24	smooth	high	0.3-1.2	present	>10	damp
6	22.6	2-5	rough	slight	0.1-0.2	absent	<10	dry
7	65.5	25-64	slight	moderate	0.1-0.4	present	>10	damp
8	16.0	3-10	slight	high	<0.1	absent	<10	dry
9	68.8	15-40	slickenside	high	0.1-0.4	absent	>10	damp
10	19.3	10-22	smooth	moderate	<0.5	absent	>10	damp
11	55.6	25-50	slight	moderate	0.4-1.2	present	>10	dry
12	62.2	20-70	smooth	high	0.1-1.5	present	>10	damp
13	75.4	50-120	slight	slight	0.3-1	absent	>10	dry
14	82.0	29-55	very	slight	<0.2	absent	<10	dry
15	75.4	25-65	rough	slight	<0.1	absent	<10	dry
16	75.4	72-135	rough	moderate	0.1-0.6	absent	<10	dry
17	72.1	55-110	very	slight	0.1-0.5	absent	<10	dry
18	85.3	75-145	slight	unweathered	<0.1	absent	<10	dry
19	22.6	1-5	slickenside	high	0.3-0.5	present	>10	damp
20	55.6	27-40	slickenside	high	0.3-0.6	present	>10	damp
21	78.7	65-95	rough	unweathered	<0.1	absent	<10	dry
22	65.5	20-50	slight	slight	0.2-0.5	absent	<10	dry
23	72.1	18-44	very	slight	<0.1	absent	<10	dry
24	78.7	70-130	smooth	moderate	0.2-1	present	>10	damp
25	58.9	25-65	slight	high	0.1-0.4	absent	<10	damp
26	78.7	52-95	rough	slight	<0.2	absent	<10	dry
27	58.9	5-25	smooth	high	0.2-0.4	absent	>10	damp
28	65.5	55-75	smooth	high	0.3-0.6	present	>10	damp
29	82.0	8-22	slight	slight	<0.1	absent	<10	dry
30	85.3	24-58	rough	moderate	<0.2	absent	<10	dry

5.2.2 SPACING OF DISCONTINUITIES

The spacing of discontinuities is the perpendicular distance between the joint planes in a rock mass. It largely influences the overall rock mass quality and controls the size of individual blocks of intact rock. Several closely spaced joints tend to give the condition of low rock mass quality, while the widely spaced ones (Plate 5.2) are much more likely to yield interlocking conditions. The spacing of individual joint planes has a strong influence on the rock mass permeability and seepage characteristics also. For the present study, the joint spacings in each slope are measured with the help of a simple measuring tape. Since the spacing varies widely, the most common range of spacing is considered for the study. The data for each slope is tabulated in column 3 of Table 5.4.

5.2.3 CONDITION OF DISCONTINUITIES

This parameter comprises several sub-parameters. These include joint roughness, joint separation (opening), continuity, weathering of joint wall rock, slickensided surface and infilling material. The parameter details are as per Indian Standard 11315 (1987). The joint roughness defines the inherent roughness and the wavy nature relative to the mean plane of discontinuity. Both roughness and waviness contribute to the shear strength. In general, the roughness of the discontinuity walls can be characterised by the waviness (large scale undulations) and by the unevenness (small scale roughness). In the present study, the roughness is estimated by observing the joint surface as rough, smooth or slickensided. The slickensided surfaces are very smooth due to previous shear displacement along the joint planes. These can be very well identified by the presence of striations on the plane of discontinuity.

The joint separation or opening is the perpendicular distance between the joint wall rocks of a discontinuity. Such openings are occasionally filled up by clayey material, commonly termed as gaugy material, otherwise, these are either empty or filled up with water. On the basis of width of the openings, the joint openings are described as closed and open (Plate 5.3). This can be measured precisely with a scale or a measuring tape calibrated in mm. Generally, these openings are very small and in some cases are even less than half a mm. In the field, the data are collected from each joint plane of each slope and the average range value is used for the analysis.

The extent to which the rock material and the discontinuities affect the behaviour of the



Plate 5.1 Highly jointed quartzite showing low RQD



Plate 5.2 Joints showing large spacing



Plate 5.3 Joint opening without filling material



Plate 5.4 Use of Schmidt hammer on joint planes

rock mass, is governed by the continuity of discontinuities. It can be crudely estimated by observing the discontinuity trace lengths on the surface of exposures. In the field, it is assessed within a numerical limit of <10m (not continuous) and >10m (continuous).

The weathering of joint wall rock is a very important parameter for engineering classification of rock mass. The weathering generally, affects the walls of joint planes and, in turn, the joint wall strength. The weathering of wall rock has been classified into five classes; fresh, slightly weathered, moderately weathered, highly weathered and completely weathered on the basis of discoloration, presence of filling material, texture and degree of friability (Bicniawaski, 1989).

The last parameter studied for the condition of joint is the filling material. It separates the adjacent rock walls of a discontinuity and is, in general, weaker than the parent rock. The common filling materials are sand, silt, clay, gouge and mylonite. The filled discontinuities, have the fillings composed of decomposed rock or disintegrated rock originated through differential weathering. The infilling has a two fold influence on stability. Firstly, the filling prevents, depending on the thickness, interlocking of the fracture. Secondly, it possesses its own characteristic properties, i.e., shear strength, permeability and deformational characteristics. In the present field data collection, only the presence or absence of the filling material in the opening of discontinuities is accounted. The data pertaining to condition of joints are given in Table 5.4.

5.2.4 GROUND WATER CONDITIONS

This is a very important parameter for rock mass stability. To know the ground water condition, water seepage needs to be assessed. The seepage describes the water flow and the free moisture present in the joint planes and is generally assessed by visual observation. Water seepage results in saturation of rock mass which ultimately increases the pore water pressure and there by reduces the shear strength of the joint wall rock.

The seepage condition of the unfilled and filled joints are assessed in the field in following categories.

- (a) The discontinuity is dry with no evidence of water flow.
- (b) The discontinuity is dry but shows evidence of water flow.
- (c) The discontinuity is wet but no free water is present.

(d) The discontinuity shows seepage, occasional drops of water but no evidence of continuous flow.

(e) The discontinuity shows a continuous flow of water.

The ground water condition on the studied slopes is estimated, on the above basis and described as completely dry, damp, wet, dripping and flowing in column 9 of Table 5.4.

5.2.5 UNIAXIAL COMPRESSIVE STRENGTH

The strength parameters of joint planes refer to the wall strength of the plane which may be lower than the rock block strength due to weathering and fracturing. The stability of a rock mass is greatly influenced by its strength which can be measured in terms of uniaxial compressive strength (UCS). The presence of a network of defective planes or surfaces of discontinuities in the rock mass, influences its mechanical and physical properties. So, it is said that the strength along discontinuities is governed by the strength of asperities (Barton and Choubey, 1977). The field testing for uniaxial compressive strength in natural condition, also known as joint wall compressive strength (JCS), provides better results.

An easy way to determine UCS is to use Schmidt hammer. There are several types of Schmidt hammer such as N-type, L-type, M-type and P-type having different impact energy. These are generally used for strength determination of concrete. Suitability of testing the joint wall rock using an L-type hammer (impact energy=0.735 Nm) has been recommended by Barton and Choubey (1977) and Jesch et al. (1979). In the present study, the L-type Schmidt hammer is used (Plate 5.4). The surfaces of the joint walls are first cleaned of the loose particles before putting the hammer perpendicular to the surface and the rebound of a spring loaded plunger, after its impact on the surface, is recorded. The rebound number is read on a scale after pressing the hammer against the surface. If it is not possible to hold the hammer perpendicular to the surface, the correction factor for inclined planes has to be applied. Each face is tested 20 times and the average value of the rebound number is obtained. Next, the density of rock is determined. Finally, the UCS is determined using a master curve (Hoek and Bray, 1981) in which UCS is given against the rebound number for different rock densities. The strength data obtained for the 30 slopes are tabulated in the 5th column of Table 5.5 which shows the UCS data for each joint set of the slopes.

Table 5.5 Strength parameter and orientation of slopes and joints

Slope No.	Rock Type	Slope orientation	Orientation of major joints	UCS (MPa)
1	Phyllite	65°/N330°	J ₁ - 60°/N175°	46.4
			J ₂ - 35°/N225°	46.4
			J ₃ - 57°/N10°	42.8
2	Phyllite	80°/N60°	J ₁ - 40°/N260°	65
			J ₂ - 75°/N205°	54
			J ₃ - 64°/N140°	68
3	Quartzite	70°/N50°	J ₁ - 85°/N100°	54
			J ₂ - 15°/N265°	77.5
			J ₃ - 75°/N165°	82.5
4	Phyllite	80°/N40°	J ₁ - 73°/N155°	52
			J ₂ - 50°/N350°	35
5	Quartzite	80°/N20°	J ₁ - 65°/N130°	161.1
			J ₂ - 20°/N80°	118.3
			J ₃ - 40°/N340°	147.5
6	Phyllite	40°/N5°	J ₁ - 22°/N140°	35.3
			J ₂ - 28°/N61°	31.4
7	Phyllite	80°/N270°	J ₁ - 55°/N175°	42.1
			J ₂ - 82°/N290°	56
			J ₃ - 38°/N175°	85
8	Metavolcanic	65°/N265°	J ₁ - 57°/N188°	32.4
9	Quartzite	70°/N315°	J ₁ - 40°/N185°	145
			J ₂ - 38°/N15°	95
			J ₃ - 60°/N290°	60

Contd...

Slope No.	Rock Type	Slope orientation	Orientation of major joints	UCS (MPa)
10	Metavolcanic	50°/N280°	J ₁ - 40°/N170°	32
			J ₂ - 80°/N270°	24
			J ₃ - 32°/N330°	21
11	Metavolcanic	70°/N295°	J ₁ - 45°/N160°	183.3
			J ₂ - 78°/N305°	102.3
			J ₃ - 62°/N340°	180.6
12	Metavolcanic	80°/N	J ₁ - 62°/N320°	38.9
			J ₂ - 28°/N185°	34.4
13	Quartzite	80°/N330°	J ₁ - 33°/N170°	161.1
			J ₂ - 65°/N5°	197.2
14	Quartzite	80°/280°	J ₁ - 66°/N200°	90
			J ₂ - 71°/N300°	161
			J ₃ - 86°/N110°	130
15	Quartzite	70°/N335°	J ₁ - 10°/N155°	135
			J ₂ - 52°/N180°	145
			J ₃ - 71°/N305°	110
			J ₄ - 73°/N95°	160
16	Quartzite	80°/N20°	J ₁ - 35°/N165°	120
			J ₂ - 73°/N325°	163.9
			J ₃ - 65°/N55°	122
17	Quartzite	80°/N350°	J ₁ - 34°/N170°	155.6
			J ₂ - 57°/N265°	183.3
			J ₃ - 56°/N25°	260.4
18	Quartzite	70°/N125°	J ₁ - 50°/N165°	70
			J ₂ - 85°/N115°	95
19	Quartzite	60°/N40°	J ₁ - 58°/N110°	68
			J ₂ - 52°/N334°	132
			J ₃ - 50°/N75°	110

contd...

Slope No.	Rock Type	Slope orientation	Orientation of major joints	UCS (MPa)
20	Quartzite	65°/N223°	J ₁ - 67°/N275° J ₂ - 40°/N175°	26.9 62
21	Quartzite	75°/N300°	J ₁ - 31°/N160° J ₂ - 86°/N200° J ₃ - 61°/N315°	248 260 252
22	Metavolcanic	70°/N280°	J ₁ - 76°/N165° J ₂ - 58°/N210° J ₃ - 50°/N295°	113.3 102 113.3
23	Quartzite	65°/N240°	J ₁ - 47°/N185° J ₂ - 84°/N135° J ₃ - 45°/N180° J ₄ - 81°/N90°	155.6 166.7 53.3 270
24	Quartzite	55°/N280°	J ₁ - 59°/N280° J ₂ - 44°/N165°	258 276
25	Epidiorite	45°/N285°	J ₁ - 42°/N320°	70
26	Quartzite	80°/N	J ₁ - 40°/N145° J ₂ - 60°/N285° J ₃ - 37°/N340°	108.3 55.4 71.2
27	Quartzite	60°/N95°	J ₁ - 35°/N5° J ₂ - 45°/N310° J ₃ - 45°/N35°	183.3 210 213.3
28	Metavolcanic	75°/N315°	J ₁ - 38°/N340° J ₂ - 73°/N255°	260 248
29	Quartzite	80°/N55°	J ₁ - 45°/N310° J ₂ - 60°/N50° J ₃ - 30°/N110°	163 102 120
30	Quartzite	75°/N350°	J ₁ - 72°/N115° J ₂ - 36°/N350°	255 272

5.2.6 ORIENTATION OF DISCONTINUITIES IN RELATION TO SLOPE

The disposition of discontinuities on the slope governs its stability to a great extent. Hence, it is essential to know the orientation of discontinuities in relation to the slope face. For this, the data pertaining to the attitude of slope as well as joint planes are required. In the present study, the strikes and dips of joint planes are measured along with the attitude of slope for all the slopes. Nearly 100 to 150 readings of the joints are collected on each slope. To work out the pole concentrations, these are plotted and contoured using stereographic projection technique. The central value of highest contour density represents the pole of major joint set. The attitude of major joint sets are then derived from these poles. The data of slope and joint orientations are given in Table 5.5.

5.3 AN OVERVIEW OF THE SMR PARAMETERS ON STUDIED SLOPES

The data pertaining to slope orientation (Table 5.5) show that most of the slopes range between 60° - 80° because these are located on road side where the local cut slope gradients are high. Although there is no major trend of slope direction, yet these may be grouped into three categories; westerly, north-westerly and north-easterly.

The different type of rocks, present along the road, are quartzite, phyllite, metavolcanic and epidiorite. Out of the 30 slopes, 18 slopes are in quartzites having different degree of hardness, jointing and fracturing.

The data collected for joint orientation show that, in most of the slopes, there exist three sets of prominent joint planes. However, in some slopes there are four sets of joint planes, e.g., in slopes 15 and 23. Similarly, there exist two sets of joint planes also, e.g., in slopes 4, 6, 12, 13, 18, 20, 24, 28 and 30. In two slopes, 8 and 25, only one set of prominent joint plane is observed. The sets of joint planes are designated as J_1 , J_2 , J_3 and J_4 and the amounts and directions of their dips are given in Table 5.5. There is no relation between the number of joint sets and the rock types, but in most cases quartzite shows 3-4 sets of joints.

All the rock types have wide ranges of strength as evident from the uniaxial compressive strength data. The quartzites show, in most of the cases, more than 100 MPa uniaxial compressive strength, the phyllites show low strength ranging from 31.4 to 85 MPa and the metavolcanics show even lesser strength. The minimum UCS value of 21 MPa, is observed in slope 10 which comprises metavolcanic rocks. However, the metavolcanics have

shown a very high strength, more than 200 MPa, in slope 28. A critical observation of these data reveals that the same rock type in the same slope may show a large variation in strength along different joint planes. This indicates that the strength largely depends on the weak and weathered planes present within a jointed rock block and that the degree of weathering and nature of weak planes differ in different joint sets of the same rock type. Hence, it is always better to assess the strength of rock mass in the field. It gives more reliable results.

The RQD data (Table 5.4) show a large variation on different slopes. The minimum value obtained is 16% showing very poor quality of rocks in the metavolcanic slope 8, while the maximum is found to be 85.3%, showing excellent quality of rocks, in the quartzitic slopes 18 and 30. In majority of the cases quartzites show RQD of 70-80%. However, in some cases, where the quartzites are highly jointed and fractured, these also show a much lower value of 22.6% (slope 19).

Spacing of discontinuities are given in the Table 5.4 in a range of minimum and maximum spacings found in different slopes. The closely spaced joint sets show a very small spacing of 1-5 cm (slope 19), while the largely spaced joints show a large spacing of 75-145 cm (slope 18).

The condition of joints depends on the five sub-parameters; roughness, weathering, opening, filling and continuity. Other than the joint opening and filling, the three sub-parameters, give a crude estimation. In majority of the cases, the joint surfaces are either slightly rough or smooth. In few slopes, the slickensided surface is also observed. The quartzites are found to vary from very rough to slightly rough. The weathering of rocks in different slopes is described as highly weathered to fresh rocks. It can be seen from the table that the degree of weathering varies, to a great extent, from one slope to another. The joint opening has a minimum range of 0.1 cm to 1 cm. The filling material wherever found has shown a more or less complete filling of soft material depending on the size of opening. Only the presence or absence of filling materials in the joint openings are taken into account.

The ground water condition in the field is estimated as dry or damp as shown in the Table 5.4. The other classes can be found only in the monsoon period when most of the slopes are either damp or wet. The worst condition, i.e., dripping or flowing is not observed in the field. The dry condition has been found in 18 slopes while the rest show damp condition. Since these observations are made in fair weather, the completely dry slopes may behave as wet

slopes during the monsoon.

5.4 DATA ANALYSIS FOR ROCK MASS RATING

Rock Mass Rating, in the present study, is the RMR_{basic} which depends on the five joint parameters; uniaxial compressive strength (UCS), rock quality designation (RQD), spacing, condition of joints and ground water condition. For the sake of clarity of expression, the term RMR_{basic} will be simply stated as RMR in the subsequent discussion. Following the rating assignment criteria of Beiniawaski, 1979 (Table 5.1), the ratings are assigned, in accordance with the evaluated joint parameters, to calculate RMR for each slope.

The assigned ratings to the different RMR parameters are given in Table 5.6. For example, to calculate RMR for slope 1, the UCS of all the three sets of joints are considered and a rating of 4 is assigned, as the strength value lies in the range of 25-50 MPa. In cases where the UCS for different joint sets falls in different classes, the value corresponding to the probable failure plane is considered. The minimum rating for UCS (<25 MPa) is 2, which exists in two joint sets of slope 10, while the maximum is 15 for UCS >250 MPa, which exists in the one joint set of slopes 17 and 28 and the two joint sets of slope 21.

The ratings for RQD show a minimum of 3 in 4 slopes and a maximum of 17 in 12 slopes. The rating 3 is assigned for very poor quality of rocks, for example, in slope 6 the RQD value is 22.6%. The rating 20 is not assigned to any slope as there is no slope showing rock mass of very good quality (RQD = 90-100%).

The ratings for joint spacings range from 5 to 15 for the spacings falling in the range of <6 cm to 60-200 cm respectively. For example, the rating of 8 is assigned to slope 1, as its joint spacings range in 6.5-20 cm. To assign the ratings for joint conditions, all the five sub-parameters are considered. For example, for slope 1, the rating is 10 as it shows slickensided surface, high weathering, 0.4-0.5 cm opening, presence of filling and continuous joint (i.e., >10 m). It is to be noted here that, all the five sub-parameters may not show similar joint condition corresponding to a particular rating. In such cases the worst condition is considered.

In the present study, the ratings for ground water condition range between 10 to 15 corresponding to respective damp and dry conditions. The other classes may exist during monsoon and are taken into account in the analysis under wet condition.

For each slope, the assigned ratings, corresponding to the five joint parameters, are

Table 5.6 Ratings of joint parameters for RMR

Slope No.	UCS	RQD	Spacing	Joint condition	Water condition	RMR
1	4	8	8	10	10	40
2	7	17	8	10	15	57
3	7	8	8	25	15	63
4	4	17	10	10	15	56
5	12	13	8	10	10	53
6	4	3	5	25	15	52
7	7	13	10	10	10	50
8	4	3	8	20	15	50
9	7	13	10	10	10	50
10	2	3	8	10	10	33
11	12	13	10	10	15	60
12	4	13	10	10	10	47
13	12	17	15	10	15	69
14	12	17	10	25	15	79
15	12	17	10	25	15	79
16	12	17	15	25	15	84
17	15	13	15	25	15	83
18	12	17	15	25	15	84
19	7	3	5	10	10	35
20	4	13	10	10	10	47
21	15	17	15	25	15	87
22	12	13	10	25	15	75
23	12	13	10	25	15	75
24	15	17	15	10	10	67
25	7	13	10	20	10	60
26	7	17	15	25	15	79
27	12	13	8	10	10	53
28	15	13	15	10	10	63
29	12	17	15	25	15	84
30	15	17	10	25	15	82

summed to obtain the RMR, as given in Table 5.6. The minimum RMR obtained is 33 for the slope 10, while the maximum is 87 for the slope 21.

5.5 ANALYSIS OF JOINT ORIENTATION

The mode of slope failure depends on the relation between the attitude of discontinuity planes and the slope face. For the three types of failures, i.e., the planar, the wedge and the topple, the nature of orientation of discontinuities in relation to the slope is shown in Fig. 5.2. The joint planes for the 30 studied slopes, determined from stereographic projection and plotted along with the slope face, are shown in the Figs. 5.3 to 5.7. The stereoplots of discontinuities and the slope provide the modes of failure, i.e., planar failure or wedge failure or both in each of the slopes. The conditions for topple failure do not exist in the slopes under study. In the present analysis, the planar and wedge types of failures are separately analysed. In case of the planar failure, only one set joint is considered, while for the wedge failure, intersection of two joint sets are considered with respect to slope.

After knowing the probable failures from the stereoplots, the values of α_j, β_j in case of planar failure, α_i, β_i in case of wedge failure and α_s and β_s are determined. The $\alpha_j, \beta_j, \alpha_i, \beta_i, \alpha_s$, and β_s are respectively the dip direction of joint plane, the dip of joint plane, the plunge direction of intersection of two joint planes, the plunge of line of intersection, the slope direction and the dip of slope face. The values of these parameters are used to calculate $|\alpha_j - \alpha_s|, (\beta_j - \beta_s)$ for the planar failure and $|\alpha_i - \alpha_s|, (\beta_i - \beta_s)$ for the wedge failure. The adjustment rating for joints, given by Romana (Table 5.2), is then used to get the numerical ratings of F_1, F_2 and F_3 for the different classes of joint orientations in relation to the slope. The values of F_1, F_2 and F_3 , corresponding to each probable modes of failure, for all the slopes are given in the Table 5.7.

For example, in slope 1 (Fig. 5.3) it is found that the probable failures are planar along the joint J_3 and wedge type along the intersection of joints J_2 and J_3 . The dip of the joint plane J_3 is $57^\circ/N10^\circ$, while the plunge of line of intersection of joints J_2 and J_3 is $16^\circ/N291^\circ$ and the dip of slope face is $65^\circ/N330^\circ$. The adjustment ratings F_1, F_2 and F_3 for slope 1 are computed as follows.

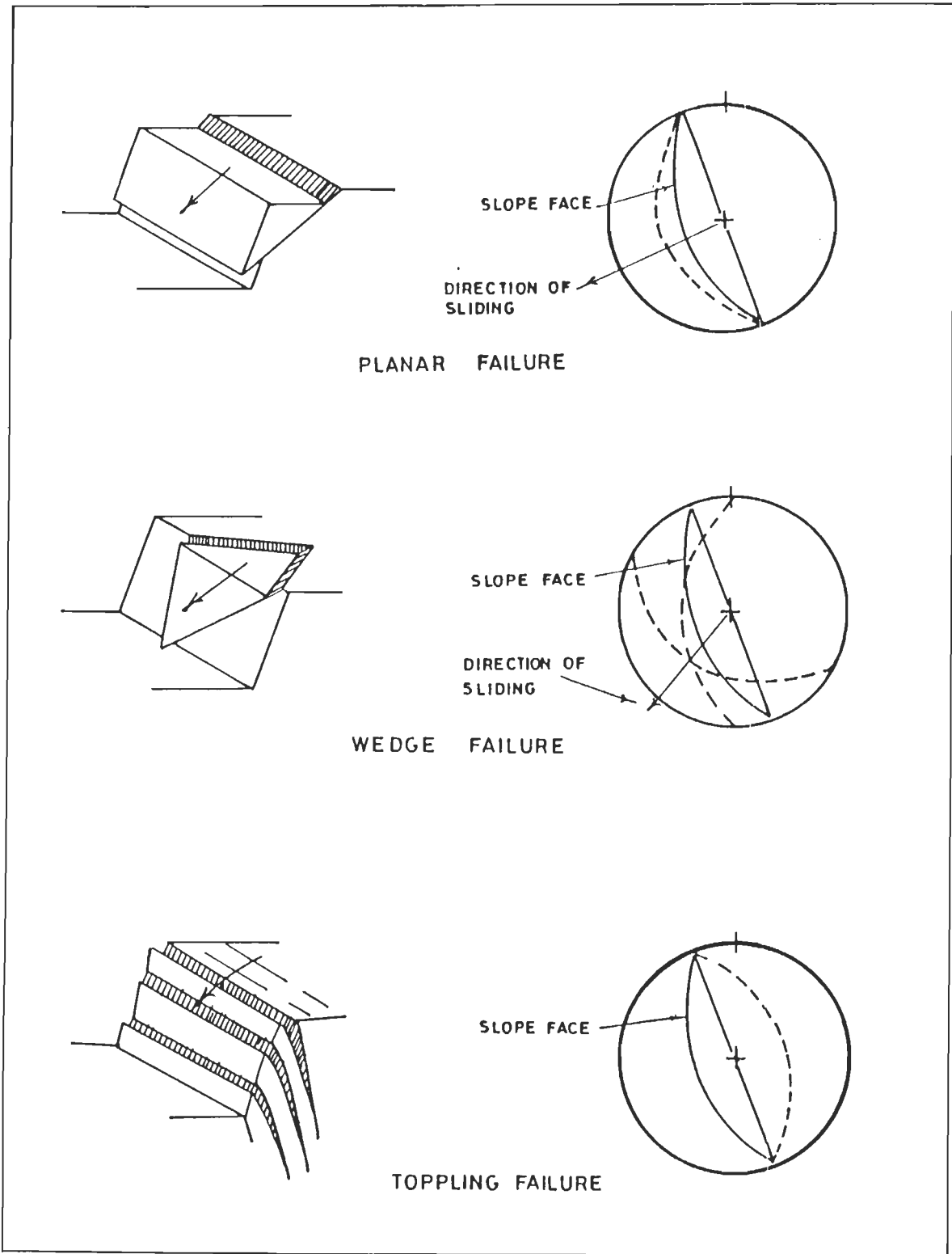


Figure 5.2 Modes of failure in rock slopes

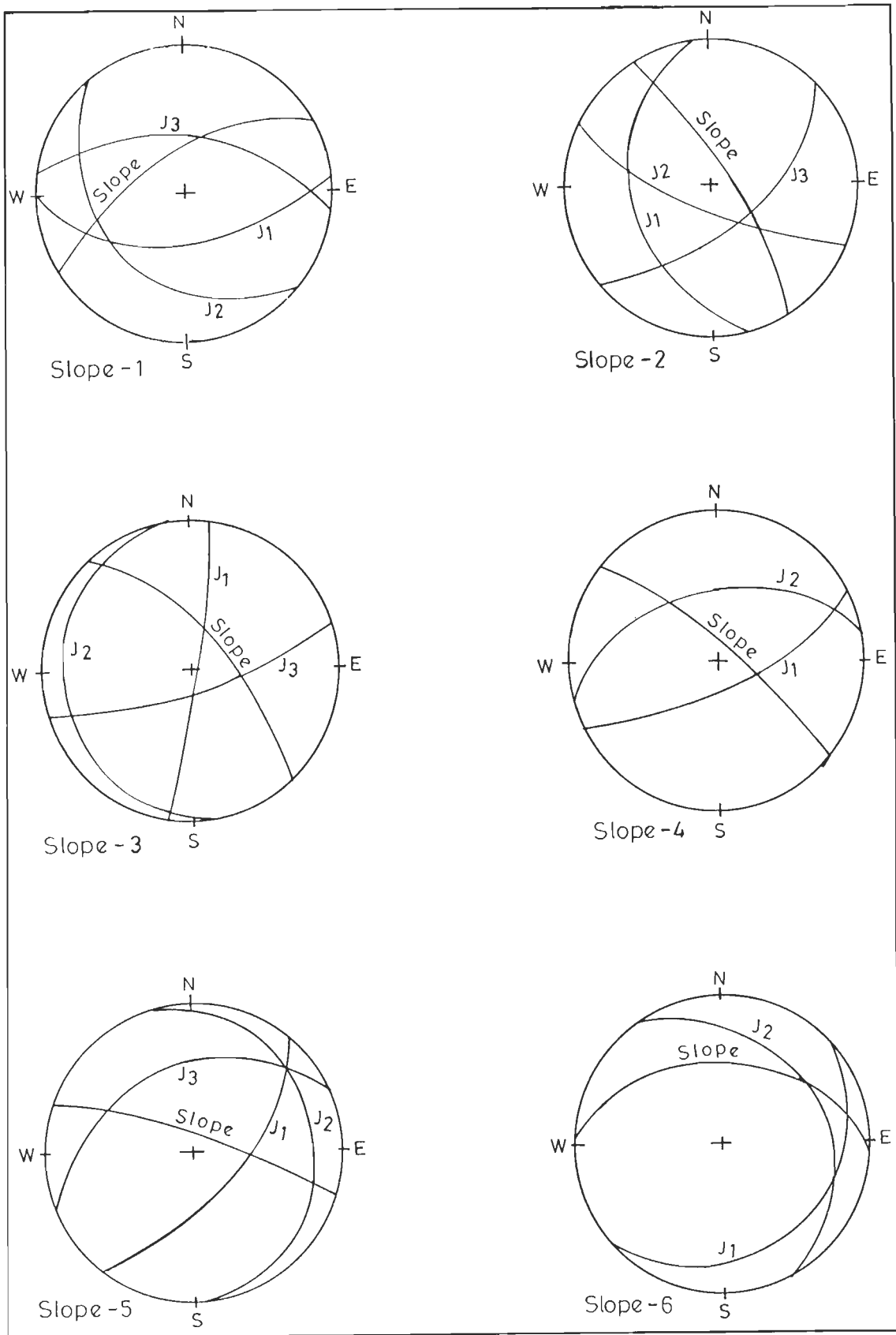


Figure 5.3 Stereoplots of slope 1 to 6 showing orientations of slope and joints

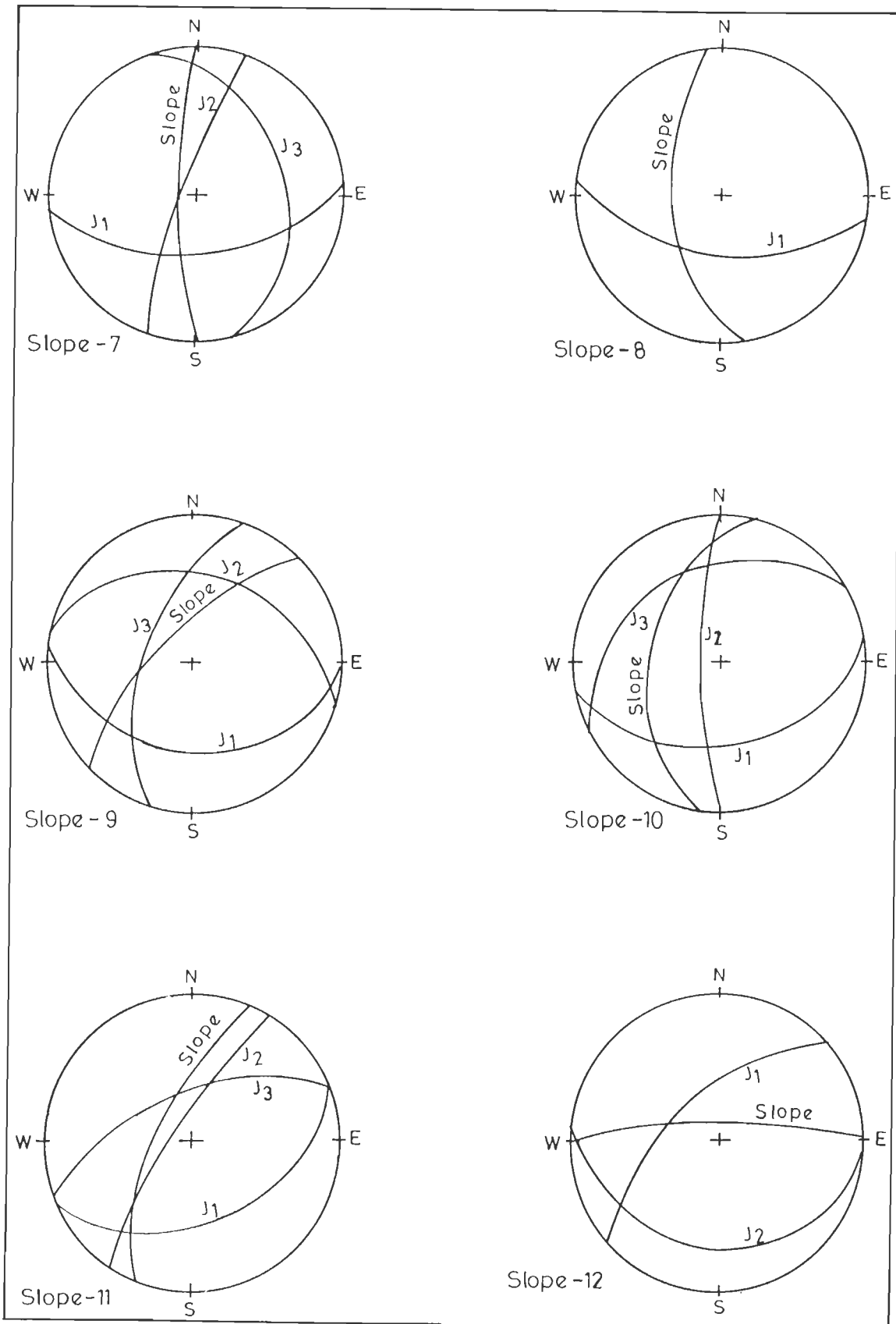


Figure 5.4 Stereoplots of slope 7 to 12 showing orientations of slope and joints

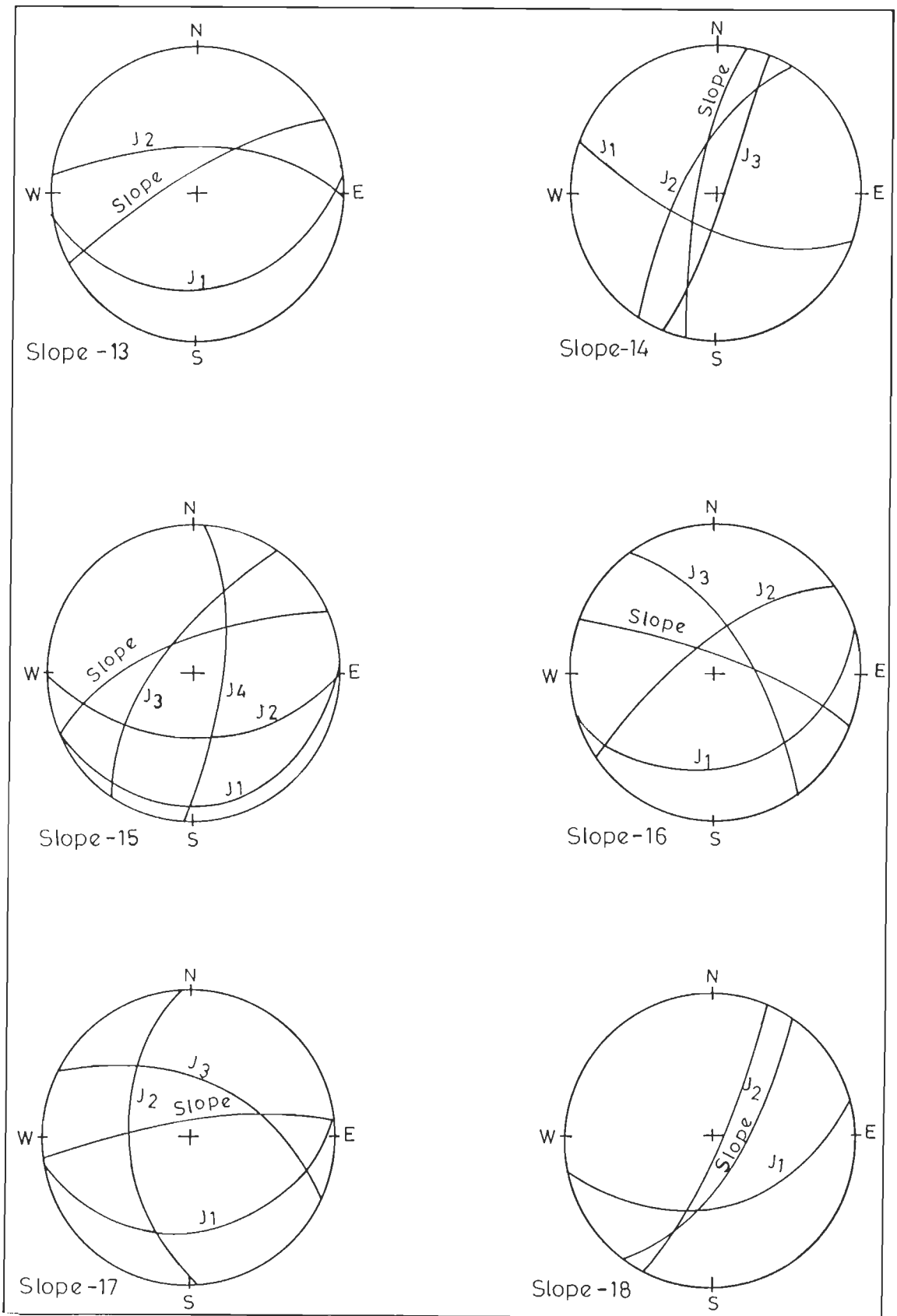


Figure 5.5 Stereoplots of slope 13 to 18 showing orientations of slope and joints

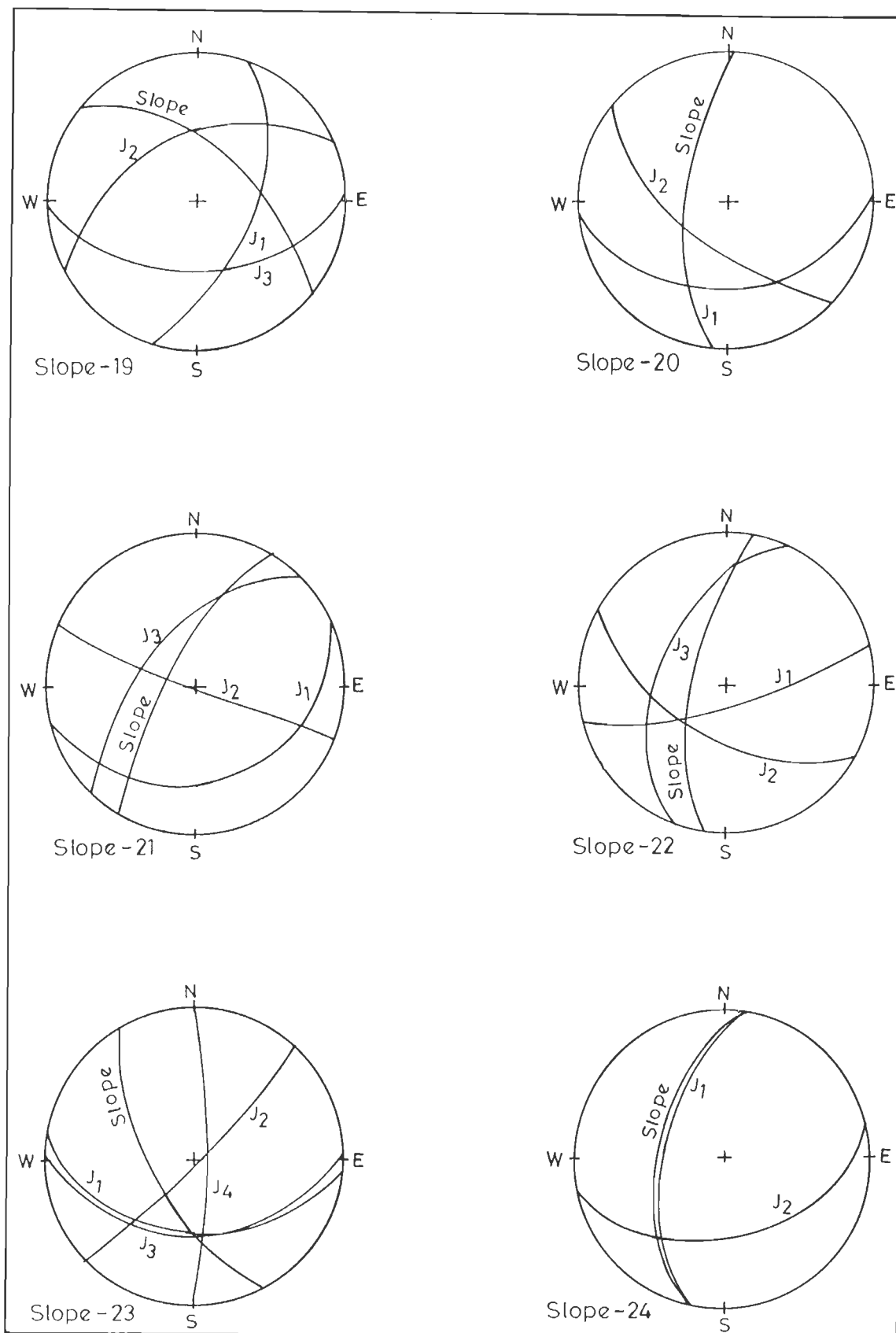


Figure 5.6 Stereoplots of slope 19 to 24 showing orientations of slope and joints

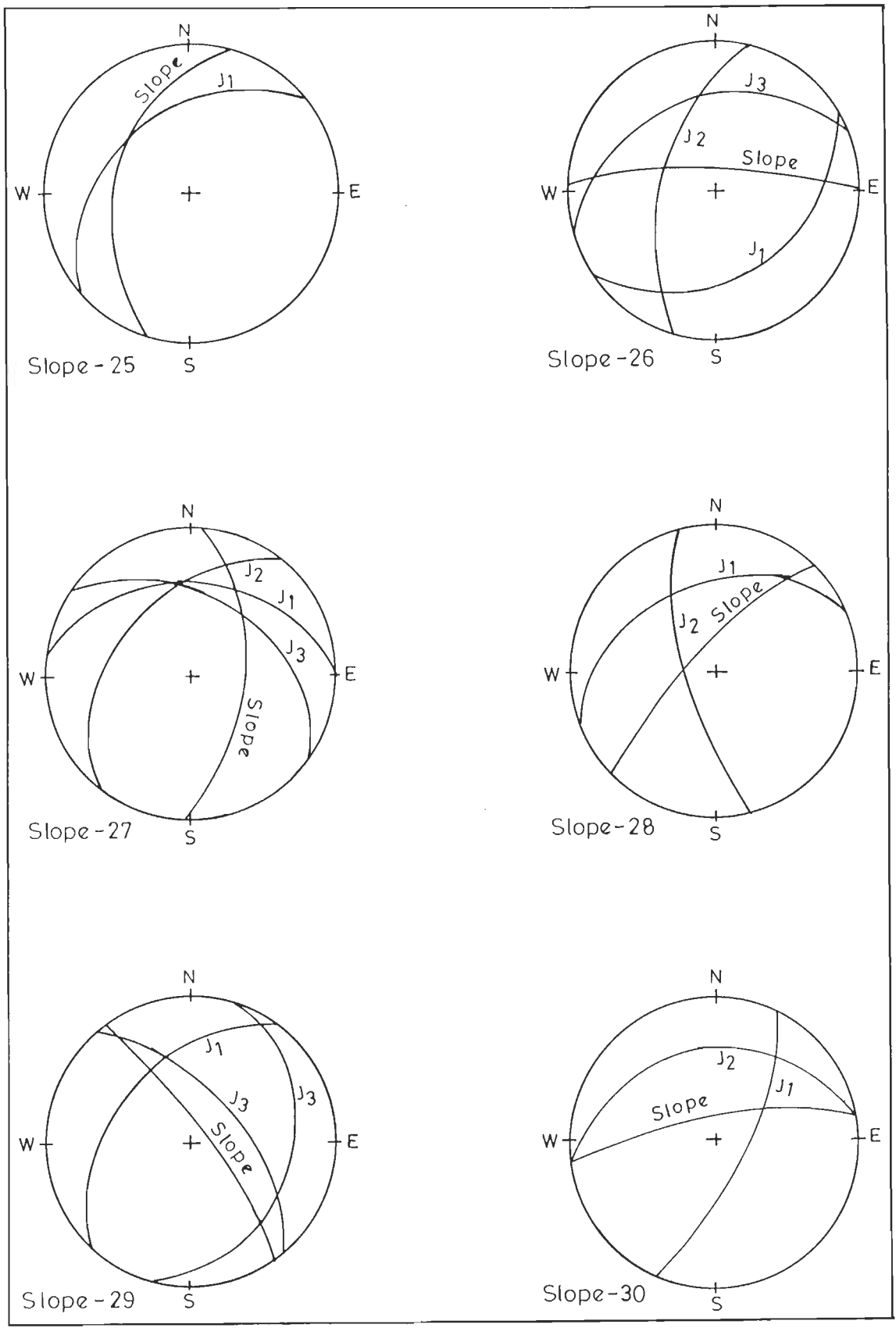


Figure 5.7 Stereoplots of slope 25 to 30 showing orientations of slope and joints

Table 5.7 Adjustment ratings for joint orientation and method of excavation

Slope No.	Probable failure modes	Joint - Slope relations (degree)	Adjustment rating for joints	Adjustment rating for excavation (F ₄)
1	Planar (J ₃) 57°/N10°	$ \alpha_j - \alpha_s = 40$ $\beta_j = 57$ $\beta_j - \beta_s = -8$	F ₁ = 0.15 F ₂ = 1 F ₃ = -50	0
	Wedge (J ₂ -J ₃) 16°/N291°	$ \alpha_i - \alpha_s = 39$ $\beta_i = 16$ $\beta_i - \beta_s = -49$	F ₁ = 0.15 F ₂ = 0.15 F ₃ = -60	
2	Planar (J ₃) 64°/N140°	$ \alpha_j - \alpha_s = 100$ $\beta_j = 64$ $\beta_j - \beta_s = -16$	F ₁ = 0.15 F ₂ = 1 F ₃ = -60	0
3	Planar (J ₁) 85°/N100°	$ \alpha_j - \alpha_s = 50$ $\beta_j = 85$ $\beta_j - \beta_s = 15$	F ₁ = 0.15 F ₂ = 1 F ₃ = 0	0
4	Wedge (J ₁ -J ₂) 11°/N69°	$ \alpha_i - \alpha_s = 29$ $\beta_i = 11$ $\beta_i - \beta_s = -69$	F ₁ = 0.4 F ₂ = 0.15 F ₃ = -60	-8
5	Planar (J ₃) 40°/N340°	$ \alpha_j - \alpha_s = 40$ $\beta_j = 40$ $\beta_j - \beta_s = -40$	F ₁ = 0.15 F ₂ = 0.85 F ₃ = -60	0
	Wedge (J ₁ -J ₃) 16°/N48°	$ \alpha_i - \alpha_s = 28$ $\beta_i = 16$ $\beta_i - \beta_s = -64$	F ₁ = 0.4 F ₂ = 0.15 F ₃ = -60	
6	Planar (J ₂) 28°/N61°	$ \alpha_j - \alpha_s = 56$ $\beta_j = 28$ $\beta_j - \beta_s = -12$	F ₁ = 0.15 F ₂ = 0.4 F ₃ = -60	0

Contd....

Slope No.	Probable failure modes	Joint - Slope relations (degree)	Adjustment rating for joints	Adjustment rating for excavation (F_4)
7	Planar (J_2) 82°/N290°	$ \alpha_j - \alpha_s = 20$ $\beta_j = 82$ $\beta_j - \beta_s = 2$	$F_1 = 0.7$ $F_2 = 1$ $F_3 = -6$	0
	Wedge ($J_1 - J_2$) 50°/210°	$ \alpha_i - \alpha_s = 60$ $\beta_i = 50$ $\beta_i - \beta_s = -30$	$F_1 = 0.15$ $F_2 = 1$ $F_3 = -60$	
8	Planar (J_1) 57°/N188°	$ \alpha_j - \alpha_s = 77$ $\beta_j = 57$ $\beta_j - \beta_s = -8$	$F_1 = 0.15$ $F_2 = 1$ $F_3 = -50$	0
9	Planar (J_3) 60°/N290°	$ \alpha_j - \alpha_s = 25$ $\beta_j = 60$ $\beta_j - \beta_s = -10$	$F_1 = 0.4$ $F_2 = 1$ $F_3 = -50$	-8
	Wedge ($J_2 - J_3$) 37°/N355°	$ \alpha_i - \alpha_s = 40$ $\beta_i = 37$ $\beta_i - \beta_s = -33$	$F_1 = 0.15$ $F_2 = 0.85$ $F_3 = -60$	
10	Planar (J_2) 80°/N270°	$ \alpha_j - \alpha_s = 10$ $\beta_j = 80$ $\beta_j - \beta_s = 30$	$F_1 = 0.85$ $F_2 = 1$ $F_3 = 0$	0
	Planar (J_3) 32°/N330°	$ \alpha_j - \alpha_s = 50$ $\beta_j = 32$ $\beta_j - \beta_s = -18$	$F_1 = 0.15$ $F_2 = 0.7$ $F_3 = -60$	
	Wedge ($J_1 - J_3$) 10°/N252°	$ \alpha_i - \alpha_s = 28$ $\beta_i = 10$ $\beta_i - \beta_s = -40$	$F_1 = 0.4$ $F_2 = 0.15$ $F_3 = -60$	
11	Planar (J_2) 78°/N305°	$ \alpha_j - \alpha_s = 10$ $\beta_j = 78$ $\beta_j - \beta_s = 8$	$F_1 = 0.85$ $F_2 = 1$ $F_3 = -6$	-8
	Planar (J_3) 62°/N340°	$ \alpha_j - \alpha_s = 45$ $\beta_j = 62$ $\beta_j - \beta_s = -8$	$F_1 = 0.15$ $F_2 = 1$ $F_3 = -50$	

Contd...

Slope No.	Probable failure modes	Joint - Slope relations (degree)	Adjustment rating for joints	Adjustment rating for excavation (F ₄)
12	Planar (J ₁) 62°/N320°	$ \alpha_j - \alpha_s = 40$ $\beta_j = 62$ $\beta_j - \beta_s = -18$	F ₁ = 0.15 F ₂ = 1 F ₃ = -60	-8
13	Planar (J ₂) 65°/N5°	$ \alpha_j - \alpha_s = 35$ $\beta_j = 65$ $\beta_j - \beta_s = -15$	F ₁ = 0.15 F ₂ = 0.85 F ₃ = -60	0
14	Planar (J ₂) 71°/N300°	$ \alpha_j - \alpha_s = 20$ $\beta_j = 71$ $\beta_j - \beta_s = -9$	F ₁ = 0.7 F ₂ = 1 F ₃ = -50	0
	Wedge (J ₁ -J ₂) 59°/N244°	$ \alpha_i - \alpha_s = 36$ $\beta_i = 59$ $\beta_i - \beta_s = -21$	F ₁ = 0.15 F ₂ = 1 F ₃ = -60	
15	Planar (J ₃) 71°/N305°	$ \alpha_j - \alpha_s = 30$ $\beta_j = 71$ $\beta_j - \beta_s = 1$	F ₁ = 0.4 F ₂ = 1 F ₃ = -6	-8
	Wedge (J ₃ -J ₄) 38°/N19°	$ \alpha_i - \alpha_s = 44$ $\beta_i = 38$ $\beta_i - \beta_s = -32$	F ₁ = 0.15 F ₂ = 0.85 F ₃ = -60	
16	Planar (J ₂) 73°/N325°	$ \alpha_j - \alpha_s = 55$ $\beta_j = 73$ $\beta_j - \beta_s = -7$	F ₁ = 0.15 F ₂ = 1 F ₃ = -50	0
	Planar (J ₃) 65°/N55°	$ \alpha_j - \alpha_s = 35$ $\beta_j = 65$ $\beta_j - \beta_s = -15$	F ₁ = 0.15 F ₂ = 1 F ₃ = -60	
	Wedge (J ₂ -J ₃) 63°/N18°	$ \alpha_i - \alpha_s = 2$ $\beta_i = 63$ $\beta_i - \beta_s = -17$	F ₁ = 1 F ₂ = 1 F ₃ = -60	

Contd....

Slope No.	Probable failure modes	Joint - Slope relations (degree)	Adjustment rating for joints	Adjustment rating for excavation (F ₄)
17	Planar (J ₃) 56°/N25°	$ \alpha_j - \alpha_s = 35$ $\beta_j = 56$ $\beta_j - \beta_s = -24$	F ₁ = 0.15 F ₂ = 1 F ₃ = -60	0
	Wedge (J ₂ -J ₃) 38°/N326°	$ \alpha_i - \alpha_s = 24$ $\beta_i = 38$ $\beta_i - \beta_s = -42$	F ₁ = 0.4 F ₂ = 0.85 F ₃ = -60	
18	Planar (J ₁) 50°/N165°	$ \alpha_j - \alpha_s = 40$ $\beta_j = 50$ $\beta_j - \beta_s = -20$	F ₁ = 0.15 F ₂ = 1 F ₃ = -60	-8
	Planar (J ₂) 85°/N15°	$ \alpha_j - \alpha_s = 10$ $\beta_j = 85$ $\beta_j - \beta_s = 15$	F ₁ = 0.85 F ₂ = 1 F ₃ = 0	
19	Wedge (J ₁ -J ₂) 28°/N40°	$ \alpha_i - \alpha_s = 0$ $\beta_i = 28$ $\beta_i - \beta_s = -32$	F ₁ = 1 F ₂ = 0.4 F ₃ = -60	0
20	Planar (J ₂) 40°/N175°	$ \alpha_j - \alpha_s = 48$ $\beta_j = 40$ $\beta_j - \beta_s = -25$	F ₁ = 0.15 F ₂ = 0.85 F ₃ = -60	0
	Wedge (J ₁ -J ₂) 36°/N203°	$ \alpha_i - \alpha_s = 20$ $\beta_i = 36$ $\beta_i - \beta_s = -29$	F ₁ = 0.7 F ₂ = 0.85 F ₃ = -60	
21	Planar (J ₃) 61°/N315°	$ \alpha_j - \alpha_s = 15$ $\beta_j = 61$ $\beta_j - \beta_s = -14$	F ₁ = 0.7 F ₂ = 1 F ₃ = -60	0
	Wedge (J ₂ -J ₃) 57°/N284°	$ \alpha_i - \alpha_s = 16$ $\beta_i = 57$ $\beta_i - \beta_s = -18$	F ₁ = 0.7 F ₂ = 1 F ₃ = -60	

Contd....

Slope No.	Probable failure modes	Joint - Slope relations (degree)	Adjustment rating for joints	Adjustment rating for excavation (F ₄)
22	Planar (J ₃) 50°/N295°	$ \alpha_j - \alpha_s = 15$ $\beta_j = 50$ $\beta_j - \beta_s = -20$	F ₁ = 0.7 F ₂ = 1 F ₃ = -60	-8
	Wedge (J ₂ -J ₃) 45°/N263°	$ \alpha_i - \alpha_s = 17$ $\beta_i = 45$ $\beta_i - \beta_s = -25$	F ₁ = 0.7 F ₂ = 0.85 F ₃ = -60	
	Wedge (J ₁ -J ₃) 36°/N244°	$ \alpha_i - \alpha_s = 36$ $\beta_i = 36$ $\beta_i - \beta_s = -34$	F ₁ = 0.15 F ₂ = 0.85 F ₃ = -60	
23	Planar (J ₁) 47°/N185°	$ \alpha_j - \alpha_s = 55$ $\beta_j = 47$ $\beta_j - \beta_s = -18$	F ₁ = 0.15 F ₂ = 1 F ₃ = -60	-8
	Wedge (J ₁ -J ₂) 42°/N220°	$ \alpha_i - \alpha_s = 20$ $\beta_i = 42$ $\beta_i - \beta_s = -23$	F ₁ = 0.7 F ₂ = 0.85 F ₃ = -60	
	Wedge (J ₂ -J ₃) 37°/N221°	$ \alpha_i - \alpha_j = 19$ $\beta_i = 37$ $\beta_i - \beta_s = -28$	F ₁ = 0.7 F ₂ = 0.85 F ₃ = -60	
24	Planar (J ₁) 59°/N280°	$ \alpha_j - \alpha_s = 0$ $\beta_j = 59$ $\beta_j - \beta_s = 4$	F ₁ = 1 F ₂ = 1 F ₃ = -6	0
25	Planar (J ₁) 42°/N320°	$ \alpha_j - \alpha_s = 35$ $\beta_j = 42$ $\beta_j - \beta_s = -3$	F ₁ = 0.15 F ₂ = 0.85 F ₃ = -50	-8
26	Planar (J ₃) 37°/N340°	$ \alpha_j - \alpha_s = 20$ $\beta_j = 37$ $\beta_j - \beta_s = -43$	F ₁ = 0.7 F ₂ = 0.85 F ₃ = -60	0
	Wedge (J ₂ -J ₃) 37°/N348°	$ \alpha_i - \alpha_s = 12$ $\beta_i = 37$ $\beta_i - \beta_s = -4$	F ₁ = 0.7 F ₂ = 0.85 F ₃ = -60	

Contd....

Slope No.	Probable failure modes	Joint - Slope relations (degree)	Adjustment rating for joints	Adjustment rating for excavation (F ₄)
27	Planar (J ₃) 45°/N35°	$ \alpha_j - \alpha_s = 60$ $\beta_j = 45$ $\beta_j - \beta_s = -15$	$F_1 = 0.15$ $F_2 = 0.85$ $F_3 = -60$	0
28	Planar (J ₁) 38°/N240°	$ \alpha_j - \alpha_s = 25$ $\beta_j = 38$ $\beta_j - \beta_s = -37$	$F_1 = 0.4$ $F_2 = 0.85$ $F_3 = -60$	0
	Wedge (J ₁ -J ₂) 38°/N331°	$ \alpha_i - \alpha_s = 16$ $\beta_i = 38$ $\beta_i - \beta_s = -37$	$F_1 = 0.7$ $F_2 = 0.85$ $F_3 = -60$	
29	Planar (J ₂) 60°/N50°	$ \alpha_j - \alpha_s = 5$ $\beta_j = 60$ $\beta_j - \beta_s = -20$	$F_1 = 1$ $F_2 = 1$ $F_3 = -60$	0
	Wedge (J ₁ -J ₃) 6°/N32°	$ \alpha_i - \alpha_s = 23$ $\beta_i = 6$ $\beta_i - \beta_s = -72$	$F_1 = 0.4$ $F_2 = 0.15$ $F_3 = -60$	
30	Planar (J ₂) 36°/N350°	$ \alpha_j - \alpha_s = 0$ $\beta_j = 36$ $\beta_j - \beta_s = -39$	$F_1 = 1$ $F_2 = 0.85$ $F_3 = -60$	0

Planar failure

$$| \alpha_j - \alpha_s | = 40 ; F_1 = 0.15$$

$$\beta_j = 57 ; \quad F_2 = 1$$

$$\beta_j - \beta_s = -8 ; \quad F_3 = -50$$

Wedge failure

$$| \alpha_i - \alpha_s | = 39 ; F_1 = 0.15$$

$$\beta_i = 16 ; \quad F_2 = 0.15$$

$$\beta_i - \beta_s = -49 ; \quad F_3 = -60$$

The calculations for all the thirty slopes are carried out in this way. In some slopes, such as slope 2, only the planar failure along J_3 is considered, while in some like slope 4, only the wedge failure along the line of intersection of J_1 and J_2 is considered. Similarly, for slope 10, two planar failures along J_2 and J_3 and wedge failure along the line of intersection of J_1 and J_3 , are considered. It reveals that an appropriate analysis of joint orientations with respect to the slope face is very important for slope stability analysis.

5.6 METHOD OF EXCAVATION

All the slopes, considered in this study, lie along the road cuts and the precise information about the method of excavation is not available. Hence, in the present study, the rating for excavation is estimated by observing the degree of disturbance on the slope which is related to the excavation technique (Swindells, 1985). In most of the cases, the nature of slope shows less disturbance, probably due to mechanical clearance of the slope material combined with some preliminary blasting. So, for these cases, the rating F_4 is assigned a value 0, which according to Table 5.3 corresponds to the category of blasting/mechanical method of excavation. For the few cases, showing major disturbance, such as irregular large fractures, overhanging rock mass etc, the rating F_4 is assigned a value -8 which falls in the category of deficient blasting. The ratings pertaining to the method of excavation for all the slopes are given in the Table 5.7.

5.7 COMPUTATION OF SLOPE MASS RATING

The Slope Mass Rating (SMR) of each slope is computed using the equation given by Romana (1985, 1988, 1991) which depends on the parameters RMR, F_1 , F_2 , F_3 and F_4 . The SMR values differ for different types of failure in a particular slope. This is because of the different ratings of F_1 , F_2 and F_3 even when the RMR and F_4 are same. Hence, it is necessary to explore all possible modes of failure and to calculate the corresponding SMR values on the slope. For example, in slope 1, the planar failure along J_3 and the wedge failure along the line of intersection of J_2 and J_3 are considered. The SMR is calculated as follows.

Planar failure along J_3

$$\text{RMR} = 40, F_1 = 0.15, F_2 = 1, F_3 = -50 \text{ \& } F_4 = 0$$

$$\begin{aligned} \text{SMR} &= 40 + (0.15 \times 1 \times -50) + 0 \\ &= 32.5 \end{aligned}$$

Wedge failure along J_2 - J_3

$$\text{RMR} = 40, F_1 = 0.15, F_2 = 0.15, F_3 = -60 \text{ \& } F_4 = 0$$

$$\begin{aligned} \text{SMR} &= 40 + (0.15 \times 0.15 \times -60) + 0 \\ &= 38.65 \end{aligned}$$

In this way, the SMR values are computed for all possible modes of failure in all the 30 slopes.

5.8 SLOPE STABILITY ASSESSMENT

The SMR classes and the corresponding stability can be obtained from the stability classes (Table 5.8) given by Romana (1985). There are five classes of stability varying from Class I, for completely stable slope, to Class V, for completely unstable slope.

Slope stability assessment is carried out by assessing the SMR values obtained for each slope. In most of the cases, there is not much difference in the SMR values for the different types of failure in an individual slope. For example, in slope 1, SMR is 32.5 (planar) and 38.5 (wedge). However, in few cases, the SMR values differ significantly, e.g., for slope 14, SMR is 44 (planar) and 70 (wedge). So, it is possible that the SMR is low along some joint plane

Table 5.8 Description of SMR Classes (Romana, 1985)

Class No.	V	IV	III	II	I
SMR	0-20	21-40	41-60	61-80	81-100
Description	very bad	bad	normal	good	very good
Stability	completely unstable	unstable	partially stable	stable	completely stable
Failures	big planar or soil like	planar or big wedges	some joints or many wedges	some blocks	none

and high along other joint plane in the same slope. Hence, for the slopes with more than one probable failure modes, the minimum SMR is considered to assess the worst stability condition. The minimum SMR, its class and the corresponding stability for the 30 slopes are given in Table 5.9.

The SMR values obtained reveal that there are only two slopes, namely slopes 19 and 20, which come under the completely unstable condition, while ten slopes, namely slopes 1, 9, 10, 12, 16, 22, 23, 28, 29 and 30, come under the unstable condition. The analysis shows that the RMR for the slope 19 is 35 while its SMR is 11. The RMR for slope 20 is 47 (considerably higher than that of the slope 19) but still its SMR is only 11.3. When the slope 16 is compared with the slope 1, both falling in unstable class, it can be seen that for slope 1, the RMR is 40 and the SMR is 32.5, while for slope 16, the RMR is 84, signifying a high rock mass quality, but the SMR is only 24. For both the cases, the value of F_4 is 0. Hence, it is inferred that the SMR is largely governed by the ratings for joint orientations (F_1 , F_2 and F_3). This shows that, even with a high rock mass rating, a slope may come under unstable condition if the orientation of joints in relation to the slope face is unfavourable. Some other slopes also show such type of results.

None of the slopes shows SMR greater than 80, i.e., none possesses a completely stable condition. Maximum number of slopes fall in the partially stable condition. While describing the stability of slopes as unstable, partially stable or some other stability class, it should always

Table 5.9 Stability classes based on SMR

Slope No.	RMR	SMR along probable failure planes	Minimum SMR	Class	Stability
1	40	$J_3 = 32.50$ $J_2-J_3 = 38.65$	32.5	IV	Unstable
2	57	$J_3 = 48$	48.0	III	Partially stable
3	63	$J_1 = 62.85$	62.85	II	Stable
4	56	$J_1-J_2 = 44.4$	44.4	III	Partially stable
5	53	$J_3 = 45.35$ $J_1-J_3 = 49.4$	45.35	III	Partially stable
6	52	$J_2 = 48.4$	48.4	III	Partially stable
7	50	$J_2 = 45.8$ $J_1-J_2 = 41$	41.0	III	Partially stable
8	50	$J_1 = 42.5$	42.5	III	Partially stable
9	50	$J_3 = 22$ $J_2-J_3 = 34.35$	22.0	IV	Unstable
10	33	$J_2 = 33$ $J_3 = 26.7$ $J_1-J_3 = 29.4$	26.7	IV	Unstable
11	60	$J_2 = 46.9$ $J_3 = 44.5$	44.5	III	Partially stable
12	47	$J_1 = 30$	30.0	IV	Unstable
13	69	$J_2 = 61.35$	61.35	II	Stable
14	79	$J_2 = 44$ $J_1-J_2 = 70$	44.0	III	Partially stable
15	79	$J_3 = 68.6$ $J_3-J_4 = 63.35$	63.35	II	Stable

Contd...

Slope No.	RMR	SMR along probable failure planes	Minimum SMR	Class	Stability
16	84	$J_2 = 76.5$ $J_3 = 75$ $J_2-J_3 = 24$	24.0	IV	Unstable
17	83	$J_3 = 74$ $J_2-J_3 = 62.6$	62.6	II	Stable
18	84	$J_1 = 67$ $J_2 = 76$	67.0	II	Stable
19	35	$J_1-J_2 = 11$	11.0	V	Completely unstable
20	47	$J_2 = 39.35$ $J_1-J_2 = 11.3$	11.3	V	Completely unstable
21	87	$J_3 = 45$ $J_2-J_3 = 45$	45.0	III	Partially stable
22	75	$J_3 = 62.8$ $J_1-J_3 = 59.35$ $J_2-J_3 = 31.3$	31.3	IV	Unstable
23	75	$J_1 = 58$ $J_1-J_2 = 31.3$ $J_2-J_3 = 31.3$	31.3	IV	Unstable
24	67	$J_1 = 61$	61.0	II	Stable
25	60	$J_1 = 45.63$	45.63	III	Partially stable
26	79	$J_3 = 43.3$ $J_2-J_3 = 43.3$	43.3	III	Partially stable
27	53	$J_3 = 45.35$	45.35	III	Partially stable
28	63	$J_1 = 42.6$ $J_1-J_2 = 27.3$	27.3	IV	Unstable
29	84	$J_2 = 24$ $J_1-J_3 = 80.4$	24.0	IV	Unstable
30	82	$J_2 = 31$	31.0	IV	Unstable

be described together with its SMR value so that its degree of stability within the class can be assessed. For example, slope 7 comes under the partially stable condition with SMR value 41 which is a marginal condition close to the next lower class, i.e., unstable. This fact should be duly considered while planning for any developmental activity.

The SMR values computed for the slopes are checked with the field conditions and it is found that the completely unstable slopes 19 and 20 are major landslide slopes. The slope 19, whose SMR has been found only 11, is the Kaliasaur landslide. Further, among the unstable slopes, the slopes 1, 9, 10, 16, 22 and 23 have shown small magnitude of slope failures. The slopes 29 and 30, falling under Class IV, i.e., unstable condition, do not show any sign of failure. Though in majority of cases, no sign of failure are observed on the slopes falling under the partially stable class, yet few slopes with lower SMR value within this class (say <50) do show a tendency to fail even when disturbed to a small extent in future. So, the partially stable condition is the transition zone and depending on the closeness of the SMR value towards the unstable or stable class, this may shift accordingly with slight changes in the existing condition. The slopes 6 and 7, though found to be in partially stable condition, are actually unstable slopes when observed in the field. The slopes 14 and 21, with lower SMR within the class III, are stable slopes. This indicates that some slopes, coming in partially stable class deviate a little from the actual field condition. However, stability conditions of slopes of completely unstable, unstable and stable classes reasonably agree with the observed field conditions. It is found that 80% assessed stability with this technique matches with the existing field conditions.

5.8.1 STABILITY ASSESSMENT UNDER WET CONDITIONS

After assessing the slope stability with the existing field conditions, an attempt is made to evaluate the worst possible stability of slopes due to high water saturation. In rainy season, the water condition on most of the slopes may change to wet condition. Hence, to assess a worst condition, the SMR is calculated with anticipated wet water condition for which the rating of 7 is assigned. The computed SMRs for wet conditions (Table 5.10) show a decrease in the stability conditions in case of a few slopes. The decrease in the SMR is more in case of slopes which are considered as dry in the existing field conditions. The table shows that three slopes, namely slope 9, 16 and 29, which are unstable under the existing water condition, fall

Table 5.10 Comparison of SMR under observed and wet conditions

Slope No.	SMR with existing water condition			SMR under wet condition		
	SMR	Class	Stability	SMR	Class	Stability
1	32.5	IV	unstable	29.5	IV	unstable
2	48	III	partially stable	40	IV	unstable
3	62.5	II	stable	54.85	III	partially stable
4	44.4	III	partially stable	36.4	IV	unstable
5	45.35	III	partially stable	42.35	III	partially stable
6	48.4	III	partially stable	42.4	III	partially stable
7	41	III	partially stable	38	IV	unstable
8	42.5	III	partially stable	34.5	IV	unstable
9	22	IV	unstable	19	V	completely unstable
10	26.7	IV	unstable	23.7	IV	unstable
11	44.5	III	partially stable	36.5	IV	unstable
12	30	IV	unstable	27	IV	unstable
13	61.35	II	stable	53.35	III	partially stable
14	44	III	partially stable	36	IV	unstable
15	63.35	II	stable	55.35	III	partially stable

Contd...

Slope No.	SMR with existing water condition			SMR under wet condition		
	SMR	Class	Stability	SMR	Class	Stability
16	24	IV	unstable	16	V	completely unstable
17	62.6	II	stable	54.6	III	partially stable
18	67	II	stable	59	III	partially stable
19	11	V	completely unstable	8	V	completely unstable
20	11.3	V	completely unstable	8.3	V	completely unstable
21	45	III	partially stable	37	IV	unstable
22	31.3	IV	unstable	23.3	IV	unstable
23	31.3	IV	unstable	23.3	IV	unstable
24	61	II	stable	58	III	partially stable
25	45.63	III	partially stable	42.63	III	partially stable
26	43.3	III	partially stable	35.3	IV	unstable
27	45.35	III	partially stable	42.35	III	partially stable
28	27.3	IV	unstable	24.35	IV	unstable
29	24	IV	unstable	16	V	completely unstable
30	31	IV	unstable	23	IV	unstable

in completely unstable class under wet condition. Out of the 12 partially stable slopes under existing water condition, 8 slopes fall in unstable class under wet condition and all the slopes of stable class are falling in partially stable class under wet condition. The SMR of completely unstable slopes, such as slopes 19 and 20, have further gone down in wet conditions (<10). This shows that, during heavy rains, if the slopes become completely wet, the stability may decrease further and the chances of failure always exist. Although some of the slopes of the partially stable class, which are changing to unstable class due to wet condition, have not so far shown failure evidences, yet the chances of failure can not be ruled out if the slopes become sufficiently saturated by retaining the rain water on slopes in future. Hence, it is always safe to assess the stability in worst possible condition.

5.10 SUMMARY

Slope Mass Rating technique, developed by Romana (1985), is used for slope stability assessment. The thirty slopes selected for this study show different degree of stability as visible from field conditions. To determine SMR, the Rock Mass Rating (RMR_{basic}) is initially determined and to it is added the factorial adjustment ratings for the joint orientation and the method of excavation of slopes. The data collected for this study is basically a detailed joint survey for each slope. The computed SMR for the 30 slopes show four types of stability conditions, i.e., from completely unstable to stable state. It is found that although in some slopes RMR values are high, showing good quality of rock, yet the corresponding SMR values are low, implying that the stability of these slopes is governed mainly by joint orientations.

The stability conditions assessed by SMR, particularly for the slopes having completely unstable, unstable and stable conditions, show that the results are in agreement with the existing field conditions. Out of the 30 slopes, 24 slopes have depicted realistic field stability conditions, so 80% predicted stability is matching. The SMR values, calculated by anticipating the worst condition under water saturation, have shown decrease in stability of slopes. Since the number of slopes studied is small for a statistical measure, the study need to be carried out with a large number of slopes, to make any conclusive statement. However, the SMR technique of stability assessment is found to be an easily applicable method which approximately evaluates the degree of stability.

In the end, it may be added that for few slopes, the assessed stability with anticipated

worst condition (wet condition) belongs to a lower degree of stability than the one to which it actually belongs in the existing field conditions. Hence, a estimate of worst stability conditions could be made using the SMR technique.

RESULTS AND DISCUSSIONS

The present work pertains to the development, evaluation and application of the techniques of landslide hazard zonation and slope stability assessment. The techniques developed during the present work as well as some of the already available techniques have been applied in Srinagar-Rudraprayag area of Garhwal Himalaya. The study involved geological mapping, preparation of the various terrain factor maps including the landslide map of the area, identification of the relationship between the landslide occurrence and the terrain factors, development and evaluation of landslide hazard zonation techniques as well as the site specific slope stability assessment. The salient results of the study are discussed here.

6.1 TERRAIN FACTORS AND LANDSLIDES

The terrain factors studied are lithology, major thrust/fault, slope, relative relief, drainage density and landuse. The existing landslide distribution is also studied.

The major rock types exposed in the area are the quartzites and the phyllites. These are associated with various volcanic flows, doleritic intrusion and occasional presence of dolomites. The only major thrust in the area is the North Almora Thrust (NAT) trending in the WNW-ESE direction. Besides this thrust, there are several local faults, the most important of these being the Kaliasaur fault.

The slope map of the area, deciphering various slope classes, has indicated that the maximum area is occupied by the 25°-35° and 35°-45° categories with small pockets of very steep slopes (>45°). From the relative relief data it has been found that bulk of the area is falling in the relief categories of 300-400 m and 400-500 m. The drainage density values, obtained from different drainage sub-basins of the area, show that the region is dominated by

the low drainage density. The landuse study, based on vegetation density, reveals that the thick forests are occupying maximum area. The landslide map, prepared using the areal photo-interpretation, shows 139 landslides in the area. Although, the landslides are distributed all over the area, yet these are more concentrated in the southern part particularly between Dewalgarh and Bachchan streams. The mean landslide density in the area has been found to be 0.313. The most important landslide, the Kaliasaur slide, located on the left bank of the Alaknanda river, is primarily due to the presence of Kaliasaur fault which has resulted in crushed and pulverised rocks on the slope and due to the continuous toe erosion by the river.

The study of relationships between the landslides and the different terrain factors has been carried out to identify the different factor categories which are conducive to landslides in the area. This relationship is based on the density of landslide (DLS) of each category of factors. Amongst all the rock types, the phyllites, being very soft and having weak foliation planes in this area have been found to be the most landslide prone. On the other hand, the quartzites, being hard and resistant, are less susceptible to landsliding. The study of landslide dependence on thrusts/faults has revealed that the presence of NAT, in the study area, is the major controlling factor for landslide occurrence. It is supported by the fact that the density of landslide has been found higher in the vicinity of this thrust. The slope angle and landslide do not show a monotonous trend. The maximum landslide density is in gentle to moderately steep slopes. This is due to the presence of weak phyllitic rocks in gentle to moderately steep slopes. The monotonous trend is not found in the case of relative relief also. The landslide density has been observed to be maximum in the higher relief of 400-500m and then for the 200-300m. The relation between drainage density and landslides has shown maximum landslide occurrence in the regions of low drainage density. This could be due to the higher seepage which, in turn, develops high pore water pressure. The landslide dependence on landuse shows a monotonous trend with density of landslide decreasing with increasing vegetation density. This confirms, there by, the role of root strength in increasing stability. The relationship study brought into focus the complex dependence of landslide occurrence on the various factors.

6.2 LANDSLIDE HAZARD ZONATION

Landslide hazard zonation study in the area has been carried out on a regional scale (1:50,000), using the three techniques viz., Subjective Regional Zonation (SRZ), Objective

Regional Zonation (ORZ) and Detailed Regional Zonation (DRZ) techniques.

In SRZ technique the landslide hazard zonation map is prepared by first assigning numerical ratings to the factors and then estimating the landslide proneness for each category of different factors. This estimation is based on the relations between landslide occurrence and different factor categories. The classification of landslide potential score, obtained from data integration, into various hazard classes is based on a subjective decision. However, subsequently it is confirmed from field checks. The SRZ map prepared using this technique, shows that the very high and high hazard zones occur very close to NAT and to the south of the Alaknanda river. The northern part of the area comprises the moderate to low hazard zones. As expected, the landslide concentration is found to be more in the zone of high hazard class. To evaluate the validation of map a quantitative measure, Hazard Index (HI) has been defined. The HI, computed for each hazard class of the map, shows that the existing landslide frequency corresponds well with the predicted potential zones.

The ORZ technique, developed using the fuzzy set theory, has reduced the amount of subjectivity present in SRZ technique by computing the grade of factor categories from the data itself and then classifying the score of landslide potential into hazard classes on the basis of frequency analysis. This study highlights the importance of objective rating assignment in zonation. The ORZ map also shows very high and high hazard zones lying to the south of Alaknanda river while to the north of it the area is mainly occupied by low and moderate hazard classes. The increase in HI values, from very low to very high hazard class, validates the quality of the map.

These regional zonation maps have rightly indicated the high hazard zones where there is a cluster of landslides, for example along the Bachchan stream. Further, a critical observation of these maps revealed that the major landslide in the area, the Kaliasaur slide, is falling in the moderate hazard zone, instead of the very high or high hazard zone. This misclassification brings into open the fact that the regional zonation of a large area may mask the fine specific details of hazard zones.

This calls for a detailed zonation study. The application of a Detailed Regional Zonation (DRZ) technique to a small part of the study area, has resulted in more detailed zones of different hazard classes. Some of the missing zones of instability are detected in the DRZ map, e.g., the Kaliasaur landslide is falling in the high hazard zone in this map.

6.3 COMPARATIVE STUDY OF THE RESULTS OF THREE TECHNIQUES

The comparative study of the zonation maps prepared using the SRZ, ORZ and DRZ techniques, reveals the broad agreement in the resulting maps.

The comparison between the SRZ and ORZ maps for the whole area has revealed the similarities in trends of hazard zones, particularly in case of high hazard zones. It has been found that the number of differing cells for these two maps is less than half of the total number of cells in the area. The majority of differing cells differed only by one hazard class. The difference of one class may be attributed to the fact that the hazard class boundaries, in both the maps are ordinal in nature and the point to point matching is not possible. So, the difference of one hazard class can be considered as insignificant.

After comparing the two zonation maps for the complete study area, the zonation maps SRZ1, ORZ1, DRZ1 prepared for the sub area, using all the three techniques, have been compared. This study has shown that considerable amount of information about the hazard zones of detailed zonation map (DRZ map) is available from the SRZ and ORZ maps. However, using the DRZ technique more refined zonation is indeed obtained, albeit at the cost of detailed field study. The pairwise comparison of the maps SRZ1, ORZ1 and DRZ1 reveals that the number of cells differing in hazard classes, is little more than half the total number of cells. However, the maximum number of cells differ only by one class, again suggesting insignificant disagreement in the maps. The SRZ2 map, prepared using class boundaries of ORZ has shown similar zonation trends as in the SRZ1 map and the comparison of the map pair SRZ2 - ORZ1 has revealed almost same percentage of cells differing in hazard classes as in case for the pair SRZ1 - ORZ1. However, considerable differences in zonation trends have been noticed in the DRZ2 map, generated from DRZ1 map using the ORZ class boundaries. This suggests that the imposition of uniform class boundaries may not be desirable where the schemes have different sets of factors, categories and rating criteria.

6.4 APPLICABILITY OF SRZ, ORZ and DRZ TECHNIQUES

The primary goal of landslide hazard zonation is to identify the landslide potential areas using a quick assessment technique. It is not always possible to carry out detailed field investigation in a large area. With the help of available information about the geology and topography of the area and the remote sensing data, considerable amount of characteristic

features of the terrain can be identified through desk study with limited field survey. This saves lot of time and money and yet a quick appraisal of a large area can be made. The data, procured in this manner, are generally used for regional landslide hazard zonation for a large area.

The SRZ technique for zonation mapping is applicable when a priori knowledge is available to suggest judicious numerical ratings for the factors and their categories. Hence, this technique has the flexibility in rating assignment. The ORZ technique, where no initial ratings are assigned, is more objective. In cases when a priori knowledge about the terrain is not available, the ORZ technique can be applied to give more representative weightages to the factors and their categories. The feasibility of the ORZ technique depends on the number of data points. The technique can be successfully used only for reasonably large number of data sets. The DRZ technique is desirable for a detailed regional zonation, whenever intensive field investigations are possible. This may help in the detailed planning of development schemes.

6.5 SITE SPECIFIC SLOPE STABILITY ASSESSMENT

The site specific slope stability assessment for individual slopes has been carried out using the Slope Mass Rating (SMR) technique. The applicability of this technique for rock slope studies has been evaluated.

The SMR technique is based on Rock Mass Rating (RMR_{basic}), joint orientations and the method of excavation of slopes. The SMR value is governed by these three factors, each of which individually governs the stability of a slope. In the SMR technique, the rating of joint orientations in relation to slope largely influences the overall SMR value of a slope. Infact a slope having a higher RMR value and showing good rock mass quality can be unsafe, if the attitude of discontinuities is unfavourable. So, the technique emphasizes the importance of discontinuity planes in relation to the slope face. The rating for the method of excavation, ranging between +15 to -8, also affects the SMR value significantly. So, depending on the characteristics of these three factors, the stability of a slope can vary from completely stable to completely unstable.

In the present work, 30 rock slopes along the Srinagar-Rudraprayag road have been studied for their stability assessment. The present analysis has shown that out of the 30 slopes, only 2 are in completely unstable condition, 10 are in unstable condition, 12 are in partially

stable condition and the remaining 6 are in stable condition. The two completely unstable slopes, assessed by SMR, are the landslide slopes. In majority of cases the slopes, assessed as unstable by SMR, have shown evidences of failure when checked in the field and the slopes of partially stable condition with lower SMR values are likely to fail in future, if their natural stability is disturbed by some external factor. Overall, it is found that 80% of the assessment matches with the existing field conditions.

Since most of the slope failures are triggered during rains, stability of the slopes is again assessed, for the worst possible condition, by anticipating water saturation. It is found that most of the slopes change over to the lower degree of stability under wet conditions. Apart from the two landslide slopes, i.e., the slopes 19 and 20 which fall in completely unstable class even in the existing field conditions, there are three more slopes namely 9, 16 and 29 which grade into completely unstable class in wet condition. So, the assessment of the stability condition under wet condition provides us with conservative stability estimates. The field applicability of the SMR technique has revealed that it can be successfully applied for site specific slope stability assessment of rock slopes.

6.6 CONCLUDING REMARKS

The landslide hazard zonation maps are useful for planning and implementation of various developmental schemes in hilly areas. It may be alluded that the main goal is to identify the high and very high hazard zones to reduce the possibility of implementing the major cost intensive developmental projects in such zones.

To study an area, the regional landslide hazard zonation should be carried out first to identify the zones of high hazard. For this, the SRZ or the ORZ technique can be used depending on the available a priori information and the size of the data set. The high hazard zones identified from regional hazard zonation should then be studied in detail for a detailed zonation mapping using the DRZ technique. Further, if felt necessary, the site specific slope stability assessment may be carried out to obtain the more specific details. Such a step by step approach will significantly help in effective planning of development schemes within the stable hill slopes. This will lead to minimal environmental degradation to the mountainous areas and thereby helping in sustainable development.

REFERENCES

- Agarwal, N.C. and Kumar, G., 1973. Geology of the Upper Bhagirathi and Yamuna valleys, Uttarkashi district, Kumaun Himalaya. *Him. Geol.*, 3, pp.1-23.
- Ahmad, A., 1976. Facies concept, correlation and classification of Palaeozoic (Pre-Blaini) Formations of Kumaun, Garhwal and Himachal Pradesh, Lesser Himalaya, India. *Geol. Surv. Ind. Misc. Pub.*, 41 (1), pp.209-240.
- Anbalagan, R., 1992. Landslide hazard evaluation and zonation mapping in mountainous terrain. *Engg. Geol.*, 32, pp.269-277.
- Anbalagan, R., Sharma, S. and Raghubanshi, T.K., 1992. Rock mass stability evaluation using modified SMR approach. *Proc. 6th Nat. Symp. on Rock Mech.*, Bangalore, India, pp.258-268.
- Auden, J.B., 1949. In Director's General Report for 1939. *Rec. Geol. Surv., India*, 78, pp.74-78.
- Barton, N and Choubey, V.D., 1977. The shear strength of rock joints in theory and practice. *Rock. Mech.*, 10 (1-2), pp.1-54.
- Bhandari, R.K., 1987. Slope stability in the fragile Himalaya and strategy for development. 9th IGS lecture, *Indian Geotech. Jour.*, 17 (1), pp. 1-78.
- Bhandari, R.K., Herath, N. and Thayalan, N., 1994. Landslide hazard zonation mapping in Srilanka - a holistic approach. *Nat. Symp. on Landslides in Srilanka*, Colombo, 1, pp.271-284.
- Bhargova, O.N., 1972. A reinterpretation of the Krol Belt. *Him. Geol.*, 2, pp.47-81.
- Bieniawski, Z.T., 1973. Engineering classification of jointed rock masses. *Trans. S. Afr. Inst. Civ. Engrs.*, 15 (12), pp.335-344.
- Bieniawski, Z.T., 1979. The geomechanics classification in rock engineering application. *Proc. 4th Int. Cong. on Rock Mech.*, Montreux, 2, pp.41-48.
- Bieniawski, Z.T., 1989. *Engineering rock mass classification*. John Willey and Sons, New York, p.251.
- Blanc, R.P. and Cleveland, G.B., 1968. Natural slope stability as related to geology, San Clemente Area, Orange and San Diego Counties, California. *California Division of Mines and Geology Special Report*, 98, p.19.
- Bowman, H.N., 1972. Natural slope stability in the city of Greater Woolongong. *N.S.W. Geol.*

Surv. Recs., 14, part 2, pp.159-222.

Brabb, E.E., 1993. Proposal for worldwide landslide hazard maps. Proc. 7th Int. Conf. and field workshop on landslides in Czech and Slovak Republics, pp.15-27.

Brabb, E.E., Pampeyan, E.H. and Bonilla, M.G., 1972. Landslide susceptibility in San Mateo County, California. U.S. Geol. Surv. Misc. Field studies Maps, MF-360.

Brand, E.W., 1988. Special lecture: Landslide risk assessment in Hong Kong. 5th Int. Symp. on landslides, Lausanne, 2, pp.1059-1074.

Campbell, D.A., 1951. Types of erosion prevalent in New Zealand. Ass. Inter. D'Hydrologie Scientific, Assemblee Generale de Bruxellers. Tome II, pp.82-95.

Carrara, A., 1983. Multivariate models for landslide hazard evaluation. Math. Geol., 15 (3), pp.403-426.

Carrara, A., Cardinali, M. and Guzzetti, F., 1992. Uncertainty in assessing landslide hazard and risk. ITC Jour., 2, pp.172-183.

Chansarkar, R.A., 1975. Geological and geomorphologic factors in landslide investigations. Proc. Seminar on landslides and toe erosion problems with special reference to Himalayan region, Gangtok, pp.84-89.

Choubey, V.D. and Litoria, P.K., 1990. Terrain classification and land hazard mapping in Kalsi Chakrata area (Garhwal Himalaya), India. ITC Jour., 1, pp.58-66.

Crozier, M.J., 1973. Techniques for the morphometric analysis of landslips. Zeitschrift fur Geomorph., 17 (1), pp.78-101.

Crozier, M.J., 1986. Landslides: Causes, consequences and environment. Croom Helm Australia Pty. Ltd., p.252.

Davis, J.C., 1986. Statistics and data analysis in geology. Second edition. John Willey and Sons, New York, p.646.

Deere, D.U., 1968. Geological consideration. In: Rock mech. in engg. practice. Eds. R.G. Stagg and D.C. Zienkiewicz, John Willey and Sons, New York, pp.1-20.

Deere, D.U., Hendron, A.J. and Cording, E.J., 1967. Design of surface and near surface construction in rocks. Proc. 8th U.S. Symp. Rock Mech., AIME, New York, pp.237-302.

Dobrovolny, E. and Schmoll, H.R., 1974. Slope stability map of Anchorage and vicinity, Alaska. U.S. Geol. Surv. Misc. Inv. Maps, I-787-E.

Doval, S.C. and Sakalani, P.S., 1980. A note on the study of minor structures in rocks of

- Srinagar area, Garhwal Himalaya, U.P. Him. Geol., 10, pp.178-190.
- Eyles, G.O., 1983. The distribution and severity of present soil erosion in New Zealand. *New Zealand Geographer*, 39 (1), pp.12-28.
- Fuches, G. and Sinha, A.K., 1978. The tectonics of the Garhwal-Kumaun Lesser Himalaya. *Jahrb. Geol., B.-A.*, 121 (2), pp.219-241.
- Gansser, A., 1964. *Geology of Himalaya*. Interscience, John Willey, London, p.289.
- Gansser, A., 1980. The division between Himalaya and Karakorum. *Geol. Bull. Univ. Peshawar*, 13, pp.9-22.
- Garg, J.K., Narayana, A., Arya, A.S., Murthy, T.V.R., Joshi, V. and Saxena, K.G., 1996. Landslide hazard zonation around Tehri dam using remote sensing and GIS techniques. *Proc. Int. Conf. on Disasters and mitigation, Madras, India*, 1, pp.A₄.41-A₄.46.
- Gupta, P. and Anbalagan, R., 1995. Landslide hazard zonation mapping of Tehri-Pratap nagar area, Garhwal Himalaya. *Jour. Rock Mech. and Tunnelling Tech., ISRM*, 1 (1), pp.41-58.
- Gupta, R.P. and Joshi, B.C., 1990. Landslide hazard zoning using the GIS approach - A case study from the Ramganga Catchment, Himalaya. *Engg. Geol.*, 28, pp.119-131.
- Haruyama, M. and Kitamura, R., 1984. An evaluation method by the quantification theory for the risk degree of landslides caused by rainfall in active volcanic area. *Proc. 4th Int. Symp. on Landslides, Toronto*, 1, pp.435-440.
- Heim, A. and Gansser, A., 1939. Central Himalaya, Geological observations of Swiss expedition, 1936. *Mem. Soc. Relv. Nat.*, 73 (1).
- Herbert, J.D., 1842. Geological map of the mountain provinces between the rivers Sutlej and Kalee. *Jour. Asiatic Sec.*, 21 (appendix).
- Hoek, E. and Bray, J., 1981. *Rock slope engineering*. 3rd ed. Inst. Min. Metall., London, pp.358.
- Huma, Io. and Radulescu, D., 1978. Automatic production of the thematic maps of slope stability. *Int. Ass. Engg. Geol. Bull.*, 17, pp.95-99.
- Hutchinson, J.N., 1968. Mass movement. In: *The Encyclopedia of Geomorphology*. Ed. R.W. Fairbridge, Reinhold, pp.688-696.
- Hutchinson, J.N., 1977. General, largely morphological classification of mass movements on slopes. Unpublished teaching hand-out, Imperial College, London.
- Indian Standard 11315, 1987. Methods for quantitative description of discontinuities in rock

mass. Part 1-10, Bureau of Indian standards, New Delhi.

Ives, J.D. and Messerli, B., 1989. *The Himalayan Dilemma: Reconciling development and conservation*. Routledge, London, p.295.

Jain, A.K., 1971. Stratigraphy and tectonics of Lesser Himalayan region of Uttarkashi, Garhwal Himalaya. *Him. Geol.*, 1, pp.25-58.

Jain, A.K., 1972. Overthrusting and emplacement of basic rocks in Lesser Himalaya, Garhwal, U.P. *Jour. Geol. Soc. Ind.*, 13 (3), pp.226-237.

Jesch, R.L., Johnson, R.B., Belscher, D.B., Yaghjian, A.D., Steppe, M.C. and Fleming, R.W., 1979. High resolution sensing techniques for slope stability studies. Rep. No. FHWA-RD-79-32, U.S. Dept. of Commerce, Natl. Bur. standards, Boulder Colo, p.138.

Joshi, B.C., 1987. Geo-environmental studies in parts of Ramganga catchment, Kumaun Himalaya. Unpublished Ph.D. Thesis, Univ. of Roorkee, Roorkee, India, p.196.

Juang, C.H., Lee, D.H. and Sheu, C., 1992. Mapping slope failure potential using fuzzy sets. *Jour. Geotech. Engg.*, 118 (3), pp.475-494.

Kasa, H., Kurodai, M., Kojima, H. and Obayashi, S., 1992. Study on landslide prediction model using satellite remote sensing data and geographical information. 6th Int. Symp. on Landslides, Christchurch, New Zealand, 2, pp.983-988.

Kawakami, H and Saito, Y., 1984. Landslide risk mapping by a quantification method. *Proc. 4th Int. Symp. on Landslides*, Toronto, 1, pp.535-540.

Khan, A.A., Dubey, U.S., Shehgal, M.N. and Awasthi, S.S., 1982. Terraces in the Himalayan tributaries of Ganga in U.P. *Jour. Geol. Soc. Ind.*, 23, pp.392-401.

Kingsbury, P.A., Hastie, W.J. and Harrington A. J., 1992. Regional landslip hazard assessment using a GIS. 6th Int. Symp. on landslides, Christchurch, New Zealand, 2, pp.995-1000.

Klir, G.J. and Folger, T.A., 1988. *Fuzzy sets, uncertainty, and information*. Englewood Cliffs, New Jersey, p.355.

Kumar, G. and Agarwal, N.C., 1975. Geology of the Srinagar-Nandprayag area (Alaknanda valley), Chamoli, Garhwal and Tehri Garhwal districts, Kumaun Himalaya, Uttar Pradesh. *Him. Geol.*, 5, pp.29-59.

Kumar, G. and Dhaundiyal, J.N., 1979. Stratigraphy and structure of Garhwal Synform, Garhwal and Tehri Garhwal Districts, U.P., a reappraisal. *Him. Geol.*, 9 (1), pp.18-41.

Kumar, G., Prakash, G. and Singh, K.N., 1974. Geology of Deoprayag-Dwarahat area, Garhwal, Chamoli and Almora districts, Kumaun Himalaya, Uttar Pradesh. *Him. Geol.*, 4,

pp.321-346.

Lakhera, R.C., Roy, A.K., Prusty, B.G. and Mittal, S.K., 1992. Landslide hazard zonation studies in parts of Garhwal Himalayas using remote sensing and GIS techniques. Proc. Nat. Symp. on Remote Sensing for sustainable development, pp.227-231.

Landry, J., 1979. Carte ZERMOS. Zones exposes a des risques lies aux mouvements du sol et du sous-sol, region de Lons-le-Saunier a Poligny (Jura), Orleans. Bur. de Rech. Geol. et Miniere, 1 map, p.14.

Majumdar, N., 1980. Distribution and intensity of landslide processes in North Eastern India - a zonation map thereof. Proc. Int. Symp. on Landslides, New Delhi, India, 1, pp.3-8.

Mark, R.K., 1992. Map of debris flow probability, San Mateo County, California. U.S. Geol. Surv. Misc. Inv. Series, Map I-1257-M.

Mehdi, S.H., Kumar, G. and Prakash, G., 1972. Tectonic evaluation of Eastern Kumaun Himalaya: a new approach. Him. Geol., 2, pp.481-501.

Mehrotra, G.S., Sarkar, S. and Dharmaraju, R., 1992. Landslide hazard assessment in Rishikesh-Tehri area, Garhwal Himalaya, India. Proc. 6th Int. Symp. on Landslides, Christchurch, New Zealand, 2, pp.1001-1007.

Mehrotra G.S., Sarkar, S., Kanungo, D.P. and Haragopal, M., 1995. Slope stability assessment using slope mass rating technique. Proc. 35th U.S. Symp. on Rock Mech., Nevada, Reno, pp.91-96.

Mehrotra, G.S., Sarkar, S., Kanungo, D.P. and Mahadevaiah, K., 1996. Terrain analysis and spatial assessment of landslide hazards in parts of Sikkim Himalaya. Jour. Geol. Soc. Ind., 47, pp.491-498.

Mehta, P.N., 1971. Some observations on the Tons Thrust and their significance. Indian Minerals, 25 (1), pp.66-68.

Meneroud, J.P., 1978. Cartographie des risques dans les Alpes-Maritimes (France). Proc. 3rd Int. Cong., Int. Ass. Engg. Geol., Sec. I, 2, pp.98-107.

Meneroud, J.P. and Calvino, A., 1976. Carte ZERMOS. Zones exposees a des risques lies aux mouvements du sol et du sous-sol a 1:25000, region de la Moyenne Vesubie (Alps-Matitimes), Orleans. Bur. de Rech. Geol. et Minieres, 1 map, p.11.

Middlemiss, C.S., 1887. Crystalline and metamorphic rocks of Lower Himalaya. Rec. Geol. Surv. Ind., 20 (3), pp.134-143.

Negi, S.S., 1982. Environmental problems in the Himalaya. Science Reporter, 19, pp.34-37.

- Neuland, H., 1976. A prediction model of landslips. *Catena*, 3, pp.215-230.
- Nilsen, T.H., Wright, R.H., Vlastic, T.C. and Spangle, W., 1979. Relative slope stability and landuse planning in the San Francisco Bay region, California. U.S. Geol. Surv. Professional paper, 944, p.96.
- Obermier, S.F., 1979. Slope stability map of Fairfax County, Virginia. U.S. Geol. Surv. Misc. Field studies Map, MF-1072.
- Pachauri, A.K. and Pant, M., 1992. Landslide hazard mapping based on geological attributes. *Engg. Geol.*, 32, pp.81-100.
- Palmstrom, A., 1982. The volumetric joint count - a useful and simple measure of the degree of rock jointing. *Proc. 4th Int. Cong., Int. Ass. Engg. Geol., Delhi*, 5, pp.221-228.
- Pant, G., 1975. Observation on the fossil valleys and gorges at the Bhagirathi and Alaknanda rivers. *Him. Geol.*, 5, pp.193-205.
- Prasad, C. and Verma, V.K., 1982. Studies in mass wasting along zones of fracturing in Garhwal Himalaya. *Himalaya: Landforms and processes*, pp.29-45.
- Radbruch-Hall, D.H. and Crowther, K.C., 1973. Map showing areas of estimated relative amounts of landslides in California. U.S. Geol. Surv. Misc. Inv. Map, I-747.
- Reger, J.P., 1979. Discriminant analysis as a possible tool in landslide investigations. *Earth Surface Processes*, 4, pp.267-273.
- Rib, H.T. and Liang, T., 1978. Recognition and Identification. In : *Landslides: analysis and control*. Eds. R.L. Schuster and R.J. Krizek, Transportation Research Board, Special Report, 176, Nat. Aca. of Sciences, Washington DC, pp.34-80.
- Rodriguez Ortiz, J.M., Hinojosa, J.A. and Prieto, C., 1978. Regional studies on mass movements in Spain. *Proc. 3rd Int. Cong., Int. Ass. Engg. Geol., Sec I, 1*, pp.267-277.
- Romana, M., 1985. New adjustment ratings for application of Bieniawski classification to slopes. *Int. Symp. on the role of rock mechanics, Zacatecas*, pp.49-53.
- Romana, M., 1988. Practice of SMR classification for slope appraisal. *Proc. 5th Int. Symp. on landslides, Lausanne*, 2, pp.1227-1231.
- Romana, M., 1991. SMR classification. *Proc. 7th Int. Cong. on rock mechanics, Aachen, Deutschland*, pp.955-960.
- Roy, A.B. and Valdiya, K.S., 1988. Tectonometamorphic evolution of the Garhwal Himalayan Thrust sheets in Garhwal region, Kumaun Himalaya. *Jour. Geol. Soc. Ind.*, 32 (3), pp.106-124.

Roy, A.K., Champati Ray, P.K. and Lakhera, R.C., 1992. A new horizon of GIS application and integrated approach in Geosciences. Proc. Silver Jubilee Seminar, IIRS, Dehradun, India, pp.34-40.

Rupke, J., 1974. Stratigraphy and structural evolution of the Kumaun Lesser Himalaya. Sed. Geol., 11, pp.81-265.

Sakalani, P.S., 1971. Structure and tectonics of the Pratapnagar area, Garhwal Himalaya. Him. Geol., 1, pp.75-91.

Sakalani, P.S., 1972. Lithostratigraphy and structure of the area between the Bhagirathi and Bhilangana rivers, Garhwal Himalaya. Him. Geol., 2, pp.342-355.

Sarkar, S., Kanungo, D.P. and Mehrotra, G.S., 1995. Landslide hazard zonation : A case study in Garhwal Himalaya, India. Mount. Res. and Dev., 15, (4), pp.301-309.

Sesagiri, D.N. and Badrinarayan, S., 1982. The Nilgiri landslides. Geol. Surv. Ind. Misc. Pub., 57, p.32.

Sharpe, C.F.S., 1938. Landslides and related phenomena. Pageant, New Jersey, p.137.

Sridevi, J. and Sarkar, S., 1993. Statistical models for instability classification. Engg. Geol., 36, pp.91-98.

Srivastava, R.N. and Ahmad, A., 1979. Geology and structure of Alaknanda valley, Garhwal Himalaya. Him. Geol., 9, pp.225-254.

Stevenson, P.C., 1977. An empirical method for the evaluation of relative landslide risk. Int. Ass. Engg. Geol. Bull., 16, pp.69-72.

Stocklin, J., 1980. Geology of Nepal and its regional frame. Jour. Geol. Soc. London, 137, pp.1-34.

Swindells, C.F., 1985. The detection of blast induced fracturing to rock slopes. Int. Symp. on the role of rock mech., Zacatecas, pp.81-86.

Takei, A., 1982. Limitation methods of hazard zones in Japan. In: Report of Japanese-Austrian joint research, forecast of disaster zone in mountainous regions, 1980-1981. Eds. Takei and Aulitzky, Kyoto Univ. Lab. of erosion control Res. Bull., 1, pp.7-25.

Thakur, V.C., 1993. Geology of Western Himalaya. Pergamon press, Oxford, p.355.

Tsiambaos, G. and Telli, D., 1992. Application of rock mass classification systems on stability of limestone slopes. 6th Int. Symp. on Landslides, Christchurch, New Zealand, 2, pp.1065-1070.

- Valdiya, K.S., 1978. Extension and analogues of the Chail Nappe in Kumaun Himalaya. *Ind. Jour. Earth Sciences*, 55, pp.1-19.
- Valdiya, K.S., 1980. Geology of Kumaun Lesser Himalaya. *Wadia Inst. of Him. Geol., Dehradun*, p.291.
- Valdiya, K.S., 1985. Accelerated erosion and landslide - prone zones in the Himalayan region. In: *Environmental regeneration in Himalaya: Strategies and concepts*. Ed. J.S. Singh. Cen. Him. Env. Ass., Nainital, pp.12-38.
- Valdiya, K.S., 1987. *Environmental Geology: Indian Context*. Tata McGraw-Hill, New Delhi, India, p.583.
- Varnes, D.J., 1958. Landslide types and processes. In: *Landslides and Engineering Practice*. Ed. E.B. Eckel, Highway Research Board, Special Rep. 29, NAS-NRC pub. 544, pp.20-47.
- Varnes, D. J., 1978. Slope movement and types and processes. In : *Landslides: Analysis and control*. Eds. R.L. Schuster and R. J. Krizek, Transportation Res. Board Special Rep. 176, Nat. Aca. of Sciences, Washington DC, pp.11-33.
- Varnes, D.J., 1984. Landslide hazard zonation: a review of principles and practice. UNESCO, France, p.63.
- Virdi, N.S., 1986. Lithostratigraphy and structure of central crystallines in the Alaknanda and Dhauliganga valleys of Garhwal, U.P. In: *Cur. trends in Geol. IX, Himalayan Thrust and associated rocks*. Ed. P.S. Sakalani, Today and Tomorrows, New Delhi, pp.156-166.
- Wagner, A., Leite, E. and Olivier, R., 1988. Rock and debris slides risk mapping in Nepal - a user friendly PC system for risk mapping. *Proc. 5th Int. Symp. on Landslides, Lausanne, 2*, pp.1251-1258.
- Ward, W.H., 1945. The stability of natural slopes. *Geographical Jour.*, pp.170-197.
- Yatsu, E., 1966. *Rock control in geomorphology*. Sozoshu, Japan, p.135.
- Yin, K.L. and Yan, T.Z., 1988. Statistical prediction models for slope instability of metamorphosed rocks. *Proc. 5th Int. Symp. on Landslides, Lausanne, 2*, pp.1269-1272.
- Zadeh, L.A., 1975. The concept of a linguistic variable and its application to approximate reasoning. *Infor. Sciences, Part I (3)*, pp.192-249.
- Zaruba, Q. and Mencl, V., 1969. *Landslides and their control*. Elsevier, Amsterdam, p.205.
- Zimmermann, H.J., 1991. *Fuzzy set theory and its application*. Second edition, Kluwer Aca., London, P.391.